Comparison of injection moulded, natural fibre reinforced composites with PP and PLA as matrices

by

JULIA PUSELETSO MOFOKENG (B.Sc. Hons)

Submitted in accordance with the requirements for the degree

MASTER OF SCIENCE (M.Sc.) IN POLYMER SCIENCE

Department of Chemistry

Faculty of Natural and Agricultural Sciences

at the

UNIVERITY OF THE FREE STATE (QWAQWA CAMPUS)

SUPERVISOR: PROF AS LUYT

07 December 2010

Declaration

We, the undersigned, hereby declare that the research in this thesis is Ms. Mofokeng's own original work, which has not partly or fully been submitted to any other University in order to obtain a degree.

_____	_____
Ms. J.P. Mofokeng	Prof. A.S. Luyt

Dedication

I would like to dedicate this thesis to my family, my mother Mme Mmakeletso and my two brothers Lefu and Lebohang Mofokeng. Most of all I would like dedicate this thesis to my late friend Nokuphila Ignitia Msibi who passed away in August this year; her dream was to have a masters degree one day, so this is for you my friend.

Abstract

Poly(lactic acid) (PLA) and polypropylene (PP) were comparatively investigated as matrices for injection moulded composites containing small (1-3 wt.%) amounts of short sisal fibre. The polymers and fibres were mechanically mixed, followed by extrusion at 190 °C and injection moulding at the same temperature. The morphology, thermal and mechanical properties, and degradation characteristics were investigated using scanning electron microscopy (SEM), Fourier-transform infrared (FTIR) spectroscopy, polarised optical microscopy (POM), differential scanning calorimetry (DSC), thermogravimetric analysis (TGA), dynamic mechanical analysis (DMA) and tensile testing. From the POM photos it seems as if the fibres are equally well dispersed in the PLA and PP matrices. The SEM photos, however, show more intimate contact and better interaction between the fibres and PLA. This improved interaction was confirmed by the FTIR results that show the presence of hydrogen bonding interaction between PLA and the fibre. This improved interaction did not seem to have a significant influence on the yield stress, stress at break or tensile modulus of PLA. In the case of PP, however, the stress at break reduced observably, while the tensile modulus almost doubled in the presence of the fibre.

The thermal stability (as determined through TGA) of both polymers increased with increasing fibre content, with a more significant improvement in the case of PP. The DSC results show a significant influence of the presence of the fibre on the crystallization behaviour of PLA, because both the melting temperature and melting enthalpy decreased with increasing fibre content, even at low fibre contents of 1-3%. This is the result of the strong interaction between PLA and the fibre, which immobilizes the PLA chains. The influence of the fibre on the melting characteristics of the PP was negligible. Both the storage and loss moduli of the PLA decreased with increasing fibre content below the glass transition of PLA, but the influence on the loss modulus was more significant. The DMA results clearly show cold crystallization of PLA around 110 °C, and the presence of fibre gave rise to higher modulus values between the cold crystallization and melting of the PLA. The presence of fibre also had an influence on the dynamic mechanical properties of PP.

The biodegradation of PLA and its composites was determined by keeping the samples in water at an elevated temperature for up to 10 days. The composites initially showed a larger mass loss than pure PLA, but after 10 days the pure PLA seemed to be more degraded. The SEM results of biodegraded samples show complete collapse of the surface of the PLA matrix after ten days.

Table of contents

List of tables

List of figures

List of symbols and abbreviations

APP	atactic polypropylene
ATR-FTIR	attenuated total reflectance Fourier-transform infrared spectroscopy
CE	chain extender
ΔH_m	enthalpy of melting
ΔH_c	enthalpy of crystallisation
DMA	dynamic mechanical analysis
EVA	ethylene vinyl acetate co-polymer
GPS	3-glycidoxypropyl trimethoxy silane
HDPE	high density polyethylene
LDI	lysine-diisocyanate
LDPE	low-density polyethylene
LLDPE	linear low-density polyethylene
MA	maleic anhydride
MAPP	maleic anhydride modified polypropylene
MA-g-PP	maleic anhydride grafted polypropylene
MCC	microcrystalline cellulose
MFI	melt flow index
PCL	polycaprolactone
PGA	poly(glycolic acid)
PHA	poly(hydroxyl alkanoate)
PHB	poly(hydroxyl butyrate)
PLA	poly(lactic acid)
POM	polarized optical microscopy
PP	polypropylene
RHF	rice-husk flour
RNCF	recycled newspaper cellulose fibre
SEM	scanning electron microscopy
TDI	toluene-2,4-diisocyanate
TGA	thermogravimetric analysis
T_c	crystllisation temperature
T_g	glass transition temperature
T_m	melting temperature

Chapter 1

Introduction

1.1 Overview

In the past years, growing environmental pollution has called for the use of natural materials for different applications. Government environmental policies have been implemented to force the industries like the automotive, packaging and construction to search for environmentally friendly or biodegradable materials to substitute the traditional non-biodegradable composites. Biodegradable polymers are materials obtained from nature or by synthetic route, whose chemical bonds are cleaved at least in one step by enzymes from the biosphere, with appropriate pH and temperature conditions and total processing time for completion. Most of the commercially available polymers are made from petroleum and they are non-biodegradable, and therefore the composites made from them are still a burden to the environment [1-8].

So far, two main technical ways have been developed to produce biodegradable materials. One deals with the compounding of traditional petroleum based polymers like thermosetting polymers (epoxy, unsaturated polyesters, phenol formaldehyde resin) or low processing temperature thermoplastic polymers (polypropylene, polyethylene) with natural fibres. The disadvantages stemming from the use of thermosets include brittleness, lengthy cure cycles and inability to repair and/or recycle damaged or scrapped parts. These disadvantages have led to the development of the thermoplastic matrix composite system. Among the thermoplastics, polypropylene was the first synthetic polymer to achieve industrial importance due to its low cost, easy processability, and excellent mechanical properties [9-10]. These composites cannot be taken as completely biodegradable materials due to the fact that the matrix is a non-biodegradable polymer.The other way mixes natural fibres with biodegradable polymers including starch, soybean plastics, cellulosic plastics, polyhydroxyalkanoate (PHA), polyhydroxybutyrate (PHB), polycaprolactone (PCL) and polylactic acid (PLA) [11-14].

The traditional definition of a composite material is a material with at least two phases, a continuous phase and a dispersed phase. The continuous phase is responsible for filling the volume and transfer loads to the dispersed phase. The dispersed phase is usually responsible for improving one or more properties of the composite [14]. In the field of composites, fibre reinforcement of matrices was initially developed using synthetic fibres such as glass, carbon and aramid, as they can be produced with a definite range of properties. Recently natural fibre reinforced polymer composites have experienced a significant growth in the composites industry. They are characterized by easy processability, good dimensional stability and excellent mechanical performance. The improved material performance primarily varies with the fibre-matrix bond strength and choice of suitable processing parameters [15-17]. The quality of the fibre reinforced composites depends considerably on the interface, because only a well formed interface allows stress transfer from the matrix to the fibre [18-19].

Natural fibres are subdivided based on their origin, coming from plants, animals or minerals. All plant fibres are composed of cellulose, while animal fibres consist of protein (hair, silk, and wool). Plant fibres include bast, leaf, or hard fibres. Bast (flax, hemp, jute) and hard fibres (sisal, coir) are commonly used in composites; therefore they are available throughout the world. They may also represent an economic interest for the agricultural sector [20-21]. Advantages of bio-fibres over the traditional reinforcing materials are cost effectiveness, low density, high toughness, acceptable specific strength properties, reduced tool wear, reduced dermal and respiratory irritation, good thermal properties, and improved energy recovery. They are renewable and biodegradable. Although there are so many advantages of natural fibres compared to inorganic or synthetic fibres, natural fibres are hydrophilic in nature. To overcome this problem the reinforcing natural fibres can be modified by physical (stretching, calendaring, thermo-treatment) and chemical methods. The most important chemical modification involves coupling methods [20,22-25].

Among the various natural fibres, sisal fibre is one of the most commercially available useful natural fibres. Sisal fibre is a hard fibre extracted from the leaves of the sisal plant *Agave sisalana*. It has a short renewal time and grows wild in the hedges of fields. The sisal fibre content of cellulose, lignin, hemi-cellulose, waxes and ash depends on the origin and age of the

fibre. Currently sisal is mainly used as ropes for the marine and agricultural industries. Other applications of sisal fibre include twines, cords, upholstery, padding and mat making, fishing nets, and fancy articles such as purses. Sisal fibre possesses a moderately high specific strength and stiffness, and can be used as a reinforcing material in polymeric resin matrices like polypropylene to make useful structural composite materials [9,16,26-28].

Polylactic acid (PLA) belongs to the family of aliphatic polyesters derived from α-hydroxy acids. PLA is a compostable polymer derived from renewable sources (mainly starch and sugars). Its degradation occurs by hydrolysis to lactic acid, which is metabolized by micro-organisms to water and carbon dioxide. Figure 1.2 shows the life cycle of PLA.

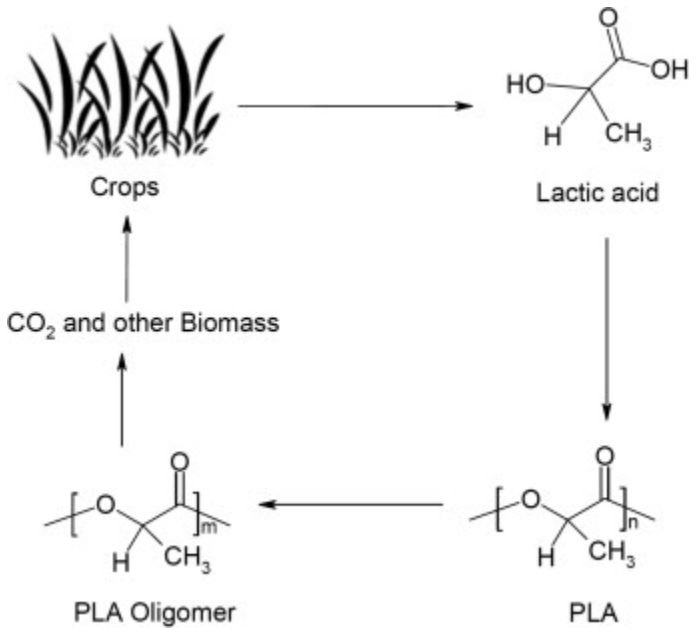

Figure 1.1 Life cycle of PLA

PLA has reasonably good optical, physical, mechanical, and barrier properties compared to the existing petroleum based polymers. The good thing about PLA is that it can be processed exactly the same way as polyolefines and other thermoplastic polymers, although the thermal stability could be better. PLA can be used for making plastic bags for household bio waste, barrier for sanitary products and diapers, planting cups, and disposable cups and plates. PLA can also be clinically used as surgical sutures, sustained drug delivery system, in bones fracture fixation

[17,29-35]. The drawback of using PLA is its brittleness, and it is also not cost effective. The problem is solved through the use of composite materials based on natural fibres [36]. The reinforcement of PLA using plant fibres has been studied with the aim of developing sustainable 'green-composites'. The Young's modulus of the PLA can be increased significantly with increasing fibre load, but the problem is loosing properties like yield strain, which results in the strength being decreased. To overcome this drawback, samples are processed by melt extrusion compounding using a twin screw extruder, followed by injection molding. [37]

The processing technique for preparing the composites is very important, and it was reported that twin screw extrusion resulted in better fibre dispersion [29]. The shear force occurring when both screws rotate in the opposite directions provides an intimate mixing between the fibre and the matrix. This plays a major role in providing the required performance such as less fibre pull outs, indicating a better fibre-matrix adhesion. Most thermoplastic-natural fibre composites were prepared through melt mixing of short natural fibres and polymer pellets through extrusion, followed by injection moulding. PLA based biodegradable composites are prepared with natural fibre as the reinforcing phase by twin screw extrusion, followed by injection molding. Injection molding is the most widely used converting process for thermoplastic articles, especially for those that are complex in shape and call for high dimensional accuracy [33,38-39].

1.2 Objectives

The present work aims at comparing the properties of polylactic acid (PLA) and polypropylene (PP) reinforced with sisal fibre at low concentrations of 1-4 and 6%. The composites were processed using a twin screw extruder, followed by injection molding. The composites' morphology was studied using scanning electron microscopy (SEM), and the dispersion of the sisal fibre in the composites was studied with polarized optical microscopy (POM). The thermal behaviour was determined by differential scanning calorimetry (DSC) and thermogravimetric analysis (TGA). The polymeric structure of these composites was further investigated by attenuated total reflectance infrared spectroscopy (ATR-FTIR) microscopy. The mechanical and thermo-mechanical properties of the composites were studied using tensile testing and dynamic mechanical analysis (DMA).

1.3 Thesis outline

The outline of this thesis is as follows:

Chapter 1:	General introduction
Chapter 2:	Literature review
Chapter 3:	Experimental
Chapter 4:	Results and discussion
Chapter 5:	Conclusions

1.3 References

1. A. Espert, F. Vilaplana, S. Karlsson. Comparison of water absorption in natural cellulosic fibres from wood and one-year crops in polypropylene composites and its influence on their mechanical properties. Applied Science and Manufacturing 2004; 35:1267-1276. DOI: 10.1016/j.compositesa.2004.04.004.
2. R. Chandra, R. Rustgi. Biodegradable polymers. Progress in Polymer Science 1998; 33:1273-1335.
3. A. Sorrentino, G. Grrasi, V. Vittoria. Potential perspectives of bio-nanocomposites for food packaging applications. Trends in Food Science and Technology 2007; 18:84-95.
4. M.Q. Zhang, M.Z Rong, X. Lu. Fully biodegradable natural fibre composites from renewable resources: All-plant fibre composites. Composites Science and Technology 2005; 65:2514-2525. DOI: 10.1016/j.compscitech.2005.06.018.
5. Q-X. Zhang, Z-Z. Yu, X-L. Xie, K. Naito, Y. Kagawa. Preparation and crystalline morphology of biodegradable starch/clay nanocomposites. Polymer 2007; 48:7193-7200. DOI: 10.1016/j.polymer.2007.09.051.
6. N. Lucus, C. Bienaime, C. Belloy, M. Queneudec, F. Silvestre, J-F Nava-Saucedo. Polymer biodegradation: Mechanisms and estimation techniques. Chemosphere 2008; 73:429-442. DOI: 10.1016/j.chemosphere.2008.06.064.

7. D. Placketta, T.L. Andersenb, W.B. Pedersenc, L. Nielsenc. Biodegradable composites based on l-polylactide and jute fibres. Composites Science and Technology 2003; 63:1287–1296.
DOI: 10.1016/j.polymdegradstab.2008.02.018
8. H-S. Yang, J-S. Yoon, M-N. Kim. Dependence of biodegradability of plastics in compost on the shape of the specimen. Polymer Degradation and Stability 2005; 87:131-135.
DOI: 10.1016/j.polymdegradstab.2004.07.016
9. S. Mukhopadhyay, R. Srikanta. Effect of ageing of sisal fibre on properties of sisal-polypropylene composites. Polymer Degradation and Stability 2008; 93:2048-2051.
DOI:10.1016/j.polymdegradstab.2008.02.018.
10. K.L. Fung, X.S. Xing, R.K. Y. Li, S.C. Tjong, Y-W. Mai. An investigation on the processing of sisal fibre reinforced polypropylene composites. Composites Science and Technology 2003; 63:1255-1258.
DOI:10.1016/S0266-3538(03)00095-2
11. X. Lu, M.Q. Zhang, M. Z Rong, D. L. Yue, G. C. Yang. Environmental degradability of self-reinforced composites made from sisal. Composites Science and Technology 2004; 64:1301-1310.
DOI: 10.1016/j.compscitech.2003.10.013.
12. S. W. Lima, I.K. Junga, K. H. Leea, B. S Jinb. Structure and properties of biodegradable gluten/aliphatic polyester blends. European Polymer Journal 1999; 35:1875-1881.
13. R.A Gross, B. Kalra. Biodegradable polymers for the environment. Green Chemistry 2002; 297:803-807.
14. J.F. Mano, R.A. Sousa, L.F. Boesel, N.M. Neves, R.L. Reis. Bioinert, biodegradable and injectable polymeric matrix composites for hard tissue replacement: State of the art and recent developments. Composites Science and Technology 2004; 64:789-817.
DOI: 10.1016/j.compscitech.2004.09.001.
15. S. Mohanty, S.K. Nayak. Dynamic and steady state viscoelastic behavior and morphology of MAPP treated PP/Sisal composites. Materials Science and Engineering A 2007; 443:202-208.
DOI: 10.1016/j.msea.2006.08.053.

16. P.V. Joseph, K. Joseph, S. Thomas. Effect of processing variables on the mechanical properties of sisal-fibre-reinforced polypropylene composites. Composites Science and Technology 1999; 59:1625-1640.
PII: S0266-3538(99)00024-X.

17. K. Oksman, M. Skrifvars, J.–F. Selin. Natural fibres as reinforcement in polylactic acid (PLA) composites. Composites Science and Technology 2003; 63:1317-1324.
DOI: 10.1016/S0266-3538(03)00103-9.

18. M. Wollerdorfer, H. Bader. Influence of natural fibre on the mechanical properties of biodegradable polymers. Industrial Crops and Products 1998; 8:105-112.
PII: S0926-6690(97)10015-2

19. S. Houshyar, R.A. Shanks, A. Hodzic. Modelling of polypropylene fibre-matrix composites using finite element analysis. eXPRESS Polymer Letters 2009; 3:2-12.
DOI: 10.3144/expresspolymlett.2009.2

20. J. Gassan, A.K. Bledzki. The influence of fibre-surface treatment on the mechanical properties of jute-polypropylene composites. Composites Part A 1997; 28A:1001-1005.
PII: S1359-835X(97)00042-0.

21. M.J. John, S. Thomas. Biofibres and biocomposites review. Carbohydrate Polymers 2008; 71:343-364.
DOI: 10.1016/j.carbpol.2007.05.040.

22. S. Panthapulakkal, M. Sain. Studies on the water absorption properties of short hemp-glass fibre hybrid polypropylene composites. Journal of Composite Materials 2007; 41:1871-1882.
DOI: 10.1177/0021998307069900.

23. A.K. Rana, A. Mandal, S. Bandyopadhyay. Short jute fibre reinforced polypropylene composites: Effect of compatibiliser, impact modifier and fibre loading. Composites Science and Technology 2003; 63:801-806.
PII: S0266-3538(02)00267-1.

24. A. Bourmaud, S. Pimbert. Investigations on mechanical properties of poly(propylene) and poly(lactic acid) reinforced by miscanthus fibres. Composites: Part A 2008; 39:1444-1454.
DOI: 10.1016/j.compositesa.2008.05.023.

25. J. Gassan. A study of fibre and interface parameters affecting the fatigue behaviour of natural fibre composites. Composites: Part A 2002; 33:369-374.
PII: S1359-835X(01)00116-6.

26. P.V. Joseph, G Mathew, K. Joseph, S. Thomas, P. Pradeep. Mechanical properties of short sisal fibre-reinforced polypropylene composites: Comparison of experimental data with theoretical predictions. Journal of Applied Polymer Science 2003; 88:602-611.
DOI: 10.1002/app.11498.

27. Y. Li, Y–W. Mai, L. Ye. Sisal fibre and its composites: A review of recent developments. Composites Science and Technology 2000; 60:2037-2055.
PII: S0266-3538(00)00101-9.

28 C.U. Kiran, G.R. Reddy, B.M. Dabade, S. Rajesham. Tensile properties of sun hemp, banana and sisal fibre reinforced polyester composites. Reinforced Plastics and Composites 2007; 26:1043-1050.

29 L-T. Lim, R. Auras, M. Rubino. Processing technologies for poly(lactic acid). Progress in Polymer Science 2008; 33:820-852.
DOI: 10.1016/j.progpolymsci.2008.05.004.

30 M.L.D. Lorenzo. Crystallization behavior of poly(L-lactic acid). European Polymer Journal 2005; 41:569-575.
DOI: 10.1016/j.eurpolymj.2004.10.020.

31 K. Molnár, J. Móczó, M. Murariu, Ph. Dubois, B. Pukánszky. Factors affecting the properties of PLA/$CaSO_4$ composites: Homogeneity and interactions. eXPRESS Polymer Letters 2009; 3:49-61.
DOI: 10.3144/expresspolymlett.2009.8

32 A. Rothen-Weinhold, K. Besseghir, E. Vuaridel, E. Sublet, N. Oudry, F. Kudel, R. Gurny. Injection-molding versus extrusion as manufacturing technique for the preparation of biodegradation of biodegradable implants. European Journal of Biopharmaceutics 1999; 48:113-121.
PII: S0939-6411(99)00034-X.

33. A. Mathew, K. Oksman, M. Sain. Mechanical properties of biodegradable composites from poly(lactic acid) (PLA) and microcrystalline cellulose (MCC). Journal of Applied Polymer Science 2005; 97:2014-2025.

DOI: 10.1002/app.21779.

34. L. Petersson, I. Kvien, K. Oksman. Structure and thermal properties of poly(lactic acid)/ cellulose whiskers nanocomposites materials. Composites Science and Technology 2007; 67:2535-2544.
DOI: 10.1016/j.compscitech.2006.12.012.

35. A.P. Gupta, V. Kumar. New emerging trends in synthetic biodegradable polymers – Polylactide: A critique. European Polymer Journal 2007; 43:4053-4074.
DOI: 10.1016/j.eurpolymj.2007.06.045.

36. D. Puglia, A. Tomassucci, J.M. Kenny. Processing, properties and stability of biodegradable composites based on mater-Bi® and cellulose fibres. Polymers for Advanced Technologies 2003; 14:749-756.
DOI:10.1002/pat.390.

37. A. Iwatake, M. Nigo, H. Yano. Cellulose nanofibre-reinforced polylactic acid. Composites Science and Technology 2008; 68:2103-2106.
DOI: 10.1016/j.compscitech.2008.03.006.

38. A.K. Mohanty, A. Widowo, M. Misra, L.T. Drzal. Effect of process engineering on the performance of natural fibre reinforced cellulose acetate biocomposites. Composites: Part A 2004; 35:363-370.
DOI: 10.1016/j.compositesa.2003.09.015.

39. W. Liu, L.T. Drzal, A.K. Mohanty, M. Misra. Influence of processing methods and fibre length on physical properties of kenaf fibre reinforced soy based biocomposites. Composite: Part B 2007; 38:352-359.
DOI: 10.1016/j.compositesb.2006.05.003.

Chapter 2

Literature review

2.1 Introduction

This chapter consists of the literature review on the natural fibre classifications and properties, and natural fibre/polymer composites. A lot of research has been done on natural fibre/polymer composites. The literature review of the different publications is summarised under (i) natural fibre/polyolefin composites, and (ii) natural fibre/biodegradable polymer composites. Each of these sections are sub-divided into sub-sections covering the morphology where different morphological observations are reported, the mechanical properties where tensile properties are discussed. Thermal properties, including melt crystallization and thermal stability, are also discussed; thermo-mechanical behaviour in which dynamic mechanical properties are reviewed, as well as the biodegradability of the natural fibre/biopolymers is discussed.

2.2 Natural fibres: Classification and properties

Besides the environmental advantage of natural fibres, there are three parameters that are first to be determined and characterised. The stiffness and strength of fibres are the basis for the reinforcement, but also the interfacial strength (adhesion) is important for efficient reinforcement [1]. Natural fibres are subdivided based on their origin, coming from plants, animals or minerals. All plant fibres are composed of cellulose, while animal fibres consist of proteins (hair, silk, and wool). Plant fibres include bast (or stem) fibres, leaf or hard fibres, seed, fruit, wood, cereal straw, and other grass fibres [2-3]. These materials form inexpensive 'new resources', which could make them more valuable for wider utilization. They are easily renewable, environmentally friendly because of their biodegradability, low density, high specific mechanical performance [4-6]. When developing countries use such materials in composites, and produce them, they become part of the global composite industry as developer and manufacturer leading to increasing revenue and job creation [7]. Lignocellulosic fibres have some unique attributes, such as being less abrasive to tooling and not causing as many respiratory problems for workers [8].

Furthermore, because they have load-bearing potential, the use of natural fibre based composites has spread to various sectors, including aircraft, construction, grain and fruit storage and footwear. Natural fibres like jute, flax, hemp coir, and sisal have all been proved to be good reinforcement in thermoset and thermoplastic matrices, and are used in automotive applications, construction as well as packaging industries. [7,9,10]

2.2.1 Sisal fibre classification and properties

Sisal fibre is a hard fibre extracted from the leaves of the sisal plant (Agave Sisalana). It is one of the four most commonly used natural fibres, and almost accounts for half the total production of textile fibres. The reason for sisal fibre being the most used fibre is the ease of cultivation of sisal plants, which have short renewal times. Though native to tropical and sub-tropical North and South America, sisal fibre is now usually grown in tropical countries of Africa, the West Indies and the Far East. A sisal plant produces about 200-250 leaves and each leaf contains 1000-1200 fibre bundles, which is composed of 4% fibre, 0.75% cuticle, 8% dry matter, and 87.25% water. The cellulose and lignin contents of sisal vary from about 50 to 61% and 3 to 4%, respectively, depending on the plant age and origin. The sisal leaf contains three types of fibre: mechanical, ribbon, and xylem [11-12]. The mechanical fibres are mostly extracted from the border of the leaf. They have a generally thickened-horseshoe shape and hardly ever divide during the extraction processes. They are the most commercially useful part of the sisal fibre. Ribbon fibres occur in association with the conducting tissues in the median line of the leaf. Figure 2.1 shows a cross-section of the sisal leaf, which indicates where mechanical and ribbon fibres are obtained from, and a picture of the sisal plant. Xylem fibres have an irregular shape and occur opposite the ribbon fibres through the connection of vascular bundles as shown in Figure 2.2. They are composed of thin-walled cells and are therefore easily broken up and lost during the extraction process.

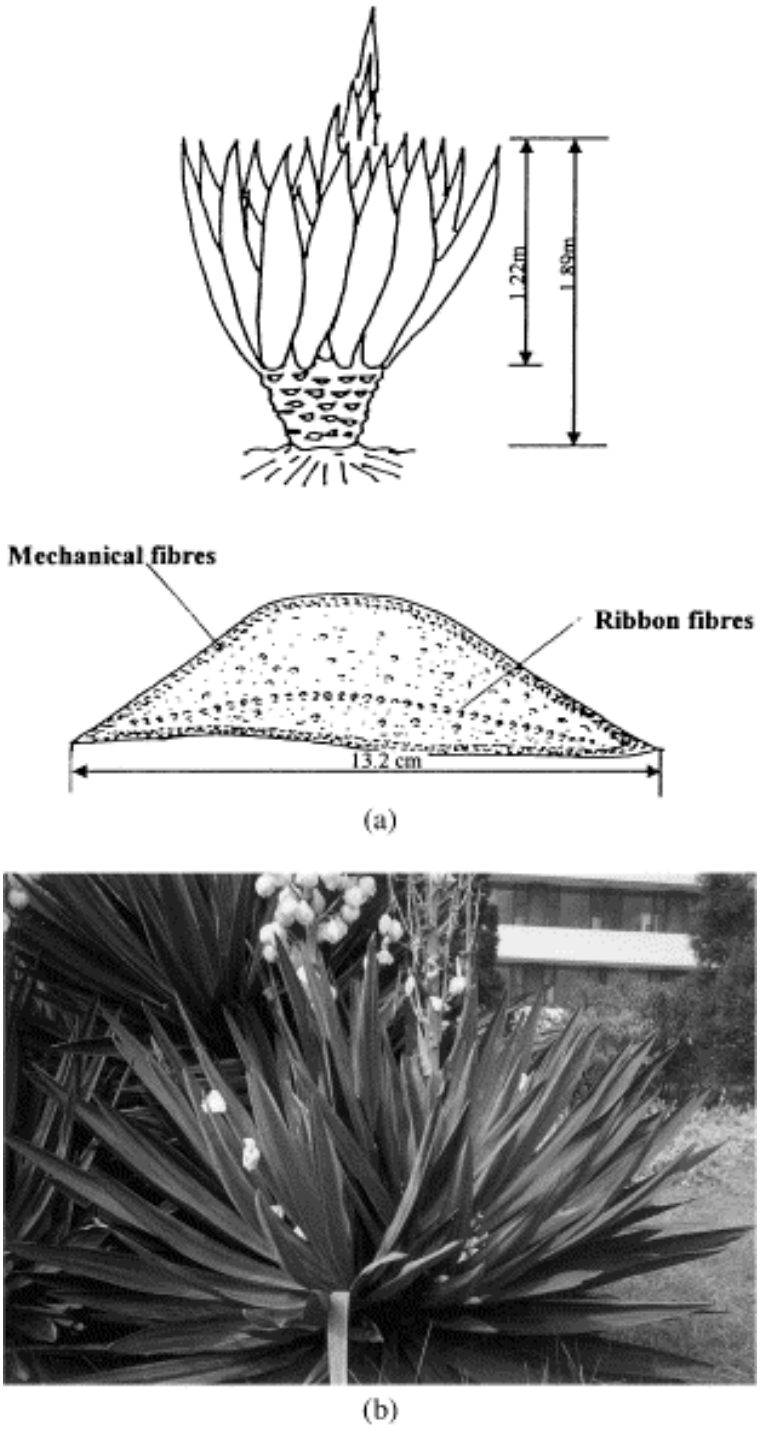

Figure 2.1 (a) Sketch of sisal plant and the cross-section of a sisal leaf; (b) Picture of a sisal plant. [11-12]

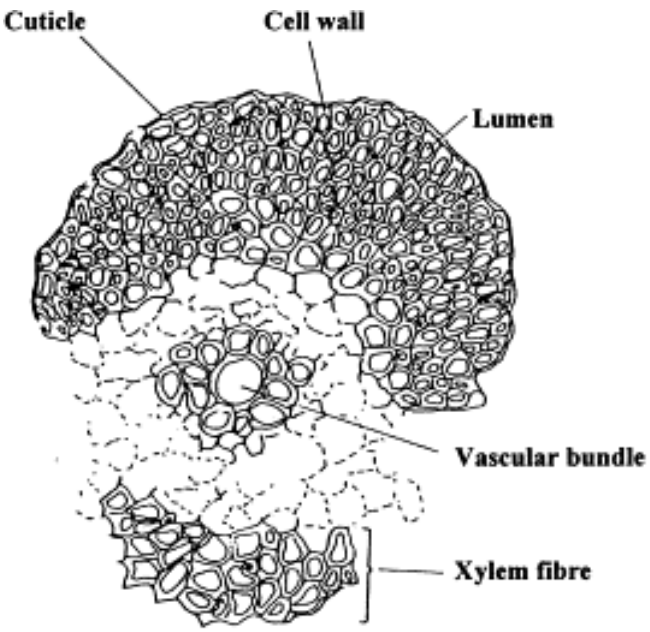

Figure 2.2 Cross-section of a ribbon-fibre bundle [11-12]

Generally the strength and stiffness of plant fibre depends on the cellulose content. Therefore the structure and properties of sisal fibre depends on the origin and the age of the fibre [12-13]. After cotton, these fibres have the highest production volume among natural fibres. Sisal fibre has also been used as reinforcement for composite materials due to its high strength, durability, and strain-to-failure. Some automotive components have already been produced using polymer matrix composites reinforced with sisal fibres [14]. The quality of a fibre reinforced composite depends considerably on the fibre–matrix interface, because only a well formed interface allows stress transfer from the matrix to the fibre. The extent of the adhesion between fibre and matrix can be described by the critical fibre length resulting from the balance of interface shear force, and normal force in the fibre. Sufficient adhesion, low fibre diameter and high tensile strength allow short critical fibre lengths [15-17]

2.3 Properties of polyolefin/natural fibre composites

Polyolefins are synthetic polymers of olefin monomers. They are the largest polymer family by volume of production and consumption. Polyolefins have enjoyed great success due to many application opportunities (automotive, packaging, medical, consumer products), relatively low cost, and wide range of properties. Classification of polyolefins can be based on their monomeric unit and chain structures. The ethylene based polyolefins include linear low density polyethylene (LLDPE), low density polyethylene (LDPE), high density polyethylene (HDPE) and ethylene vinyl acetate co-polymer (EVA), while polypropylene is classified atactic, syndiotactic or isotactic [18].

Polypropylene (PP) was the first synthetic polymer to achieve industrial importance due to its low cost, easy processability and excellent mechanical properties. The monomer propylene is a hydrocarbon gas mainly produced from petroleum refining. The polypropylene chain comprises a monomer with an asymmetric carbon atom at the C2 position, –CH2- CH(CH3)–, and hence the polymer may exist in three types (isotactic, syndiotactic and atactic) of molecular configurations depending upon the relative orientations of the methyl side groups [19]. Atactic polypropylene (APP) is a side product of polypropylene production. Because the structure of the polymer chain is not regular, APP is less resistant to chemical attack and weaker than other types of PP such as isotactic and syndiotactic PP. Thus, APP is an undesired and unemployed product in the petrochemical industry [20]. Both isotactic and syndiotactic forms have methyl groups situated regularly with respect to adjacent groups along the molecular chain, and have fibre-forming character due to their potential for creating order in the polymer structure. Currently, isotactic polypropylene is the most crystalline and main commercially available stereoisomer for use in oriented fibres, films and tapes [19]. Because of its wholly aliphatic hydrocarbon structure, polypropylene by itself burns very rapidly with a relatively smoke-free flame and without leaving a char residue. It has a high self-ignition temperature (570 ºC) and a rapid decomposition rate and hence has a high flammability [21]. PP possesses outstanding properties such as low density, good flex life, sterilisability, good surface hardness, very good abrasion resistance, and excellent electrical properties [22]. PP has been widely used in apparel, upholstery, floor coverings,

hygiene medical, geotextiles, car industry, automotive textiles, various home textiles, and wall-coverings [19].

Today synthetic polymers are combined with various reinforcing fillers in order to improve the mechanical properties and obtain the characteristics demanded in actual applications [23]. Natural fibres added as fillers to synthetic polymers reduce the product cost by replacing oil derived material with a cellulose-rich natural polymer. A further advantage is when the natural fibres act as reinforcement and improve the mechanical properties of the polymer matrix [24].

2.3.1 Morphology

Rahman *et al.* [23] investigated the effect of fibre loading on the mechanical properties and morphology of jute reinforced polypropylene, where raw, oxidized, and urotropine post-treated fibres were used. The composites were prepared by first mixing with a single screw extruder, followed by injection moulding of the materials. They reported an improvement in the fibre/matrix adhesion with oxidized fibre composites. The fibre/matrix adhesion was further improved by introducing urotropine in the composites, which was seen from the reduced agglomeration of the fibres. Botev *et al.* [25] reported a weak matrix-fibre interaction between polypropylene and basalt fibre. Their TEM pictures showed that the fibre surface was not covered with the polymer, and well defined holes of pulled-out fibres were observed. Bourmaud *et al.* [26] evaluated the mechanical properties of PP/reed fibre and PLLA/reed fibre composites. They also studied the influence of chemical modification of the matrix on the composites' mechanical properties by using maleic unhydride grafted polypropylene (PP-g-MA) and maleic anhydride grafted polylactic acid (PLA-g-MA). The materials were prepared using a twin screw extruder followed by injection moulding. Their SEM results showed weak interfacial bonding in the unmodified polymer composites, while the maleic anhydride (MA) modified composites showed improved fibre-matrix interaction.

Pimenta *et al.* [27] studied the mechanical properties of PP and maleic anhydride modified polypropylene (MAPP) composites with sisal fibre treated with sodium hydroxide (NaOH). Examination of the SEM results showed no major signs of fibre pull-out, which clearly indicated

a strong adhesion between the reinforcement and the matrix, showing that the MAPP coupling was effective. Untreated and water-treated fibres had diameters of approximately 100–200 μm, and the NaOH treated fibres had diameters around 10–20 μm. This decrease in fibre diameter was reported to be caused by the partial elimination of the lignin during NaOH treatment. Ichazo *et al*. [28] investigated the effect of different kinds of coupling agents and compatibilisers on the mechanical, morphological, and thermal properties of wood fibre (WF)-reinforced polypropylene, as well as its water absorption. They found that the functionalised PP and the use of silane improved the adhesion and dispersion of the particles. Alkali treatment was reported to only improve the dispersion of the WF particles, but not its adhesion to the polymer matrix. This was explained to be due to the better availability of OH groups in the particles' surfaces, which in turn favoured the water absorption and hence the composite swelling. Bledzki *et al.* [29] investigated the effect of fibre loading for abaca fibre reinforced composites with PP, and compared them with jute and flax reinforced PP composites, in terms of their mechanical properties, structural and odour emission properties. The samples were prepared by first mixing with an extruder, followed by injection moulding. Their SEM results showed good abaca fibre/PP adhesion, even though there were some debonding and fibre pull-outs of the untreated fibres. The interfacial interaction was improved further when the coupling agent MAPP was introduced. Therefore the debonding and pull-outs of fibres were reduced, which was an indication of better morphology.

2.3.2 Mechanical properties

Wambua *et al*. [30] evaluated several different natural fibre–polypropylene composites to determine if they had the ability to replace glass fibre–reinforced materials. Polypropylene with a very high melt flow index was used to help in fibre-matrix adhesion and to ensure proper wetting of the fibres. Samples were prepared with 40% fibre content of kenaf, coir, sisal, hemp, and jute. Tensile and impact tests were performed to compare the properties of these composites to those made with glass fibre. The tensile strengths all compared well with that of glass, except for the coir, but the only fibre giving comparable flexural strength was hemp. They showed with kenaf fibres that increasing the fibre weight fraction increased the ultimate strength, tensile modulus, and impact strength. However, the composites showed low impact strengths compared to glass

mat composites. This study demonstrated that natural fibre composites have a potential to replace glass in many applications that do not require very high load bearing capabilities.

Joseph *et al.* [31] studied the water absorption characteristics of sisal fibre/PP composites. Their work concentrated on the dependence of fibre loading and the influence of chemical treatment. They also investigated the effect of temperature on the water absorption phenomena. They reported that at 28 ºC the tensile strength of untreated sisal/PP composites with different fibre loadings decreased with increase in immersion time in water. The treated composites showed better tensile strength than the untreated composites, although both treated and untreated composites showed a decrease in tensile strength when they were immersed in boiling water for 7 h. Joseph and co-workers [15] also carried out a detailed investigation on sisal fibre reinforced polypropylene composites with special reference to the effect of fibre length, processing conditions, fibre loading and interfacial adhesion. A fibre length of 2 mm was found to be best for a good balance of properties in the case of melt mixed composites. Composites containing longitudinally oriented fibres showed better mechanical properties than those of transverse and random orientations. When the tensile properties of melt-mixed and solution-mixed composites were compared, the melt-mixed composites showed better properties than the solution-mixed composites.

Bourmaud *et al.* [26] investigated the tensile properties of their composites using nanoindentation. They reported an increase in tensile modulus of PP/reed fibre composites with increasing fibre and compatibilizer loading, and an increase in tensile modulus when mixing natural fibres into a PP matrix. These improvements were attributed to better dispersion of the fibre bundles in the PP matrix. The introduction of compatibiliser into the composites was reported to have improved the fibre/matrix interfacial interactions, resulting in a better morphology. Thus, because of the improved morphology, the mechanical properties were also improved. Karnani *et al.* [32] studied the mechanical properties of injection moulded samples of various MA modified and unmodified PP with silane treated kenaf fibre composites. A comparison was made between the mechanical properties of kenaf and sisal fibre reinforced composites. The addition of 20% untreated kenaf fibre into the polymer matrix gave rise to a significant increase in tensile modulus and stiffness of the composites without compatibilizer.

The compatibilized PP/kenaf composites were reported to exhibit greater tensile strength and elongation at break than the uncompatibilised composites or the neat PP. This was attributed to the increase in toughness of the composites after addition of MAPP. When compared with the sisal fibre reinforced PP composites, the kenaf fibre reinforced PP composites showed better mechanical properties for all the systems (modified and unmodified). The tensile strengths of kenaf reinforced composites were reported superior to that of sisal reinforced composites, but the impact strengths were poorer. This was attributed to the differences in the origins of these fibres.

Botev *et al.* [25] studied the suitability of untreated basalt fibres as reinforcing agents for polypropylene. The samples were prepared by melt mixing of the components, followed by pressing to make films. They reported that both the strain and stress at yield decreased after incorporation of the fibre in the PP matrix. In their case the lower yield stress was explained on the basis of poor adhesion between the polar basalt fibres and the non-polar PP. They further reported that a lack of interfacial bonds made efficient load transfer from the matrix to the fibres impossible. The fibres disturbed the continuity of the matrix instead of reinforcing it. The mechanical properties were improved after the incorporation of a maleic anhydride grafted polypropylene (PP-g-MA) coupling agent.

2.3.3 Thermal properties

2.3.3.1 Melting and crystalisation

Joseph *et al.* [33] studied the transcrystallisation and thermal behaviour of both chemically treated and untreated sisal fibre reinforced isotactic polypropylene. They reported that the addition of untreated sisal fibre to the PP matrix resulted in an increase in the crystallinity, crystallisation temperature (T_c), and enthalpy of crystallization as the fiber content increased. This behaviour was attributed to the nucleating ability of sisal fibre for the crystallisation of PP. The sisal fiber had a maginal effect on the melting temperature (T_m), and no correlation with fibre content was established. They further reported that the different treatments (permanganate ($KMnO_4$), MAPP, toluene-2,4-diisocyanate (TDI)) favoured both T_m and the T_c of the composites as they both increased. This was attributed to the compatibility between the fibre and the matrix

resulting in a better interaction after the chemical treatments. Rosa *et al.* [34] reported the same behaviour when studying the influence of rice-husk on the thermal and viscoelastic properties of PP composites, with and without coupling agent. The crystallization temperature (T_c) shifted to higher temperatures as the rice-husk content was increased (10, 20, 30 and 40 wt%). This increase in T_c was considered to be due to the nucleation by rice-husk, and was further explained as the fibres acting as sites for heterogeneous nucleation, thus inducing the crystallisation of the matrix. The presence of rice-husk had no effect on the melting temperature of PP. The addition of MAPP apparently had no effect on the thermal behaviour of PP and the composites.

Amash *et al.* [35] studied the morphology, thermal and viscoelastic behaviour of isotactic PP reinforced with two types of cellulose fillers (short- and micro-fibres). MAPP at low wt% was introduced as an interface modifier. The DSC results clearly showed that the addition of small amounts of cellulose fibres (both short and micro) into PP resulted in an increase in T_c of the polymer matrix. For the PP–microfibre composites this increase was significant. This was explained by the assumption that the cellulose fibres acted as efficient nucleating agents for the crystallization of PP. The addition of cellulose fibres into PP caused only a marginal effect on the melting temperature, and no correlation with the fibre content could be established. Ichazo *et al.* [28] reported that when treated and untreated WFs were added to PP, the crystallisation temperature (T_c) increased. Addition of maleic anhydride grafted PP into the PP/WF composites increased the T_c even further. The melting temperature of the PP did not change, neither with the addition of WF nor with the treatments.

2.3.3.2 Thermal stability

Joseph *et al.* [33] reported the TGA results of untreated and treated PP/sisal composites. Sisal fibre was found to have three degradation processes (60-200 ºC – dehydration as well as degradation of lignin, and cellulose decomposition around 350 ºC). The degradation of PP was reported to be around 398 ºC, and the addition of sisal fibre improved the thermal stability of PP. It was concluded that this increase in thermal stability was due to improved fibre/matrix interaction. Rosa and co-workers [34] studied the thermal stability of PP and PP/rice husk composites, and they reported similar results as Joseph and co-workers. The composites showed

two degradation steps: the first due to the husk degradation around 300 ºC, and the second due to the degradation of PP in the composites. The temperature of the maximum degradation rate of PP in the composite was reported to be higher than that of the neat PP. They suggested that the filler induced some kind of thermal stabilisation on the PP molecules. MAPP was reported not to have any effect on the temperature of maximum degradation rate of PP.

Mamun *et al.* [36] used enzymatic (fungamix) and a combination of enzymatic and chemical (natural digestion) methods to study the influence of abaca fibre reinforced polypropylene composites. It was assumed in the TGA results that the total moisture content (free and bonded) on the fibre was removed before 150 ºC. The weight at 150 ºC was considered as initial weight and the starting decomposition temperatures of the fibres were defined at 2% weight loss. The decomposition temperature of the fangamix treated fibres increased by 8 ºC, and that of the natural digestion treated fibre by 4 ºC. These increases in decomposition temperatures were reported to be due to the removal of smaller molecules from the fibre surface. Bledzki *et al.* [37] observed that the thermal stability improved with increasing degree of acetylation. They reported that the acetylated flax fibre showed the best thermal stability, which was the result of the removal of wax, lignin and hemicellulose from the fibre surface.

Canetti *et al*. [38] studied the effect of lignin, and its content, on the thermal degradation behaviour of PP/lignin blends in oxidative and inert atmospheres. The morphology and the supermolecular structure of the PP/lignin blends, prepared by melt mixing of the components, were also investigated. In general, the thermal degradation temperature and the char yield increased with an increase in the amount of lignin in the blend. The char is a carbon-based residue that undergoes slow oxidative degradation. The increase in char yield was more pronounced when the experiments were carried out in air, where the interactions between the PP and the charring lignin led to the formation of a protective surface shield able to reduce the oxygen diffusion towards the polymer bulk.

2.3.3.3 Thermo-mechanical properties

Dynamic mechanical analysis has been used by many researchers to investigate the morphological and viscoelastic properties of composites materials. The damping (tan δ) measurements give practical information on glass transitions (T_g) and other relaxations. The storage modulus determines the materials' stiffness. Yang *et al*. [39] studied the effect of lignocellulosic filler and a MAPP compatibilising agent on the thermal properties and viscoelastic behaviour of polypropylene bio-composites. They reported higher storage modulus (E') values for all the composites at all temperatures when compared to neat PP. The wood flour (WF) composites were stiffer than the rice-husk flour (RHF) composites because of the higher lignin and holocellulose content in WF. The increase in the E' values was apparently caused by the reinforcement effect of the lignocellulosic filler, which facilitated stress transfer across the interface from the PP to the filler. The damping (tan δ) characteristics of the composites were reported to decrease as the fibre loading was increased, while the incorporation of the natural filler did not significantly affect the glass transition temperature. The compatibilized composites showed more improved viscoelastic behaviour than the untreated composites because of improved interfacial adhesion, thereby lowering the molecular mobility in the interfacial region.

Huda *et al*. [40] evaluated the mechanical and thermo-mechanical properties of recycled newspaper cellulose fibre (RNCF)-reinforced PLA biocomposite materials, and they compared it to those of similarly prepared PP composites. The composites were micro-compounded and moulded, and had a cellulose content of 30 wt%. They found that the incorporation of the fibres gave rise to a considerable increase in the storage modulus and a decrease in the tan δ values for both PP and PLA. This was due to the reinforcement imparted by the cellulose fibres that allowed the stress transfer from the matrices to the fibre. Fung *et al.* [41] investigated injection moulded sisal fibre reinforced PP composites. The weak sisal fibre/PP interface was improved by PP maleation (MA-g-PP). A DMA evaluation of maleated and non-maleated composites was carried out. They found that the E' of PP increased in the presence of sisal fibre. The glass transition temperature (T_g) did not change as function of fibre loading. It was reported that the presence of MAPP in the composites showed a shift of the tan δ peak towards lower temperatures. This

decrease in T_g and was related to the stronger interfacial bonding between MAPP and the sisal fibre.

Amash and Zugenmaier [35], in their analysis of cellulose filler (CF) reinforced isotactic PP, found that the viscoelastic behaviour of PP was considerably affected by the presence of CFs. An increase in the storage modulus (E') and reduced damping values were observed with increasing fibre content. This was due to reinforcement effects and interfacial adhesion between fibres and matrix in the presence of MAPP. Mohanty *et al.* [42] did an extensive investigation into the viscoelastic behaviour of PP/sisal fibre composite melts, both in steady and dynamic modes. The variation of the linear viscoelastic properties of the composites at different angular frequencies was also investigated. The steady state viscosity of the composites increased with the incorporation of fibres. The composites treated with MAPP showed enhanced viscosity values due to improved fibre-matrix adhesion. All the composites exhibited pseudoplastic characteristics that can be represented by a power law equation. The swelling ratio of the PP decreased in the composites, but the dynamic properties (*G'*, *G''*, η^* and tan δ) increased with reinforcement. An investigation of the morphology of the extrudates revealed efficient fibre-matrix adhesion in the treated composites.

2.4 Properties of natural fibre composites with biodegradable polymers

Biodegradable polymers can be classified into four families. The first family is agro-polymers (e.g. polysaccharides) obtained from biomass by fractionation. The second and third families are polyesters, obtained by fermentation from biomass or from genetically modified plants (e.g. PHA, polyhydroxyalkanoate), and by synthesis from monomers obtained from biomass (e.g. PLA, polylactic acid). The fourth family is polyesters that are totally synthesized by a petrochemical process (e.g. PCL, polycaprolactone; PEA, polyesteramide; aliphatic or aromatic copolyesters). A large number of these biodegradable polymers (biopolymers) are commercially available. They show a range of properties, and they can compete with non-biodegradable polymers in different industrial fields. Polylactic acid (PLA) products are mainly in packaging, and it can be used in the production of plastic bags for household wastes, barriers for sanitary products and diapers, planting cups, disposable cups and plates. PLA also finds uses in other less

conventional applications, such as housing for laptop computers electronics. These days PLA composites can also be used in automotive industry to manufacture an interior headliner (interior ceiling) in automobiles [2,7,43-45]

Biodegradable plastics are becoming more important because environmental pollution by non-degradable plastics has assumed dangerous proportions, especially in the developing countries. Research efforts are currently focused on developing a new class of fully biodegradable 'green' composites. These are made by combining natural fibres with biodegradable matrices [2]. The prefix 'bio' can only be attractive if material costs are moderate and customer acceptance can be guaranteed. Therefore, biodegradable polymer composites or biocomposites which are in competition with PP equivalents should be processed the same way as PP. They should also be filled with comparable fibres, so that their properties will be evaluated comparatively. Biomaterials should also be processed with comparable processing techniques. For this purpose, the choice of tailor-made reinforcing fibres is of central importance [46-48]. Less work has been done to study composites with matrices which originate from renewable raw materials. There are many different polymers of renewable materials, for example poly(lactic acid), cellulose esters, poly(hydroxyl butyrates), starch and lignin based plastics. The problems with these polymers have been poor commercial availability, poor processability, low toughness, high price and low moisture stability. The long-term properties of renewable materials are also very important, especially if the products are not single use applications [49]. As these materials have limited mechanical properties for several applications, and an increase in tensile strength can be achieved by compounding them with fibres, provided that the fibres show a higher tensile strength and Young's modulus and a lower elongation than the matrix [17].

Poly(α-hydroxy acid) such as poly(glycolic acid), PGA, or poly(lactic acid), PLA, are crystalline polymers with a relatively high melting point [2]. Recently PLA has been highlighted because of its availability from renewable resources like corn. PLA is a biodegradable thermoplastic polymer with good mechanical properties. It is produced on a large scale from the fermentation of corn starch to lactic acid, and subsequent chemical polymerization. PLA can also be processed in the same way as polyolefins [50]. Possible applications of PLA include food packaging for meat and soft drinks, films for the agro-industry and non-wovens in hygienic products [51]. PLA

is a crystalline polymer with a relatively high melting point, and it is a hydrophobic polymer because of the incorporation of the CH_3 side groups. A viable method to improve the mechanical properties and reduce the overall cost of biodegradable plastics is to use natural fibres as reinforcements.

2.4.1 Morphology

Avella *et al.* [50] studied the interfacial adhesion of PLA/kenaf fibre composites with particular attention to the effect of compatibilisation on the composites. Their SEM pictures showed that the kenaf fibres were not wholly embedded into the PLA matrix in the uncompatibilised samples. The fibres were also strongly damaged and some de-bonding phenomena was observed for the uncompatibilised samples. This was apparently due to the poor fibre/matrix adhesion. An improvement in the interfacial adhesion was observed for the compatibilised samples. The fibres were welded into the PLA and the absence of voids indicated that no de-bonding phenomena occurred. The reactive compatibilisation allowed a significant improvement in fibre/matrix interfacial adhesion.

Huda *et al.* [52] observed different behaviour when they investigated the mechanical and thermo-mechanical properties of wood fibre reinforced PLA. They reported that there was good adhesion between the wood fibre and the PLA. The coupling agent MAPP had a negative effect on the morphology of the PLA/wood fibre composites. Graupner [53] assumed that lignin strengthens the bond between fibre and matrix. The author examined to what extent adding powdery lignin changes the mechanical properties of cotton fibre reinforced PLA. Kenaf/PLA composites were used as reference materials. The SEM analysis showed that adhesion between the fibre and matrix, as well as between the individual layers of the multilayer webs, could be improved by the presence of lignin. The untreated cotton/PLA composites showed clear delaminations of the individual layers of the multilayer web, but fewer delaminations were observed in the lignin-treated cotton/PLA. No delaminations were found in the kenaf/PLA composites.

2.4.2 Mechanical properties

Duigou *et al.* [54] studied the recyclability of flax/PLLA studied the recyclability of flax/PLLA, prepared through extrusion and injection moulding, and compare them with equivalent PP composites prepared in the same way. The Young's modulus of the flax/PLLA composites increased, but the stress at break was not enhanced by the reinforcement. The strain at failure decreased with increasing fibre content, which was caused by the poor fibre/matrix interaction and the low aspect ratio of the fibres due length reduction during the injection moulding process. Tao *et al.* [55] investigated the mechanical and thermal properties of ramie and jute fibre reinforced PLA composites prepared by using a two-roll mill followed by melt pressing. The neat PLA had a lower tensile strength than the composites. The increase in tensile strength was explained as being the result of stress transfer from the matrix to the strong fibre. However, when the amount of fibre was more than 30%, the tensile strength of the composites decreased to even lower values than that of neat PLA. This was because the dispersion of the fibre in the PLA matrix became bad. The tensile strength of the PLA/ramie composites was higher than that of the PLA/jute composites. Elongation at break of the PLA-based composites decreased compared to that of pure PLA, due to the bad dispersion of fibre in the matrix.

Huda *et al*. [40], in their investigation of recycled newspaper cellulose fibre (RNCF) reinforced PLA biocomposites, found that the presence of RNCF improved the tensile modulus of PLA. This indicated better stress transfer because of good interfacial adhesion between the polymer and the fibre. However, the tensile strength at break of the PLA was reduced by the incorporation of RNCF. Ochi [56] investigated the most suitable moulding conditions, as well as the mechanical and biodegradation properties of biodegradable composites using kenaf fibres as a reinforcement in PLA. They reported that the tensile strength of kenaf fibres decreased at 200 ºC. The tensile strength of kenaf fibres heat-treated at 180 ºC for 30 min was similar to that of the non-heat-treated fibres. At 160 ºC, the tensile strength of the heat-treated kenaf fibres did not decrease, even with longer heating times. Based on these results, the processing temperature for the fabricating of kenaf fibre-reinforced composites should be kept below 160 ºC, 60 min or 180 ºC, 30 min to prevent strength reduction due to thermal degradation.

2.4.3 Thermal properties

2.4.3.1 Melting and crystallization

Methew *et al.* [57] focused on the crystallisation of PLA in the presence of different cellulose-based reinforcements for heat treated and untreated samples (PLA, PLA/microcrystalline cellulose (MCC), PLA/cellulose fibers (CFs), and PLA/wood flour (WF)). Generally the glass transition temperatures (T_g) were higher for all fibre reinforced samples. This showed that the polymer relaxation was delayed due to the chain restriction as a result of increased crystallinity. The cold crystallization was reduced in the presence of fibres due to the nucleating ability of the reinforcement. Pilla *et al.* [58] investigated the effect of adding epoxy-based chain extender (CE) on the cell morphology and mechanical properties of solid and microcellular PLA. The chain extender clearly separated the PLA melting peaks into two. This double melting peak was attributed to the different crystalline morphologies obtained during the different crystallisation processes such as melt-crystallisation (from cooling) and cold crystallisation.

A study by Huda *et al*. [40] revealed the nucleation ability of the RNCF on PLA crystallization. An increase in the crystallization temperature with the introduction of the fibres was observed. The glass transition temperature and crystalline melting point of PLA did not change after reinforcement with RNCF. The crystallisation temperature of the RNCF-reinforced PLA composites decreased as compared to neat PLA, which signifies that the cellulose fibres hinder the migration and diffusion of PLA molecular chains to the surface of the nucleus in the composites. Misra *et al.* [59] investigated the properties and processing of recycled newspaper fibre as a possible reinforcement for 'green' composites. The crystallization enthalpy (ΔH_c), crystallization temperature (T_c), and melting enthalpy (ΔH_m) changed with the addition of cellulose fibres. T_g and T_m of the composites did not change significantly up to 30% fibre content. Though T_c for PLA matrix in the composites changed with increasing the cellulose content, ΔH_c remained nearly unchanged. These results suggest that cellulose fibres did not significantly affect the crystallization behaviour of PLA up to 30% cellulose content.

Duigou *et al.* [60] studied the mechanisms which govern the long-term durability of flax/PLLA composites in a marine environment. Two preparation methods were used, (injection moulding and film stacking). The sample used was 30/70 w/w flax fibre/PLLA in 60 L seawater at different temperatures (4, 20, 40, 60 and 80 ºC). They reported that the T_g of PLLA was hardly affected by the immersion, but that the melting enthalpy increased during the immersion at 20 and 40 ºC. The increase in ΔH_m was reported to be due to the crystallization phenomenon, but they also indicated that it might be an indication of degradation due to ageing. The T_g of the injection moulded samples were lower (by 3 ºC) than those of the film stacked samples, whereas their melting enthalpy were higher (by 18 J g^{-1}) after the immersion at 20 ºC. This suggested higher degradation for the injection moulded samples. They concluded that the influence of ageing was significant in the injection moulded samples. The ageing caused a decrease in the T_g of the samples, which was greater at higher water temperatures.

2.4.3.2 Thermal stability

Huda *et al.* [61] reported that there are three stages of degradation for wood fibre (WF) namely; cellulose, hemicellulose, and lignin. The degradation of neat PLA started at higher temperatures than that of WF, and the thermal stability of the PLA decreased with an increase in the WF content. This was concluded as an indication of the weak interfacial bonding, therefore, resulting in the weak compatibility between the fibre and the matrix.

Lee *et al.* [59] investigated the mechanical and thermal properties, chemical structure and morphology of PLA bio-composites as a function of kenaf fibre loading level and of silane coupling agent concentration. In all of their TGA curves they observed two main degradation regions. One was due to the thermal degradation of cellulose, hemicelluloses, and lignin in the kenaf fibre, and the other at higher temperature was attributed to the depolymerisation of the PLA. The onset of thermal decomposition of the bio-composites was slightly lower than that of pure PLA, indicating that introduction of the fibres reduced the thermal stability. However, the thermal stability of the silane treated bio-composites was slightly better than that of the untreated ones. The residual mass of the biocomposites increased when 5 pph of silane was used. Tao *et al.* [55], in their investigation of ramie/PLA and jute/PLA composites, observed that the composites

showed a lower degradation temperature than PLA. They reported that this might be due to the decrease of relative molecular mass of PLA as well as the effect of incorporation of the fibres. The explanation given by the authors for the decrease of the relative molecular mass seems not to be satisfactory, as the conditions which were used to prepare the neat polymer and the composites were the same. The effect of fibre in the degradation PLA matrix seems to be more reasonable.

2.4.3.3 Thermo-mechanical properties

The DMA results of RNCF reinforced PLA biocomposites showed that the incorporation of the fibres gave rise to a remarkable increase in the storage modulus, and a decrease in the tan δ values [40]. The RNCF-reinforced PLA composites also had better damping characteristics than neat PLA. The same authors investigated the influence of a coupling agent and processing parameters on the mechanical properties of wood-fibre/PLA composites [58]. The samples were prepared using a single screw extruder then followed by injection moulding. The incorporation of WF into PLA gave rise to a considerable increase in the storage modulus (E') and a decrease in the tan δ values. The addition of MAPP into the composites apparently reduced the E' of these composites. The DMA results of PLA/kenaf composites showed that both the storage modulus (E') and loss modulus (E") increased with fibre content [50]. The highest E' and E" improvements were recorded for the compatibilised composites. They also observed a pronounced decrease of the maximum value of the tan δ as a function to the fibre content and reactive compatibilisation. The temperature relative to the maximum of tan δ, which corresponds to the glass transition temperature (T_g), was also influenced by the reactive compatibilisation procedure. The decrease in T_g and the increase in E' and E" suggested that the compatibilisation procedure was able to promote better fibre-matrix adhesion.

Lee *et al.* [59], in their investigation of PLA/kenaf composites, observed that the glass transition shifted to higher temperatures and broadened upon the incorporation of the kenaf fibres. The E' values of the biocomposites were significantly higher than that of pure PLA over the whole temperature range. Treatment with 3-glycidoxypropyl trimethoxy silane (GPS) further enhanced the storage modulus values. The silane coupling agent was reported not to significantly affect the dynamic mechanical properties of the samples. PLA/cellulosic short-fibre biocomposites showed

higher storage modulus values than pure PLA [43]. The glass transition temperatures, derived from the loss modulus curves, slightly shifted to higher temperatures, which is an indication of restricted molecular movement because of better interaction between the fibre and the matrix.

2.4.4 Biodegradability of natural fibre/polylactic acid composites

Yang *et al.* [60] studied the biodegradation of plastics through laboratory-controlled composting, in order to investigate the effect of the surface area of the plastics on their biodegradability. They found that polypropylene (film and powder) can be safely used as a negative control for the biodegradation tests. No degradation was observed over a period of 45 days. The biodegradation of PLLA was very slow, and the profile of the accumulated amount of CO_2 was sigmoidal. The reason for this slow degradation was that PLLA must first be hydrolysed abiotically to low-molecular-weight substances [61]. Then the substance will be mineralized into CO_2 by microbes. Due to the fact that few microbes are able to directly degrade PLLA, the degradation was slow. The powder PLLA degraded faster than the film, and the film PLLA preserved its shape all through the biodegradation test.

Lee *et al*. [62] studied biocomposites with designable interfacial properties from biodegradable polymers. PLA and PBS were used as biodegradable polymers, and the reinforcement was bamboo fiber (BF). Lysine-diisocyanate (LDI) was used as a bio-based coupling agent. The weight of the samples decreased almost linearly with elapsed degradation time. The degradation of pure PLA was slower than that of all the composites, indicating that BF improved the degradation of the polymers. All composites treated with LDI coupling agent were more difficult to degrade than those without. The reason for this is that the improved interfacial adhesion between the polymer matrix and BF will reduce the area exposed to enzyme hydrolysis, resulting in a decreasing degradation rate. The composting for less than two weeks was reported [56] to have no effect on kenaf/PLA composites as no change was observed. The weight loss of kenaf/PLA composites rapidly increased (38 %) upon composting for four weeks. The results were reported to indicate the enzymatic degradation of the cellulosic chains in kenaf fibres degrades fibre strength. In addition, fibres and polymer that experienced a decrease in polymerisation degraded into water and carbon dioxide.

2.5 References

1. A.K. Mohanty, M. Misra, G. Hinrichsen. Biofibres, biodegradable polymers and biocomposites: An overview. Macromolecular Materials and Engineering 2000; 276/277:1-24.
   DOI:10.1002/(SICI)1439-2054(20000301)
2. M.J. John, S. Thomas. Biofibres and biocomposites. Carbohydrate Polymers 2008; 71:343-364.
   doi:10.1016/j.carbpol.2007.05.040
3. A.K. Bledzki, J. Gassan. Composites reinforced with cellulose based fibres. Progress in Polymer Science 1999; 24:221-274.
   PII: S0079-6700(98)00018-5
4. M.Q. Zhang, M.Z. Rong, X. Lu. Fully biodegradable natural fiber composites from renewable resources: All-plant fiber composites. Composites Science and Technology 2005; 65:2514-2525.
5. R.A. Shanks, A. Hodzic, D. Ridderhof. Composites of poly(lactic acid) with flax fibers modified by interstitial polymerization. Journal of Applied Polymer Science, 2006; 101:3620-3629.
6. K Joseph, R.D.T. Filho, B. James, S. Thomas, L.H. de Carvalho. A review on sisal fiber reinforced polymer composites. Revista Brasileira de Engenharia Agrícola e Ambiental, 1999; 3:367-379.
7. K.G. Satyanarayana, G.G.C. Arizaga, F. Wypych. Biodegradable composites based on lignocellulosic fibers - An overview. Progress in Polymer Science 2009; 34:982-1021. DOI:10.1016/j.progpolymsci.2008.12.002.
8. A. Espert, F. Vilaplana, S. Karlsson. Comparison of water absorption in natural cellulosic fibres from wood and one-year crops in polypropylene composites and its influence on their mechanical properties. Composites: Part A 2004; 35:1267-1276. DOI:10.1016/j.compositesa.2004.04.004.
9. A.K. Bledzki, A.A. Mamun, A. Jaszkiewicz, K. Erdmann. Polypropylene composites with enzyme modified abaca fibre. Composites Science and Technology 2010; 70:854-860.
   DOI:10.1016/j.compscitech.2010.02.003.

10. M. Zampaloni, F. Pourboghrat , S.A. Yankovich, B.N. Rodgers, J. Moore, L.T. Drzal, A.K. Mohanty, M. Misra. Kenaf natural fiber reinforced polypropylene composites: A discussion on manufacturing problems and solutions. Composites: Part A 2007; 38:1569-1580.
DOI:10.1016/j.compositesa.2007.01.001.
11. E. T. N. Bisanda, M.P. Ansell. Properties of sisal-CNSL composites. Journal of Materials Science 1992; 27:1690-1700.
12. Y. Li, Y-W. Mai, L. Ye. Sisal fibre and its composites: A review of recent developments. Composites Science and Technology 2000; 60:2037-2055.
PII: S0266-3538(00)00101-9.
13. S. Mishra, A. K. Mohanty, L.T. Drzal, M. Misra, G. Hinrichsen. A review on pineapple leaf fibers, sisal fibers and their biocomposites. Macromolecular Materials and Engineering 2004; 289:955-974.
14. F. de Andrade Silva, N. Chawla, R.D. de Toledo Filho. An experimental investigation of the fatigue behaviour of sisal fibers. Materials Science and Engineering A 2009; 516:90-95.
DOI:10.1016/j.msea.2009.03.026.
15. P.V. Joseph, K. Joseph, S. Thomas. Effect of processing variables on the mechanical properties of sisal-fibre-reinforced polypropylene composites. Composites Science and Technology 1999; 59:1625-1640.
PII: S0266-3538(99)00024-X.
16. S-Y. Fu, C-Y. Yue, X. Hu, Y-W. Mai. Analyses of the micromechanics of stress transfer in single- and multi-fiber pull-out tests. Composites Science and Technology 2000; 60:569-579.
17. M. Wollerdorfer, H. Bader. Influence of natural fibres on the mechanical properties of biodegradable polymers. Industrial Crops and Products 1998; 8:105-112.
PII: S0926-6690(97)10015-2.
18. D. Nwabunma. Overview of polyolefin composites. In: D. Nwabunma, T. Kyu (editors). Polyolefin Composites. John Willy and Sons, Inc. USA (2008) p.3-4.
19. S. Zhang, A.R. Horrocks. A review of flame retardant polypropylene fibres. Progress in Polymer Science 2003; 28:1517-1538.

DOI:10.1016/j.progpolymsci.2003.09.001.

20. L. Ballice, R. Reimert. Classification of volatile products from the temperature-programmed pyrolysis of polypropylene (PP), atactic-polypropylene (APP) and thermogravimetrically derived kinetics of pyrolysis. Chemical Engineering and Processing 2002; 41:289-296.
PII: S0255-2701(01)00144-1.

21. S. Mukhopadhyay, R. Srikanta. Effect of ageing of sisal fibres on properties of sisal-polypropylene composites. Polymer Degradation and Stability 2008; 93:2048-2051.
DOI:10.1016/j.polymdegradstab.2008.02.018.

22. A.J. Nuñez, P.C. Sturm, J.M. Kenny, M.I. Aranguren, N.E. Marcovich, M.M. Reboredo. Mechanical characterization of polypropylene–wood flour composites. Journal of Applied Polymer Science 2003; 88:1420-1428.

23. M.R. Rahman, M.M. Huque, M.N. Islam, M. Hasan. Improvement of physico-mechanical properties of jute fiber reinforced polypropylene composites by post-treatment. Composites: Part A 2008; 39:1739-1747.
DOI:10.1016/j.compositesa.2008.08.002.

24. N.M. White, M.P. Ansell. Straw-reinforced polyester composites. Journal of Materials Science 1983; 18:1549-1556.

25. M. Botev, H. Betchev, D. Bikiars, C. Panayiotou. Mechanical properties and viscoelastic behaviour of basalt fiber-reinforced polypropylene. Journal of Applied Polymer Science 1999; 74:523-531.
CCC 0021-8995/99/030523-09

26. A. Bourmaud, S. Pimbert. Investigations on mechanical properties of poly(propylene) and poly(lactic acid) reinforced by miscanthus fibers. Composites: Part A 2008; 39:1444-1454.
DOI:10.1016/j.compositesa.2008.05.023.

27. M.T.B. Pimenta, A.J.F. Carvalho, F. Vilaseca, J. Girones, J.P. López, P. Mutjé, A.A.S. Curvelo. Soda-treated sisal/polypropylene composites. Journal of Polymers and the Environment 2008; 16:35-39.
DOI: 10.1007/s10924-008-0080-0

28. M.N. Ichazo, C. Albano, J. González, R. Perera, M.V. Canal. Polypropylene/wood flour composites: Treatment and properties. Composite Structure 2001; 54:207-214.
PII: S0263-8223(01)00089-7.

29. A.K. Bledzki, A.A. Mamun, O. Faruk. Abaca fibre reinforced PP composites and comparison with jute and flax fibre PP composites. eXPRESS Polymer Letters 2007; 1: 755-762.
DOI: 10.3144/expresspolymlett.2007.104.

30. P. Wambua, J. Ivens, I. Verpoest. Natural fibres: Can they replace glass in fibre reinforced plastics? Composites Science and Technology 2003; 63:259-1264.
DOI:10.1016/S0266-3538(03)00096-4.

31. P.V Joseph, M.S. Rabello, L.H.C. Mattoso, K. Joseph, S. Thomas. Environmental effect on the degradation behaviour of sisal fibre reinforced polypropylene composites. Composites Science and Technology 2002; 62:1357-1372.
PII: S0266-3538(02)00080-5.

32. R. Karnani, M. Krishnan, R. Narayan. Biofiber-reinforced polypropylene composites. Polymer Engineering and Science 1997; 37:476-483.

33. P.V. Joseph, K. Joseph, S. Thomas, C.K.S. Pillai, V.S. Prasad, G. Groeninckx, M. Sarkissova. The thermal and crystallization studies of short sisal fibre reinforced polypropylene composites. Composites: Part A 2003; 34:253-266.
PII: S1359-835X(02)00185-9.

34. S.M.L. Rosa, S.M.B. Nachtigall, C.A. Ferreira. Thermal and dynamic-mechanical characterization of rice-husk filled polypropylene composites. Macromolecular Research 2009; 1:8-13.

35. A. Amash, P. Zugenmaier. Morphology and properties of isotropic and oriented samples of cellulose fibre-polypropylene composites. Polymer 2000; 41:1589-1596.
PII: S0032-3861(99)00273-6.

36. A.K. Bledzki, A.A. Mamun, A. Jaszkiewicz, K. Erdmann. Polypropylene composites with enzyme modified abaca fibre. Composites Science and Technology 2010; 70:854-860.
DOI:10.1016/j.compscitech.2010.02.003.

37. A. K. Bledzki, A. A. Mamun1, M. Lucka-Gabor, V. S. Gutowski. The effects of acetylation on properties of flax fibre and its polypropylene composites. eXPRESS Polymer Letters 2008; 1:413–422.
DOI: 10.3144/expresspolymlett.2008.50.

38. M. Canetti, F. Bertini, A. De Chirico, G. Audisio. Thermal degradation behaviour of isotactic polypropylene blended with lignin. Polymer Degradation and Stability 2006; 91:494-498.
DOI:10.1016/j.polymdegradstab.2005.01.052.

39. H-S. Yang, D.J. Gardner, H-J. Kim. Viscoelastic and thermal analysis of lignocellulosic material filled polypropylene bio-composites. Journal of Thermal Analysis and Calorimetry 2009; 98:553-558.
DOI 10.1007/s10973-009-0324-9.

40. M.S. Huda, L.T. Drzal, M. Misra. A study on biocomposites from recycled newspaper fiber and poly(lactic acid). Industrial & Engineering Chemistry Research 2005**;** 44:5593-5601.
DOI**:** 10.1021/ie0488849.

41. K.L. Fung, R.K.Y. Li, S.C. Tjong. Interface modification on the properties of sisal fiber-reinforced polypropylene composites. Journal of Applied Polymer Science 2002; 85:169–176.

42. S. Mohanty, S.K. Nayak. Dynamic and steady state viscoelastic behaviour and morphology of MAPP treated PP/sisal composites. Materials Science and Engineering A 2007; 443: 202–208.
DOI:10.1016/j.msea.2006.08.053.

43. A.P. Mathew, K. Oksman, M. Sain. Mechanical properties of biodegradable composites from poly lactic acid (PLA) and microcrystalline cellulose (MCC). Journal of Applied Polymer Science 2005; 97:2014-2025.
DOI: 10.1002/app.21779.

44. L-T. Lim, R. Auras, M. Rubino. Processing techniques for poly(lactic acid). Progress in Polymer Science 2008; 33:820:852.
DOI: 10.1016/j.progpolymsci.2008.05.004.

45. B-H. Lee, H-S. Kim, S. Lee, H-J. Kim, J.R. Dorgan. Bio-composites of kenaf fibers in polylactide: Role of improved interfacial adhesion in the carding process. Composites Science and Technology 2009; 69:2573-2579.
DOI:10.1016/j.compscitech.2009.07.015.

46. A.K. Bledzki, A. Jaszkiewicz, D. Scherzer. Mechanical properties of PLA composites with man-made cellulose and abaca fibres. Composites: Part A 2009; 40:404–412.
DOI:10.1016/j.compositesa.2009.01.002.

47. R. Mani, M. Bhattacharya. Properties of injection moulded blends of starch and modified biodegradable polyesters. European Polymer Journal 2001; 37:515-526.
PII: S0 01 4 -3 05 7 (00)0 0 15 5 -5.

48. A.K. Bledzki, A. Jaszkiewicz. Mechanical performance of biocomposites based on PLA and PHBV reinforced with natural fibres - A comparative study to PP. Composites Science and Technology 2010; 70:1687-1696.
DOI:10.1016/j.compscitech.2010.06.005.

49. K. Oksman, M. Skrifvarsb, J.-F. Selinc. Natural fibres as reinforcement in polylactic acid (PLA) composites. Composites Science and Technology 2003; 63:1317-1324.
DOI:10.1016/S0266-3538(03)00103-9.

50. M. Avella, G. Bogoeva-Gaceva, A. Bežarovska, M.E. Errico, G. Gentile, A. Grozdanov. Poly(lactic acid)-based biocomposites reinforced with kenaf fibers. Journal of Applied Polymer Science 2008; 108:3542-3551.
DOI: 10.1002/app.28004.

51. S. Jacobsen, H-G. Fritz , P. Degée, P. Dubois ,R. Jérôme. New developments on the ring opening polymerisation of polylactide. Industrial Crops and Products 2000; 11:265-275.
PII: S0926-6690(99)00053-9.

52. M.S. Huda, L.T. Drzal, A.K. Mohanty, M. Misra. Wood fiber reinforced poly(lactic acid) composites. 5th Annual SPE Automotive Composites Conference, Troy, Michigan, 12-14 September 2005.

53. N. Graupner. Application of lignin as natural adhesion promoter in cotton fibre-reinforced poly(lactic acid) (PLA) composites. Journal of Materials Science 2008; 43:5222–5229.
DOI 10.1007/s10853-008-2762-3.

54. A.L. Duigou, I. Pillin, A. Bourmaud, P. Davies, C. Baley. Effect of recycling on mechanical behaviour of biocompostable flax/poly(L-lactide) composites. Composites: Part A 2008; 39:1471-1478.
DOI: 10.1016/j.compositesa.2008.05.008.

55. Y. Tao, L. Yan, R. Jie. Preparation and properties of short natural fiber reinforced poly(lactic acid) composites. Transactions of Nonferrous Metals Society of China 2009; 19:651-655.

56. S. Ochi. Mechanical properties of kenaf fibers and kenaf/PLA composites. Mechanics of Materials 2008; 40:446–452.
DOI:10.1016/j.mechmat.2007.10.006.

57. A.P. Mathew, K. Oksman, M. Sain. The effect of morphology and chemical characteristics of cellulose reinforcements on the crystallinity of polylactic acid. Journal of Applied Polymer Science 2006; 101:300-310.
DOI: 10.1002/app.23346.

58. S. Pilla, A. Kramschuster, L. Yang, J. Lee, S. Gong, L-S. Turng. Microcellular injection-molding of polylactide with chain-extender. Materials Science and Engineering C 2009; 29:1258-1265.
DOI: 10.1016/j.msec.2008.10.027.

59. M.S. Huda, A.K. Mohanty, L.T. Drzal, E. Schut, M. Misra. "Green" composites from recycled cellulose and poly(lactic acid): Physico-mechanical and morphological properties evaluation. Journal of Materials Science 2005; 40:4221 – 4229.

60. A. Le Duigou, P. Davies, C. Baley. Seawater ageing of flax/poly(lactic acid) biocomposites. Polymer Degradation and Stability 2009; 94:1151–1162.
DOI:10.1016/j.polymdegradstab.2009.03.025.

61. M.S. Huda, L.T. Drzal, M. Misra, A.K. Mohanty. Wood-fiber-reinforced poly(lactic acid) composites: Evaluation of the physicomechanical and morphological properties. Journal of Applied Polymer Science 2006; 102:4856–4869.
DOI 10.1002/app.24829.

62. H-S. Yang, J-S. Yoon, M-N. Kim. Dependence of biodegradability of plastics in compost on the shape of specimens. Polymer Degradation and Stability 2005; 87:131-135. DOI:10.1016/j.polymdegradstab.2004.07.016.

63. J. George, M.S. Sreekala, S. Thomas. A review on interface modification and characterization of natural fiber reinforced plastic composites. Polymer Engineering and Science 2001; 41(9):1471-1485

64. N. Lucas, C. Bienaime, C. Belloy, M. Queneudec, F. Silvestre, J-E. Nava-Saucedo. Polymer biodegradation: Mechanisms and estimation techniques. Chemosphere 2008; 73:429–442.
DOIO:10.1016/j.chemosphere.2008.06.064.

65. S-H. Lee, S. Wang. Biodegradable polymers/bamboo fiber biocomposite with bio-based coupling agent. Composites: Part A 2006; 37: 80–91.
DOI:10.1016/j.compositesa.2005.04.015

Chapter 3

Experimental

3.1 Materials

3.1.1 Sisal fibre

Agave sisalana (sisal) fibre was obtained from the National Sisal Marketing Committee in Pietermaritzburg, South Africa. It has a diameter range of 100–300 μm, average tensile strength of 490 MPa, average modulus of 11350 MPa, and elongation at break of 5%.

3.1.2 Polylactic acid (PLA)

PLA (Polylactide) polymer 3051D was supplied by Nature-Works LLC in Europe. The density of the PLA was 1.25 g cm^{-3}, MFI (210 ºC / 2.16 kg) of 10-25 g/10 min, relative viscosity of 3.0-3.5, crystalline melting temperature of 150-165 ºC, glass transition temperature of 55-65 ºC, tensile strength at yield of 48 MPa, and tensile elongation at yield of 2.5%.

3.1.3 Polypropylene (PP)

Polypropylene TIPPLENE H 116F homopolymer was supplied by the Tiszai Chemical Group Plc in Hungary as opaque crystalline pellets. This is a high melt flow polymer that was designed for fibres from medium to high spin speeds, as well as offer good homogeneity, stable extrusion and excellent processability. It has the following properties: tensile strength at yield of 34.5 MPa, MFI (230 ºC / 2.16 kg) of 25 g/10 min, and tensile elongation at yield of 10%.

3.2 Methods

3.2.1 Preparation of composites

Two sample preparation methods were used, in each method the sisal was cut into 5 mm long fibres, and dried in an oven at 130 for six hours to eliminate moisture absorbed. The PLA was also dried in an oven at 85 ºC for six hours before it could be used. PP was used directly from the bag without drying. In the first method both the PLA and PP composites were prepared using a Brabender PLASTICORDER PL 2100 extruder at 205 ºC at the sisal fibre content of 2, 4 and 6 wt%. The granulated samples were injection moulded at the same temperature of 205 ºC.

In the second method the PLA and PP composites with sisal fibre content of 1-3 wt% were extruded at 190 ºC. After the extrusion PLA/sisal granulated composites were placed in the oven at 120 ºC for three hours to recrystallize. After the annealing process the PLA samples were dried in the oven at 85 ºC followed by injection moulding at 190 ºC. The PP and its composites were injection moulded immediately after they were pelletized. Table 3.1 lists the compositions of the samples prepared. An Arburg 320C Allrounder 600-250 injection moulder was used to prepare 2 mm thick and 80 x 80 mm flat sheet samples, and the injection moulding parameters were as follows:

Injection volume	50 cm^3
Swith-over point	12 cm^3
Injection pressure	600-700-740 bars (1-2-3 wt% sisal content)
Holding pressure	600 bars
Holding time	20 s
Cooling time	30 s
Back pressure	30 bar
Melt temperature	190 ºC/205
Mould temperature	20 ºC

Table 3.1 Compositions of the investigated samples

PLA/sisal (205 ºC)	PP/sisal (205 ºC)	PLA/Sisal (190 ºC)	PP/Sisal (190 ºC)
100/0	100/0	100/0	100/0
98/2	98/2	99/1	99/1
96/4	96/4	98/2	98/2
94/6	94/6	97/3	97/3

3.2.2 Optical microscopy (OM)

The optical microscope is a primary tool for phase identification. It enlarges an image by sending a ray of light through the object, the condenser lens focuses the light on the sample and the objective lens magnifies the ray, which contains the image to the projector lens so that the image can be viewed by the observer [1-2].

A CETI (Belgium) optical microscope was used to study the fibre dispersion in the polymers, and a 10x magnification was used for each composition.

3.2.3 Scanning electron microscopy (SEM)

The scanning electron microscope is an instrument that produces a largely magnified image that uses electrons instead of light to form an image. A beam of electrons is produced at the top of the microscope by an electron gun. The electron beam follows a vertical path through the microscope, which is held in a vacuum. The beam travels through electromagnetic fields and lenses, which focus the beam down toward the sample. Once the beam hits the sample, electrons and X-rays are ejected from the sample. Detectors collect these X-rays, backscattered electrons, and secondary electrons and convert them into a signal that is sent to a monitor screen, producing the final image [2].

A Shimadzu ZU SSX-550 Superscan scanning electron microscope was used to study the fracture surfaces of the samples. The samples were dipped in liquid nitrogen, broken using tweezers, and

one broken piece was mounted on an aluminium SEM sample holder with glue. The mounted samples were sputter coated with gold, under an argon gas flow for 20 minutes. The coated samples were left to dry at room temperature for two hours before SEM could be performed. The SEM analyses were done at 15 kV and at magnifications of 50, 100, 250 and 300x.

3.2.4 Fourier transform infrared spectroscopy (FTIR)

FTIR spectroscopy is a technique that provides information about the chemical bonding or molecular structure of materials; determines the amount of components in the mixture, and whether they are organic or inorganic. It is mostly used to characterize organic materials. The technique works on the fact that bonds and groups of bonds vibrate at characteristic frequencies. A molecule that is exposed to infrared rays absorbs infrared energy at frequencies that are characteristic to that molecule.

Attenuated total reflectance Fourier-transform infrared (ATR-FTIR) spectroscopy is a technique used for analysis of the surfaces of materials. It is suitable for the characterization of materials which are either too thick or too strongly absorbing to be analyzed by transmission infrared spectroscopy. ATR is commonly used to analyze solids, gases, and liquids. When an IR beam travels from a medium of high reflective index (e.g. diamond crystal) to a medium of low reflective index (sample), some amount of light is reflected back to the sample, and this results in the IR spectrum of the sample.

FTIR-microscope is in principle the same as most optical microscopes. The IR radiation from the spectrometer is directed onto the sample through the series of mirrors and lenses. The light emerging from the sample is channeled into a detector, and then the picture of the sample is viewed on the screen [3-5].

A Perkin-Elmer Spectrum 100 FTIR spectroscope fitted with a PIKE Miracle$_{TM}$ ATR, equipped with a diamond crystal, and a Perkin Elmer Multiscope FTIR microscope was used to study the chemical bonding and molecular structure of the composites and polymers. The IR spectra were

recorded between 4000 and 650 cm^{-1} at a resolution of 8 cm^{-1}. A clean, empty diamond crystal was used for the collection of background spectrum.

3.2.5 Differential scanning calorimetry (DSC)

DSC is a technique used to study the thermal transitions of a material during heating or cooling. A thermal transition is the process whereby changes like glass transitions, melting, or crystallization occur when the sample or material is heated or cooled at a controlled rate. A differential scanning calorimeter consists of two compartments, the control side which contains an empty aliminium pan, and the sample side with contains an aluminium pan with a sample (5-10 mg). The DSC has to be calibrated before the samples can be run. Zinc and indium are calibration standards with known onset temperatures and enthalpies of melting. Glass transition temperature, melting temperatures and crystallization temperatures are some of the thermal transitions that can be observed by DSC [6-7].

A Perkin-Elmer DSC 7 differential scanning calorimeter from Waltham, Massachusetts, USA was the DSC instrument used to characterize the samples. The instrument was computer controlled and the calculations were performed using Pyris software. All the analyses were performed under nitrogen flow (20 ml min^{-1}). The onset temperatures of melting of zinc (419.5 ºC), and indium (156.7 ºC) standards, together with the melting enthalpy of indium (28.4 J g^{-1}), were used for the calibration of the DSC instrument. The PP samples (5-10 mg) were analysed from 25 to 180 ºC at a rate of 10 ºC min^{-1}, while the PLA samples were analysed from 25 to 160 ºC at the same rate. The samples were heated, cooled, and reheated under the same conditions mentioned above. Three samples from each composition were analysed. Only the second heating scan was used to determine the melting enthalpies and temperatures. The crystallization enthalpies and temperatures were determined from the first cooling scan.

3.2.6 Thermogravimetric analysis (TGA)

TGA is a technique mainly used to characterize the thermal stability, decomposition, and degradation of materials under controlled conditions. TGA utilizes a highly sensitive

microbalance and a quick response furnace. The balance is located above the furnace and is thermally isolated from the furnace. A precision hang-down wire is suspended from the balance into the furnace. At the end of the hang-down wire is the sample pan, and its position in the furnace should be extremely reproducible. The data is recorded as a TGA curve of mass % or mass as a function of time or temperature. Calibration of the machine is very important as it gives correct onset temperature positions of the materials within a five percent error [6,8]. TGA can be calibrated using Curie point standard materials.

The TGA analyses were carried out in a Perkin-Elmer TGA7 thermogravimetric analyzer, from Waltham, Massachusetts, U.S.A. Nitrogen was used as the purge gas at the rate of 20 mL min^{-1}. The samples (5-10 mg) were heated from 30 to 600 ºC at a rate of 10 ºC min^{-1}. The TGA instrument was computer controlled and the calculations performed on the curves were done using Pyris software.

3.2.7 Dynamic mechanical analysis (DMA)

DMA is a technique used to determine changes in sample properties resulting from changes in five experimental variables: temperature, time, frequency, force, and strain. DMA applies a small sinusoidal stress or strain to the sample and causes a sinusoidal deformation of the sample. The resulting stress or strain response is measured. The DMA analyses samples that can be in bulk solid, film, fibre, gel, or viscous liquid form. Interchangeable clamps are employed to allow the measurement of many properties including modulus, damping, creep, stress relaxation, glass transitions, and softening points. It is particularly useful for measuring transitions in polymers that cannot be detected by other techniques like DSC [9-13].

A Perkin-Elmer Diamond DMA was used in determining the thermo-mechanical properties of all the samples. The samples, with the dimensions 50 x 12 x 1 mm, were analysed in the bending mode and the parameters were as follows:

Start temperature	-60 ºC
Limit temperature	170 ºC
Rate	5 ºC min^{-1}
L amplitude	10 um
Minimum tension	300 mN
Tension force gain	1.5
Frequency	1 Hz
Force amplitude default value	1000 mN

3.2.8 Tensile testing

A tensile test is a fundamental mechanical test where a carefully prepared specimen is loaded in a controlled manner while measuring the applied load and the elongation of the specimen over some distance. Tensile tests are used to determine the modulus of elasticity, elastic limit, elongation, proportional limit, and reduction in area, tensile strength, yield point, yield strength and other tensile properties. The main product of a tensile test is a load *versus* elongation curve which is then converted into a stress *versus* strain curve [13-14].

A Hounsfield H5KS universal tensile testing machine was used to analyse the composites, and dumbbell shaped samples were tested. The gauge length was 35 mm, and the extension speed 5 mm min^{-1}. At least six samples were tested for each composition, and the results are presented as an average for tested samples. Figure 3.1 illustrates a typical sample used for tensile testing.

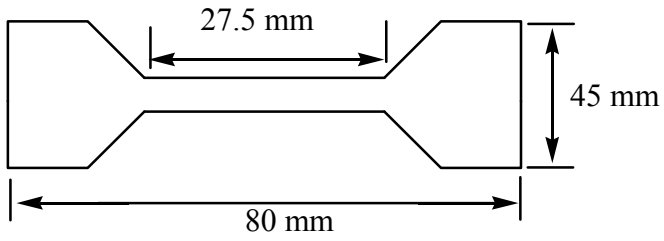

Figure 3.1 Dumbbell shape sample dimensions for tensile testing

3.2.9 Biodegradation test

The biodegradability of the samples was tested by cutting five pieces (10 x 10 x 2 mm) from each composition. The samples were dried in the oven at 80 for 4 hours and each sample's mass was recorded, and they were placed in labeled vials. All the vials were filled with distilled water, sealed, and placed in an oven at 80 ºC for 10 days. After every 2 days one of the five samples for each composition was removed and rinsed with distilled water. The rinsed samples were then dried in an oven at 80 ºC for 2 days and the mass was recorded. The SEM analyses of the 'degraded' samples were carried out. The biodegradation was monitored by observing the physical change and by monitoring the differences in mass of the specimens. Equation 3.1 was used to calculate the mass remaining after immersion in water for 10 days. W_0 is the weight of the sample before immersion, W_i is the weight of the sample after immersion, and W_{loss} (%) is the percentage weight loss after immersion.

$$W_{loss}(\%) = W_0 - W_i / W_0 * 100 \qquad (3.1)$$

3.3 References

1. T. Euler, S.E. Hausselt, D.J. Margolis, T. Breuninger, X. Castell, P.B. Detwiler, W. Denk. Eyecup scope-optical recordings of light stimulus-evoked fluorescence signals in the retina. Pflugers Archiv European Journal of Physiology 2009; 457:1393-1414.
   DOI 10.1007/s00424-008-0603-5.
2. K.J. Van Den Berg, M. Daudin, I. Joosten, B. Wei, R. Morrison, A. Burstoek. A composition of a light microscopy techniques with scanning electron microscopy for imaging the surface cleaning of paintings. 9th International Conference on NDT of Art, Jerusalem, Israel, 25-30 May 2008.
3. B.C. Smith. Fundamentals of Fourier Transform Infrared Spectroscopy. CRC Press: Boca Raton, Florida (1996).
4. J. Schmitt, H-C. Flemming. FTIR-spectroscopy in microbial and material analysis. International Biodeterioration & Biodegradation 1998; 41:1-11.
   PII: SO964-8305(97)00067-X.

5. A. Subramanian, J. Ahn, V.M. Balasubramaniam, L. Roudriguez-Saona. Determination of spore inactivation during thermal and pressure-assisted thermal processing using FT-IR specroscopy. Journal of Agricultural and Food Chemistry 2006; 54:10300-10306.
DOI**:** 10.1021/jf0622174.
6. P.J. Haines. Thermal Methods of Analysis: Principles, Applications and Problems. Blackie Academic and Professional: London (1995).
7. V.J. Griffin, P.G. Laye. Differential thermal analysis and differential scanning calorimetry. In: E.L. Charstey and S.B. Warrington. Thermal analysis – Techniques & Applications. Royal Society of Chemistry: Cambridge (1992).
8. D. Dollimore. Thermogravimetry. In: E.L. Charstey and S.B. Warrington. Thermal Analysis – Techniques & Applications. Royal Society of Chemistry: Cambridge (1992).
9. M. Reading. Thermomechanical analysis and dynamic mechanical analysis. In: E.L. Charstey and S.B. Warrington. Thermal analysis – Techniques & Applications. Royal Society of Chemistry: Cambridge (1992).
10. A.B. Bashaiwoldu, F. Podczeck, J.M. Newton. Application of dynamic mechanical analysis (DMA) to the determination of the mechanical properties of coated pellets. International Journal of Pharmaceutics 2004; 274:53-63.
DOI:10.1016/j.ijpharm.2003.09.028
11. F. Oulevey, N.A. Burnham, G. Gremaud, A.J. Kulek, H.M. Pollock, A. Hammiche, M. Reading, M. Song, D.J. Hourston. Dynamic mechanical analysis at the submicron scale. Polymer 2000; 41:3087-3092.
PII: S0032-3861(99)00601-1
12. A.B. Bashaiwoldu, F. Podczeck, J.M. Newton. Application of dynamic mechanical analysis (DMA) to determine the mechanical properties of pellets. International Journal of Pharmaceutics 2004; 269:329-342.
DOI:10.1016/j.ijpharm.2003.12.030.
13. N. Aldred, T. Wills, D.N. Williams, A.S Clare. Tensile and dynamic mechanical analysis of the distal portion of mussel (Mytilus edulis) byssal threads. Journal of the Royal Society Interface 2007; 4:1159-1167.
DOI: 10.1098/rsif.2007.1026.

14. A. Naranjo, M. del Pilar Noriega, T. Osswald, A. Roldán-Alzate, J.D. Sierra. Plastics Testing and Characterization, Industrial Applications. Carl Hanser Verlag: Munich (2008).

Chapter 4

Results and discussion

4.1 Optical and scanning electron microscopy

To test the matrix/fibre adhesion and composite morphology, polarized optical microscopy (POM) and scanning electron microscopy (SEM) investigations were undertaken. The POM pictures of the PLA and PP composites with sisal fibre are shown in Figure 4.1. For the PLA composites the fibres generally seem to be well dispersed (Figure 1(a-c)), while the fibres in the PP composites are also dispersed, but there seems to be some agglomeration.

The SEM micrographs in Figures 4.2 show that for the PLA composites there are some fibre breakages (Figures 4.2(c) and 4.2(d)) and a minimal number of fibre pull-outs (Figures 4.2(e) to 4.2(h)). It seems as if some of the fibres at the fracture surface show the matrix covering their surfaces. The presence of matrix coverage on the fibre surfaces, and the fibre breakages indicate good interaction between the fibre and the matrix which results in better interfacial adhesion. The gaps between the fibre and the PLA matrix in Figures 4.2(d) and 4.2(e) clearly indicate that the fibre was trying to pull-out but that it could not, which also indicates good fibre/matrix interaction. Huda *et al.* [1] investigated the mechanical and thermo-mechanical properties of wood fibre reinforced PLA, and compared them with wood fibre reinforced PP composites that were processed in the same way by a micro-compounding moulding system. They reported that there was a good adhesion between the wood fibre and the PLA, and that the MAPP coupling agent had no effect on the morphological properties of the PLA/wood fibre composites. This is in line with our own observations.

The SEM photos in Figures 4.3(c) to 4.3(h) seem to show surprisingly good adhesion between the hydrophilic sisal fibre and the hydrophobic PP polymer, which does not reflect in the properties that will be discussed later in this chapter. Most of the fibres at the fracture surface are still attached to PP. The fibre breakages and the seemingly lack of fibre pull-outs in all the pictures seem to indicate good matrix/fibre adhesion. The reason for this may be that, at the high temperature used for composite preparation, the viscosity of the PP (because of its high melt flow index) was low enough for it to penetrate the pores on the fibre surfaces.

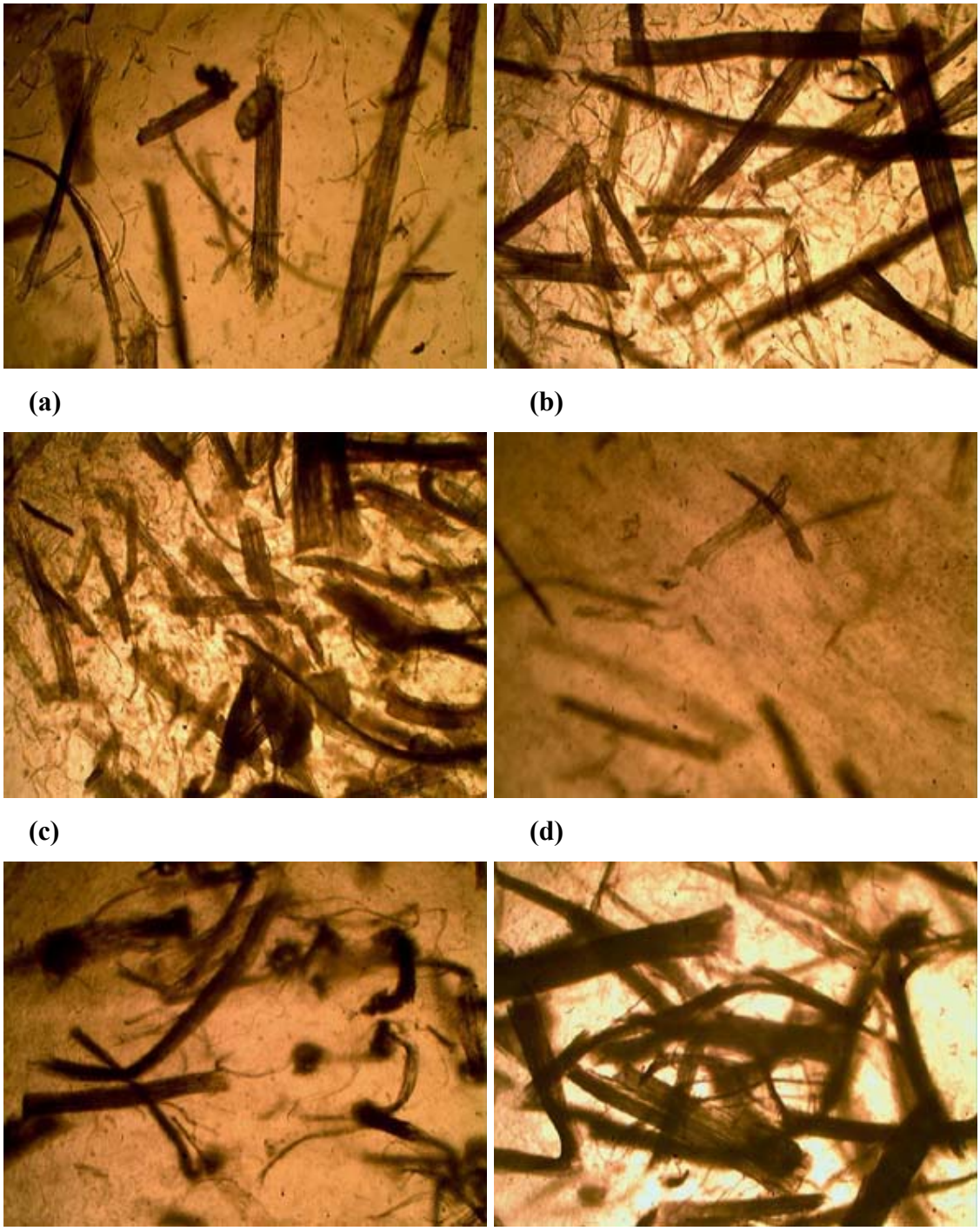

(a) **(b)**

(c) **(d)**

(e) **(f)**

Figure 4.1 POM photos of (a) 98/2 w/w PLA/sisal, (b) 96/4 w/w PLA/sisal, (c) 94/6 w/w PLA/sisal, (d) 98/2 w/w PP/sisal, (e) 96/4 w/w PP/sisal, and (f) 94/6 w/w PP/Sisal

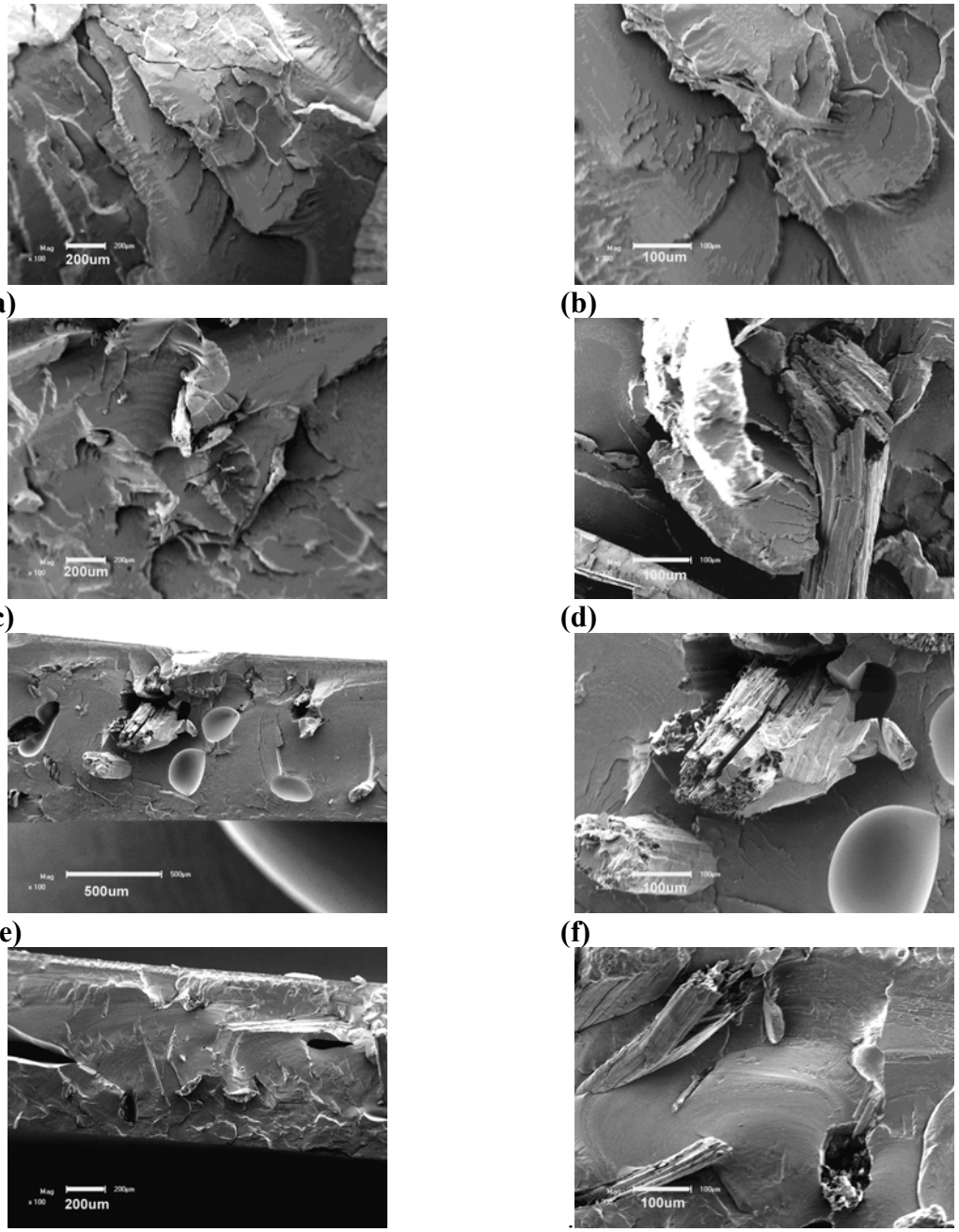

Figure 4.2 SEM micrographs of the fracture surfaces of PLA ((a) 100x magnification & (b) 300x magnification), the 99/1 w/w PLA/sisal composite ((c) 100x magnification & (d) 300x magnification), the 98/2 w/w PLA/sisal composite ((e) 100x magnification & (f) 300x magnification), and the 97/3 w/w PLA/sisal composite ((g) 100x magnification & (h) 300x magnification)

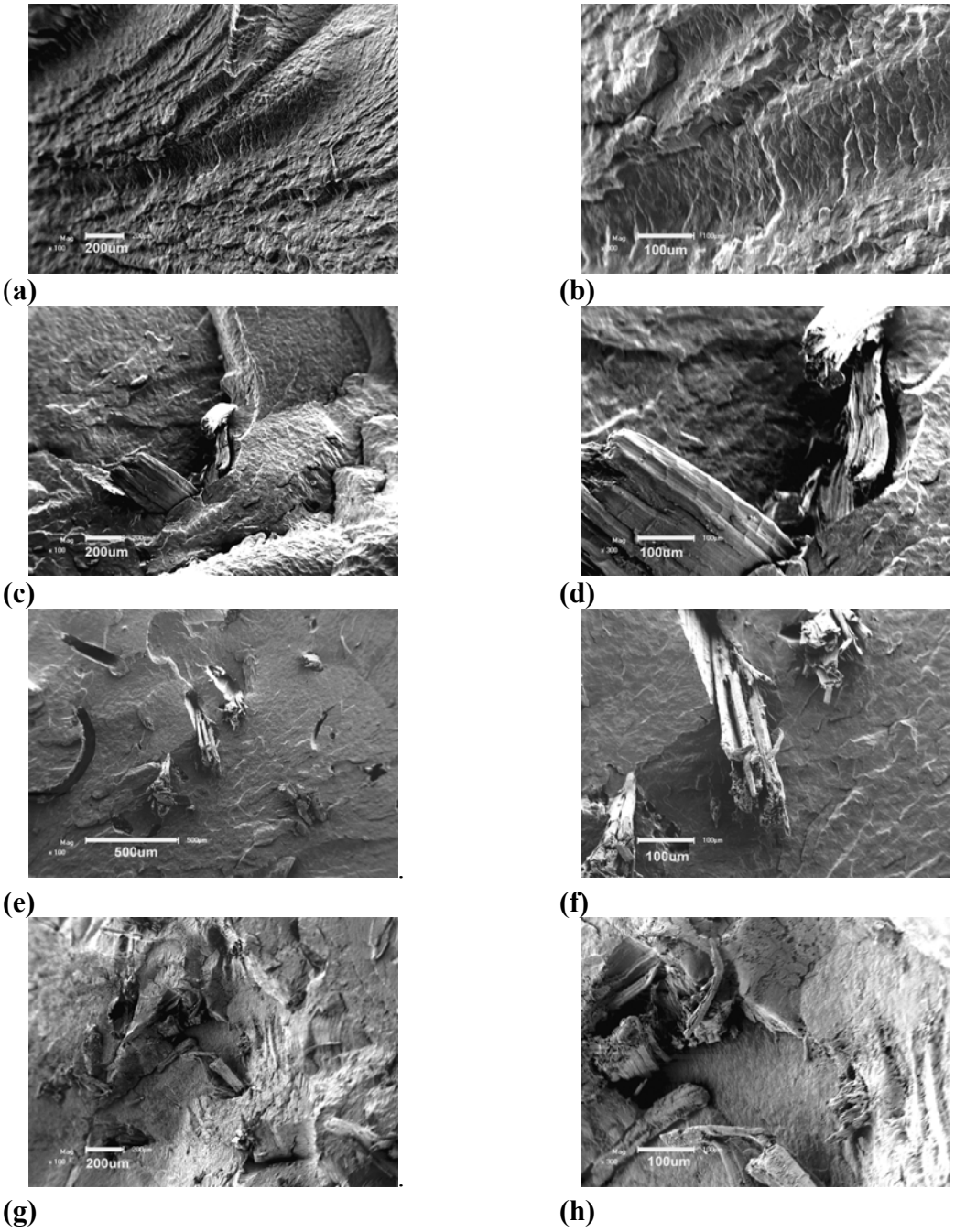

Figure 4.3 SEM micrographs of the fracture surfaces of PP ((a) 100x magnification & (b) 300x magnification), the 99/1 w/w PP/sisal composite ((c) 100x magnification & (d) 300x magnification), the 98/2 w/w PP/sisal composite ((e) 100x magnification & (f) 300x magnification), and the 97/3 w/w PP/sisal composite ((g) 100x magnification & (h) 300x magnification)

4.2. Fourier transform infrared (FTIR) spectroscopy

To examine the existence and the type of interfacial bond in the composites, FTIR experiments were performed and compared with those of the neat PP and PLA at the range from 4000 to 650 cm^{-1}. The regions of interest for PLA and the composites are 1780 and 1680 cm^{-1} for the C=O stretch, and 3600-3000 cm^{-1} for the O-H stretch. The peaks at about 1750 and 1180 cm^{-1}, which belong to the C=O stretching and the C-O-C stretching of PLA, are clearly visible in all the PLA spectrums (Figures 4.4 and 4.5). The O-H band around 3500 cm^{-1} for the as prepared PLA and the PLA/sisal composites (Figure 4.4) is very small and it does not increase as the fibre load was increased. The intensity of the C=O stretch (1750 cm^{-1}) for the as prepared samples increased a little when compared to the C=O for the annealed samples (Figure 4.5). This may be attributed to the fibres being degraded during the processing time as the temperature used was above 200 ºC for the injection moulding [3-4]. The O-H band for the annealed neat PLA and the PLA/sisal composites became more pronounced and broader, and shifted to slightly lower wavenumbers, as the fibre content was increased. This is probably due to the "free" hydroxyl groups that are now engaged in hydrogen bonding [2]. There is a development of a small peak just below the carbonyl peak at 1650 cm^{-1}. This is an O-H peak that originated from the unresolved hydroxyl group bending of the absorbed water usually carried by cellulose [5-6].

Figure 4.6 shows the FTIR spectra of the PP and the PP/sisal composites that were prepared in the same way as the as prepared samples of PLA above. The same observations can be made in terms of the O-H band, which does not show due to the probability of fibre degradation. In this case the matrix PP does not have a carbonyl group, so the only carbonyl should be from the sisal fibre. The only change in this case is the appearance of weak carbonyl group (1750 cm^{-1}) band for the sample with the highest sisal content in the spectrum of the 94/6 w/w PP/sisal sample. The spectra in Figure 4.7 are for the PP and PP/sisal composites that were prepared at the same temperature as that used for the annealed PLA samples. The spectra of the composites all show a C=O peak around 1750 cm^{-1}, and another peak at 1648 cm^{-1} which increased in intensity as the fibre content increased. The peak at 1648 cm^{-1} is the same O-H peak as that observed in Figure 4.5 that originated from the unresolved hydroxyl group bending of the absorbed water [5]. The peak around 3350 cm^{-1} is the O-H band that is found in sisal fibre.

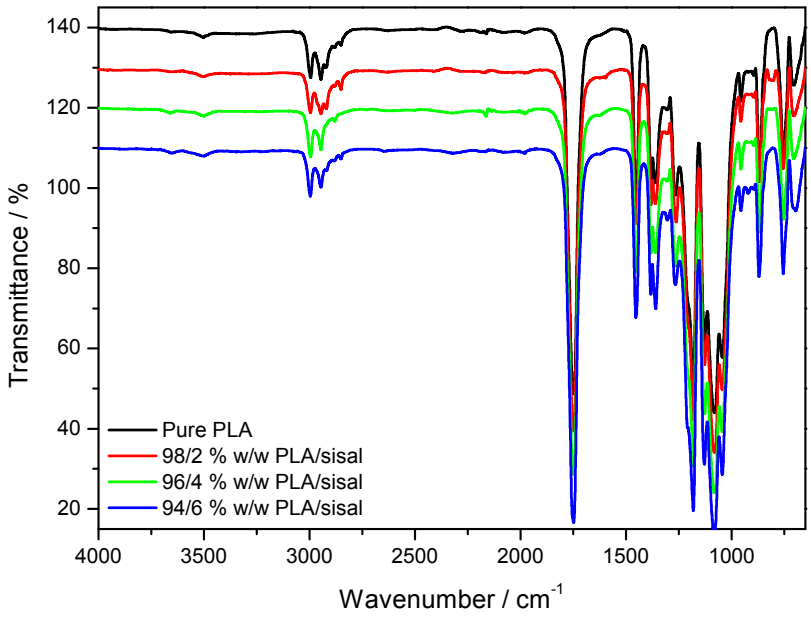

Figure 4.4 FTIR spectra of PLA and its composites at 2, 4 and 6 wt% sisal content

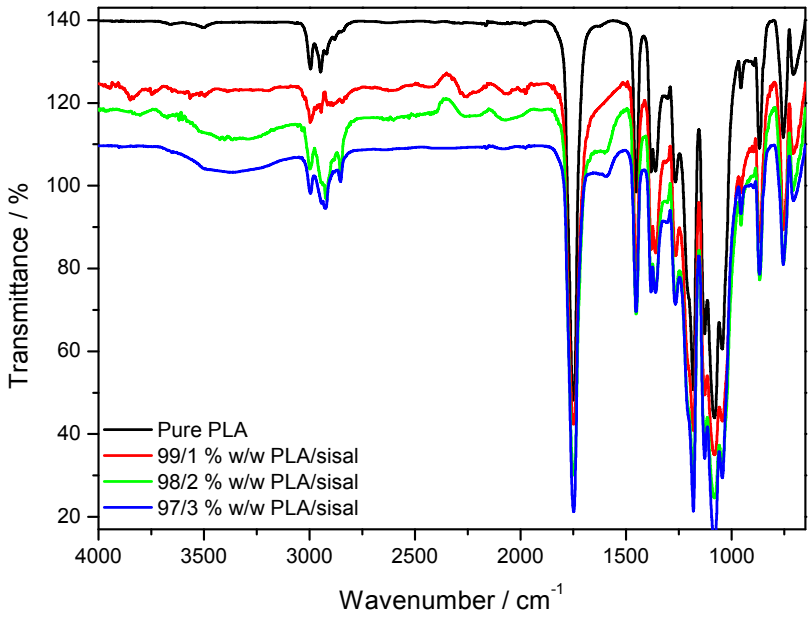

Figure 4.5 FTIR spectra of annealed PLA and its composites at 1-3 wt% sisal content

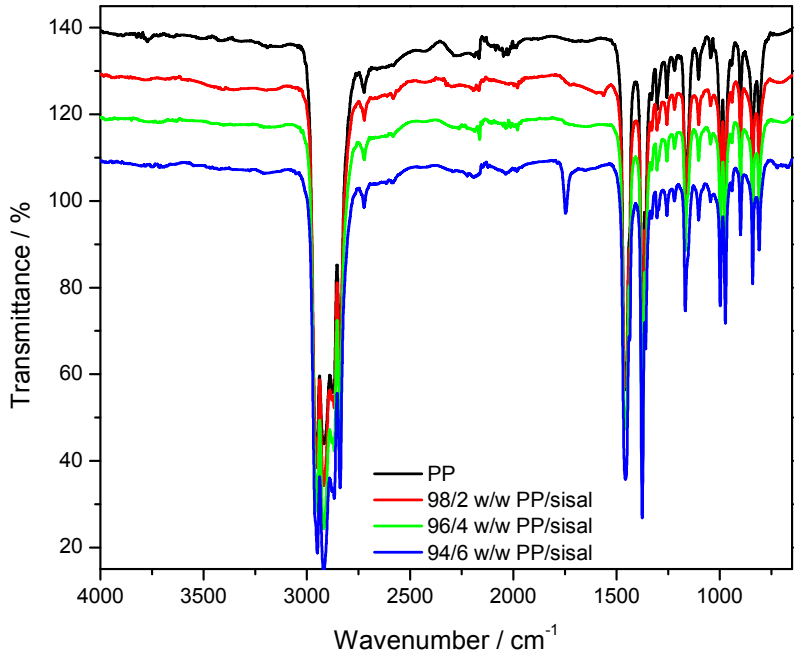

Figure 4.6 FTIR spectra of PP and its composites at 2, 4 and 6 wt% sisal content

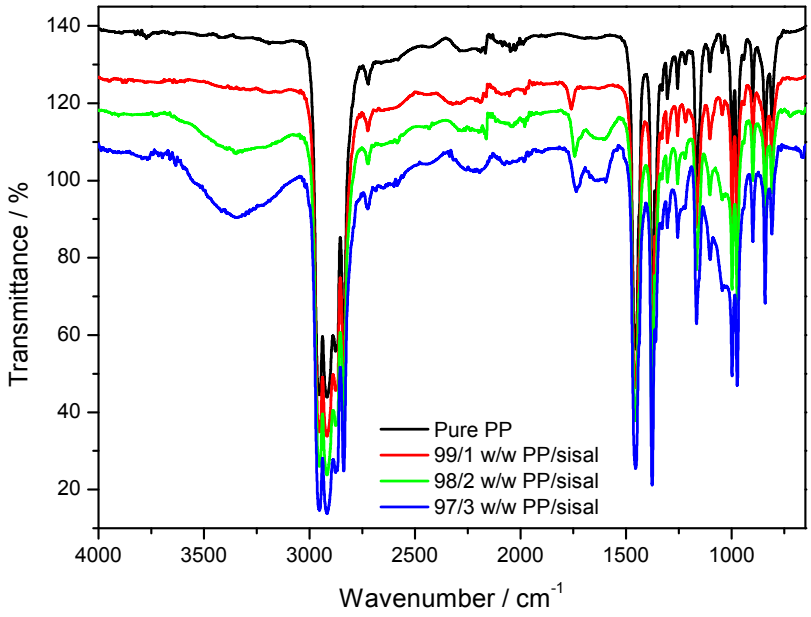

Figure 4.7 FTIR spectra of PP and its composites at 1-3 wt% sisal content

4.3 Thermogravimetric analysis (TGA)

The TGA curves for all the samples are shown in Figures 4.8 to 4.11, and the temperatures at 20 and 70% mass loss are summarized in Table 4.1**.** One of the goals when incorporating sisal fibre into the two polymers was to increase the temperature region in which PLA and PP can be useful [7]. Sisal fibre loses moisture around 100 ºC. The degradation of the sisal fibre is a two-step degradation process as indicated by the two mass loss steps at 285 and 357 ºC. The first step is due to the thermal depolymerization of hemicellulose and the glycosidic linkages of cellulose. The second step is due to the cellulose decomposition which produces a relatively high char residue [8-12]. For both the unannealed and annealed PLA samples only one degradation step was observed for the neat polymer and for the composites, and the thermal stability increased with increasing sisal content, as can be seen in the increase in T_{20} values in Table 4.1. It seems as if the surrounding polymer protected the fibre from lower-temperature degradation, and as if the interaction between the fibre and the polymer retards the degradation process and/or restricts the diffusion of volatile degradation products out of the sample.

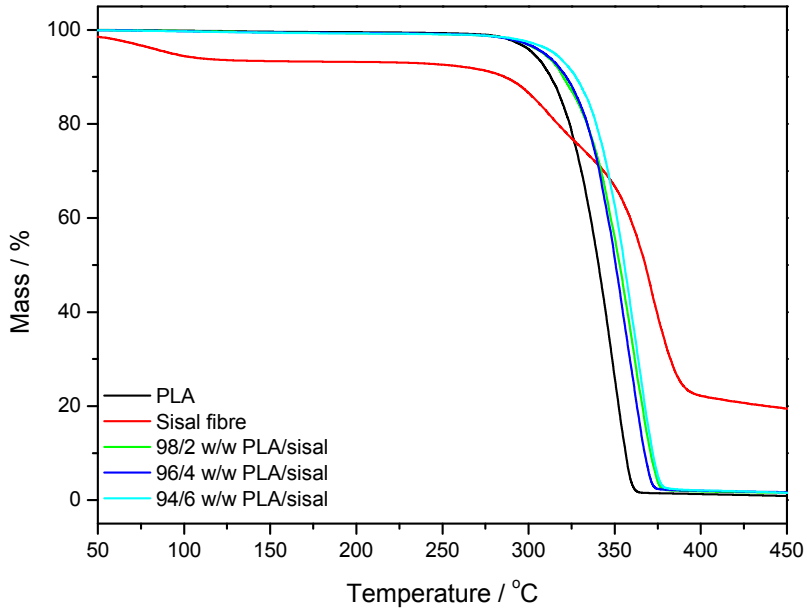

Figure 4.8 TGA curves of as prepared PLA and PLA/sisal fibre composites prepared at 205 ºC

The annealed PLA starts degrading at a higher temperature than the unannealed sample, and the increase in degradation temperature with increasing sisal content is not so significant (Figure 4.9 and Table 4.1). Lim *et al.* [13] reported that annealing PLA at temperatures above the glass transition temperature and below the melting temperature increases the crystallinity of PLA and improves its thermal stability. My DSC results, reported and discussed in the next section, clearly indicate a higher crystallinity for the annealed PLA, and the improved thermal stability in my case can therefore also be linked with this higher crystallinity.

Table 4.1 TGA results of all the investigated samples

Sample	$T_{20\%}$ / ºC	$T_{70\%}$ / ºC
PLA (as-prepared)	344.8	348.4
Sisal	318.5	382.3
98/2 w/w PLA/sisal	351.7	358.7
96/4 w/w PLA/sisal	349.8	362.3
94/6 w/w PLA/sisal	350.9	363.9
PLA (annealed)	345.0	368.7
99/1 w/w PLA/sisal	352.2	375.1
98/2 w/w PLA/sisal	350.5	374.2
97/3 w/w PLA/sisal	349.9	372.9
PP(205 ºC)	377.9	417.0
98/2 w/w PP/sisal	428.3	454.6
96/4 w/w PP/sisal	430.6	458.2
94/6 w/w PP/sisal	435.3	459.5
PP(190 ºC)	387.9	427.9
99/1 w/w PP/sisal	439.7	467.6
98/2 w/w PP/sisal	443.8	469.6
97/3 w/w PP/sisal	446.5	469.6

The degradation of sisal in the composites was not observed as a separate step (Figures 4.8 and 4.9), and we assume that this was due to the small fibre contents and the good interaction between the fibre and PLA. Huda *et al.* [14] investigated the morphology and mechanical properties of wood fibre reinforced PLA in the presence of a maleic anhydride modified polypropylene (MAPP) coupling agent. They reported that the presence of wood fibre decreased the thermal stability of the PLA, which according to them was due to the weak interfacial bonding between the fibre and the matrix, leading to a weak compatibility. This is different from our findings which show that adding sisal fibre to PLA increased the degradation temperature of PLA. Avella *et al.* [15] studied the interfacial adhesion in PLA/kenaf fibre composites with particular attention to the compatibilisation effect in the composites. They reported that the MAPP compatibilised and uncompatibilised PLA/kenaf composites showed a single degradation step, and that neither the fibre nor the compatibiliser had any effect on the thermal degradation temperatures of PLA. The reason given was the comparable degradation temperatures of kenaf and PLA. Lee and co-workers [16] found that the incorporation of bamboo fibre in a PLA matrix significantly affected the thermal degradation temperature of PLA. Their composites showed lower thermal degradation temperatures (more than 50 ºC differences) compared to neat PLA. The reason given was the decrease in molecular weight of the PLA by the high knitting temperature (180 ºC).

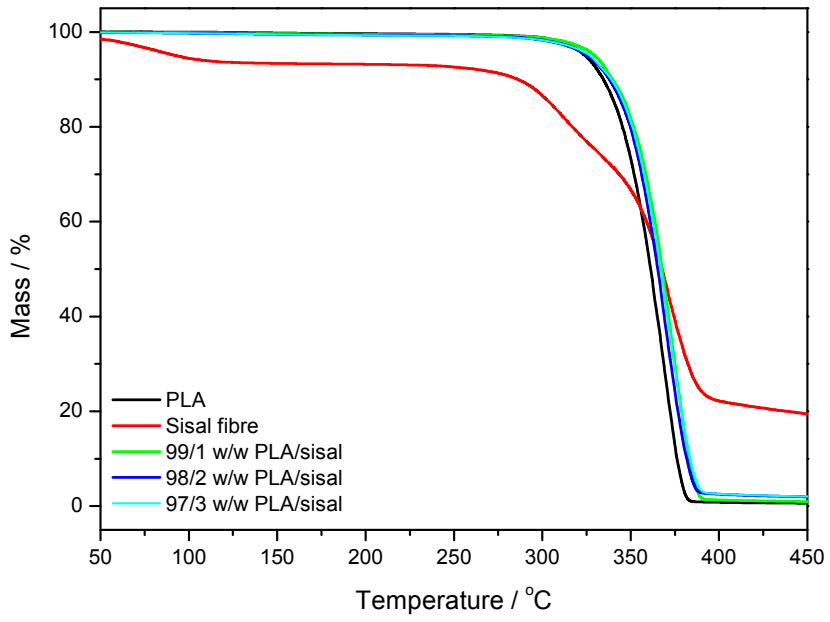

Figure 4.9 TGA curves of PLA (annealed at 120 °C) and PLA/sisal fibre composites prepared at 190 ºC

Pure PP shows a single degradation step around 383 ºC, while the composites show two degradation steps. The small mass loss around 330 ºC is the result of the degradation of sisal fibre, while the major step around 440 ºC is the result of the degradation of PP. The degradation temperatures of the composites significantly increase with an increase in the fibre content (Figures 4.10 and 4.11). Salemane *et al.* [17] reported the same behaviour when PP was filled with wood flour (WF) at different WF particle sizes (<38 and 300-600 μm). The composites with <38 μm particle size showed a one step thermal degradation at temperatures higher than that of the PP and the WF. The composites prepared with 300-600 μm WF particles also showed an increase in thermal degradation temperature, but two degradation steps were observed. This was attributed to the higher PP crystallinity in the presence of the filler. In our case the DSC results show a decrease in crystallinity in the presence of sisal fibre for the samples processed at 205 ºC. Completely different DSC results were observed for the samples processed at 190 ºC, as the crystallinity increased with an increase in sisal fibre content. The fibre probably started degrading at higher temperatures because of the thermal protection by the thermally more stable PP that surrounded the fibre. The increased thermal stability of the PP is probably because the presence of fibre might have (i) immobilised the free radicals formed during the initiation of the degradation of the polymer chains, and (ii) the inhibition of the diffusion of volatile degradation products because of the interaction with the fibre. The thermal degradation temperatures of the samples prepared at 205 ºC are lower than the ones for the samples prepared at 190 ºC. This can be attributed to the partial degradation of the fibres at the higher preparation temperature used during the processing. This is confirmed by the FTIR results which show the disappearance of the -OH peak for the samples prepared at 205 ºC.

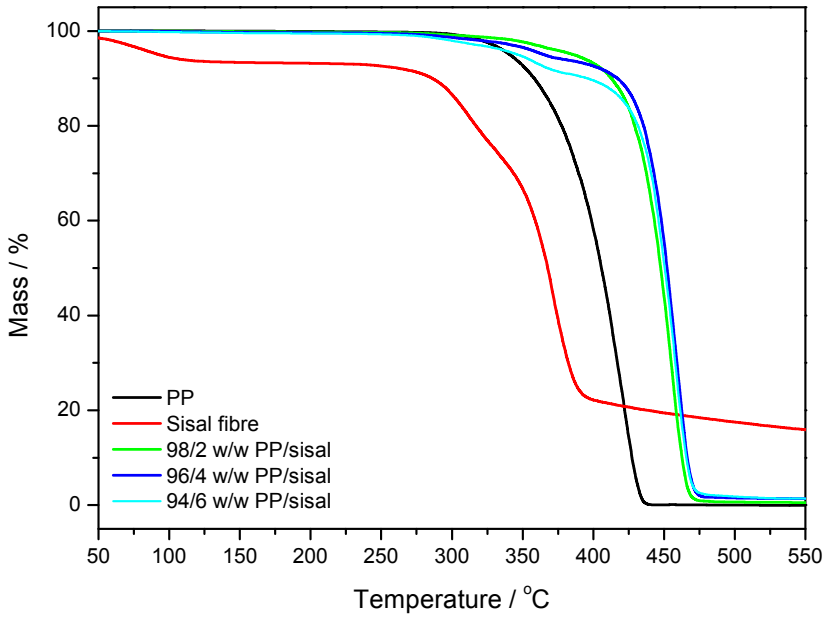

Figure 4.10 TGA curves of PP and PP/sisal composites prepared at 205 ºC

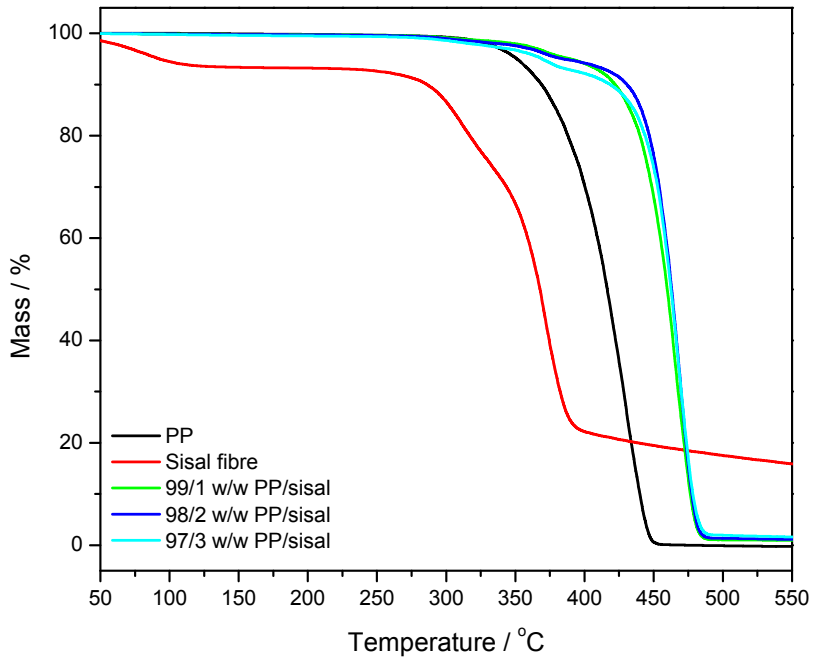

Figure 4.11 TGA curves of PP and PP/sisal composites prepared at 190 ºC

4.4 Differential scanning calorimetry (DSC)

Figures 4.12 and 4.13 and Table 4.2 show the DSC results of the as prepared and annealed PLA, as well as of the PLA/sisal composites prepared at 205 ºC and 190 ºC. The glass transition temperature seems to decrease observably with increasing fibre content for the as prepared composites. This is not something which is generally observed for natural fibre composites, and an explanation is not immediately apparent. However, there are publications that claim that the fibre, at low contents, may act as a plasticizer in the polymer matrix [18-19]. This behaviour may also be linked with the partial degradation of the fibre at this temperature, because similar behaviour was not observed for the samples prepared at the lower temperature (Table 4.2). The cold crystallisation (exothermic transition around 130 ºC) for the as-prepared samples did not change much with an increase in sisal fibre content. The melting temperature (T_m) of these samples increased marginally with an increase in sisal fibre content (Figure 4.12 and Table 4.2). This shows that the crystal sizes slightly increased in the presence of sisal fibre, indicating that the fibres may have acted as nucleating agents. Only one melting peak was observed for the as-prepared samples. This shows that only one type of crystalline structure was present in the composites.

Table 4.2 DSC results of all the investigated PLA and PLA/sisal composite samples

Sample (205 ºC)	**T_g / ºC**	**T_m / ºC**
PLA(as prepared)	60.0 ± 0.1	150.4 ± 0.3
98/2w/w PLA/sisal	60.1 ± 0.4	151.1 ± 0.2
96/4w/w PLA/sisal	59.1 ± 0.2	151.0 ± 0.1
94/6w/w PLA/sisal	55.6 ± 0.1	152.4 ± 1.4
Sample (190 ºC)		
PLA(annealed)	63.7 ± 0.5	153.9 ± 0.5
99/1 w/w PLA/sisal	63.4 ± 0.2	170.1 ± 0.5
98/2 w/w PLA/sisal	63.1 ± 0.2	165.4 ± 0.8
97/3 w/w PLA/sisal	63.2 ± 0.3	156.0 ± 1.3

Glass transition temperature(T_g); Peak temperature of melting (T_m)

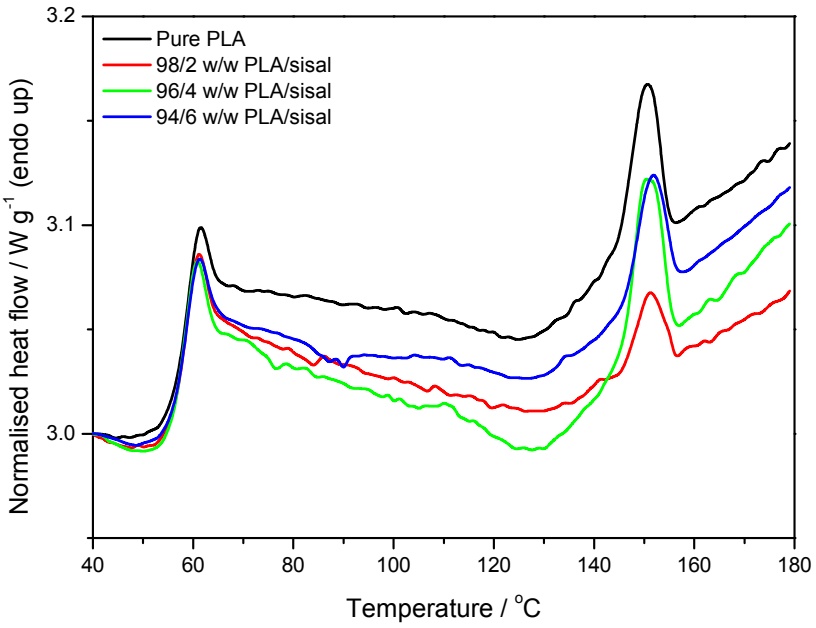

Figure 4.12 DSC heating curves of as prepared PLA and PLA/sisal fibre composites prepared at 205 ºC

The results of the annealed PLA samples are shown in Figure 4.13. The glass-transition, cold crystallisation, and melting of the samples are clearly observed in the curves. The glass transition of the annealed neat PLA shows a sharp transition called a hysteresis peak. This happens mostly with annealed semicrystalline polymers. The reason for this endothermic hysteresis peak is not a lowering of the enthalpy of the polymer due to annealing, but a change in the kinetics of unfreezing [20]. The sharpness and the intensity of the hysteresis peak decrease in the presence of the sisal fibre. This is the indication that the presence of fibre in some way changed the morphology of the amorphous fractions in the polymer during the cooling process. The glass transition of the annealed PLA samples is higher than that of the as-prepared samples, and it did not change for the fibre composites (Table 4.2). The reason for this is that the annealing produced more, and more perfect, crystals that acted as physical crosslinks and reduced the mobility of the amorphous fraction in the polymer.

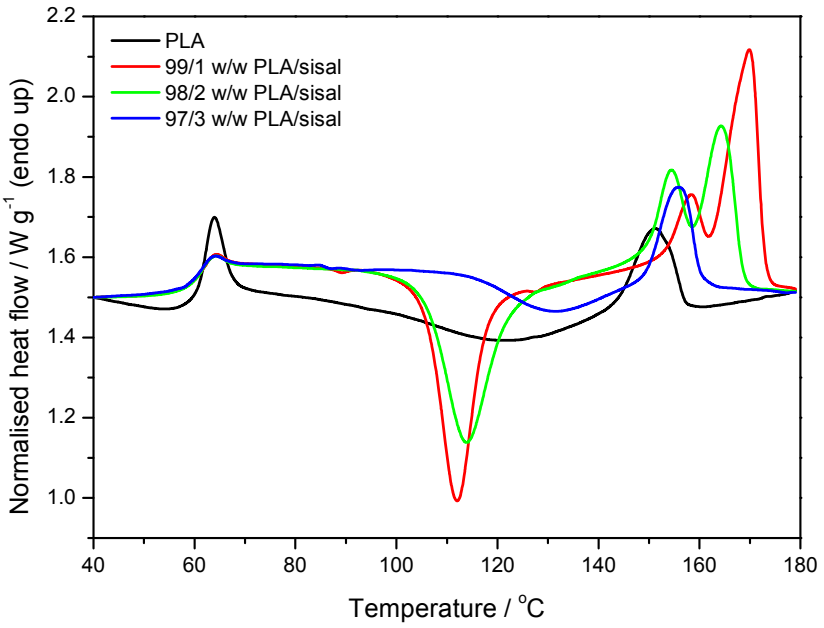

Figure 4.13 DSC heating curves of PLA (annealed at 120 °C) and PLA/sisal composites prepared at 190 ºC

The exothermic transition around 110 ºC is due to the cold crystallization of PLA, and it is sharp and well resolved for the sample containing 1 wt% of sisal fibre. This peak shifts to higher temperatures and also decreases in intensity with further increase in the sisal fibre content. The fibres can either act as nucleation sites for the crystallization of the polymer, or restrict the mobility of the polymer chains. These two actions may always be present when a polymer is cooled in the presence of well dispersed short fibres. When only 1% of sisal fibre was present, the nucleation by the short fibres was probably dominant, giving rise to a large extent of cold crystallization and the formation of two melting peaks. This is an indication of two crystal fractions (meta-stable and perfected crystals) [20] formed during the original cooling of the sample and the subsequent cold crystallization. As the fibre content increased (2 wt%), the cold crystallisation peak intensity decreased and it shifted to higher temperatures. The intensity of the second melting peak also decreased, and both melting peaks shifted to lower temperatures. This indicates that the immobilization effect became more dominant. At higher fibre content (3 wt%) the cold crystallisation peak shifted to even higher temperatures and its intensity decreased significantly, and the second melting peak completely disappeared. This shows that the

immobilization effect was even more dominant, but the fact that the melting temperature for this composite was still higher than that of neat PLA shows that some fibres still acted as nucleating agents.

Lezak *et al.* [21] worked with PLA mixed with different natural fillers and reported that the cold crystallisation peak shifted to higher temperatures as the filler content increased. Further additions of the fillers diminished the appearance of the cold crystallisation peak, but they could not explain why that was happening. Both Lezak *et al.* [21] and Masirek *et al.* [22] observed a double melting peak when they have filled PLA with natural fillers. They reported that the presence of the two melting peaks has in the past been attributed to lamellar reorganization, which was likely the result of less stable crystals formed at relatively low temperatures. Pilla *et al.* [23] investigated the effect of adding an epoxy-based chain extender (CE) on the cell morphology and mechanical properties of solid and microcellular PLA. They reported that the presence of CE separated the melting peak into two individual peaks. This was attributed to the different crystalline morphology (e.g. thickness of the lamellar structure and size of the spherulites) obtained during different crystallization processes such as melt-crystallization (from cooling) and cold crystallization.

The melting enthalpy calculations should have been done by subtracting the enthalpy of the cold crystallisation peak from that of the melting peaks. The cold crystallisation peaks for most of the samples were ill-defined, and therefore it was decided not to report or discuss any changes in enthalpies or total crystallinities.

Figures 4.14 to 4.17 illustrate the DSC heating and cooling curves, and Table 4.3 summarizes the DSC results, for PP and the PP/sisal fibre composites prepared at 205 ºC and 190 ºC. Figure 4.14 shows that the T_m and the broadness of the PP melting peak decreases with an increase in fibre content. This decrease in T_m is probably due to a decrease in the average crystallite size, while the narrowing of the peaks indicating a narrower crystal size distribution. The experimental melting enthalpies were lower than the calculated ones, indicating a lower total crystallinity for the composites. All these observations can be explained assuming that the short fibres act as nucleation sites for the formation of smaller, but more equally sized PP crystals. The lower total

crystallinity of PP in the composites is probably the result of some immobilization of the PP chains by the well-dispersed sisal fibres.

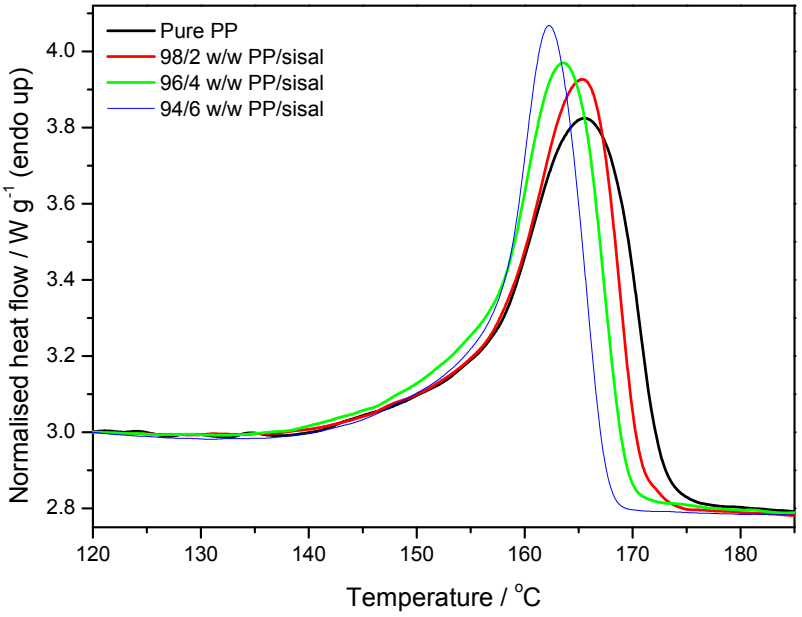

Figure 4.14 DSC heating curves of PP and PP/sisal composites prepared at 205 ºC

The crystallisation temperature (T_c) values of the PP in the PP/sisal fibre composites that were prepared at 205 ºC (Figure 4.15) increased with increasing sisal fibre content. This indicates that the fibres acted as nucleating agents, hence the PP in the composites started crystallizing at higher temperatures. Normally, upon cooling, the polymer will crystallize at a given temperature, and an effective nucleating agent will cause the T_c of the polymer to increase, because crystallization will start earlier during the cooling process. This behaviour can be explained by the fibre surfaces acting as nucleation sites for the crystallization of the polymer matrix [24].

Table 4.3 DSC results of all the investigated PP and PP/sisal composite samples

Sample (205 ºC)	**ΔH_m^{exp} / J g^{-1}**	**ΔH_m^{calc} / J g^{-1}**	**T_m / ºC**
PP	65.5 ± 0.5	65.5	166.4 ± 0.3
98/2 w/w PP/sisal	63.2 ± 0.1	64.8	165.9 ± 0.6
96/4 w/w PP/sisal	61.2 ± 0.9	64.2	164.0 ± 0.2
94/6 w/w PP/sisal	54.8 ± 0.7	63.5	162.4 ± 0.3
	ΔH_c^{exp} / J g^{-1}	**ΔH_c^{calc} / J g^{-1}**	**T_c / ºC**
PP	-90.8 ± 0.6	-90.8	107.6 ± 0.4
98/2 w/w PP/sisal	-90.6 ± 1.0	-90.0	112.2 ± 0.3
96/4 w/w PP/sisal	-86.8 ± 0.4	-89.0	113.0 ± 0.3
94/6 w/w PP/sisal	-85.3 ± 1.7	-88.1	114.1 ± 0.1
Sample (190 ºC)	**ΔH_m^{exp} / J g^{-1}**	**ΔH_m^{calc} / J g^{-1}**	**T_m / ºC**
PP	63.2 ± 2.3	63.2	165.9 ± 1.9
99/1 w/w PP/sisal	65.7 ± 7.5	62.6	168.0 ± 2.8
98/2 w/w PP/sisal	70.0 ± 1.8	61.9	167.7 ± 0.8
97/3 w/w PP/sisal	71.3 ± 5.1	61.3	167.7 ± 1.4
	ΔH_c^{exp} / J g^{-1}	**ΔH_c^{calc} / J g^{-1}**	**T_c / ºC**
PP	-91.7 ± 0.8	-91.7	112.1 ± 0.6
99/1 w/w PP/sisal	-95.3 ± 1.6	-90.8	120.6 ± 0.2
98/2 w/w PP/sisal	-87.5 ± 1.3	-89.9	120.3 ± 0.9
97/3 w/w PP/sisal	-89.8 ± 1.7	-89.0	120.2 ± 0.8

Peak temperature of melting (T_m); Melting enthalpy (ΔH_m); Peak temperature of crystallization (T_c); Crystallization enthalpy (ΔH_c),

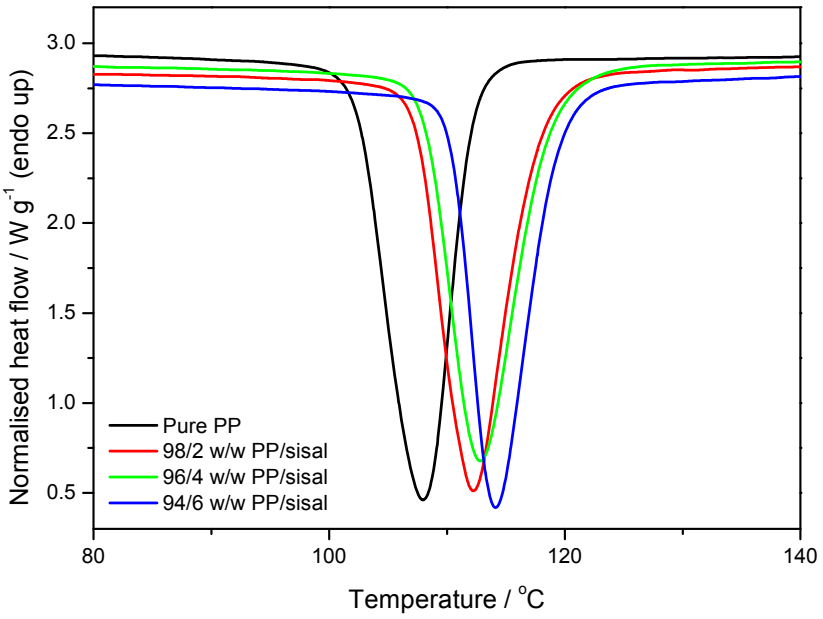

Figure 4.15 DSC cooling curves of PP and PP/sisal composites prepared at 205 ºC

The DSC results of the PP/sisal composites prepared at 190 °C are totally different from those prepared at 205 °C. In this case the melting temperatures of the composites are higher than that of pure PP, and the experimental melting enthalpies are higher than the calculated ones. There is not such a narrowing of the melting peaks, and there is also a much bigger difference between the crystallization temperature of pure PP and those of the composites. The only differences between these two sets of samples are (i) the compounding and injection moulding temperatures, and (ii) the possibility that polypropylenes from different batches were used for the preparation of the composites. Since the composites were prepared in a collaborator's laboratory in Hungary, we could not confirm whether the same PP was used for all the composite preparations. Since sisal starts degrading at 200 °C, it is quite possible that the slightly degraded fibre interacted less strongly with the PP in the case of the samples prepared at 205 °C, and as a result was less effective as a nucleating agent.

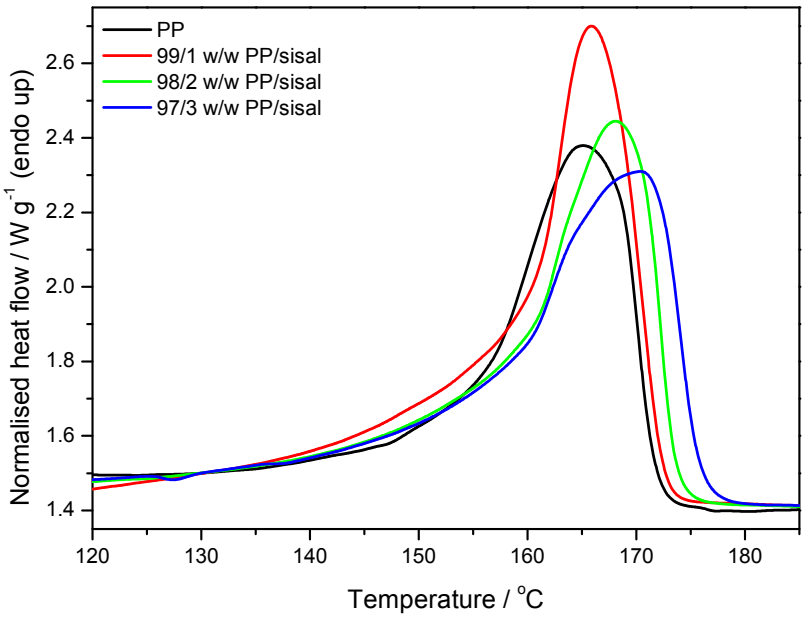

Figure 4.16 DSC heating curves of PP and PP/sisal composites prepared at 190 ºC

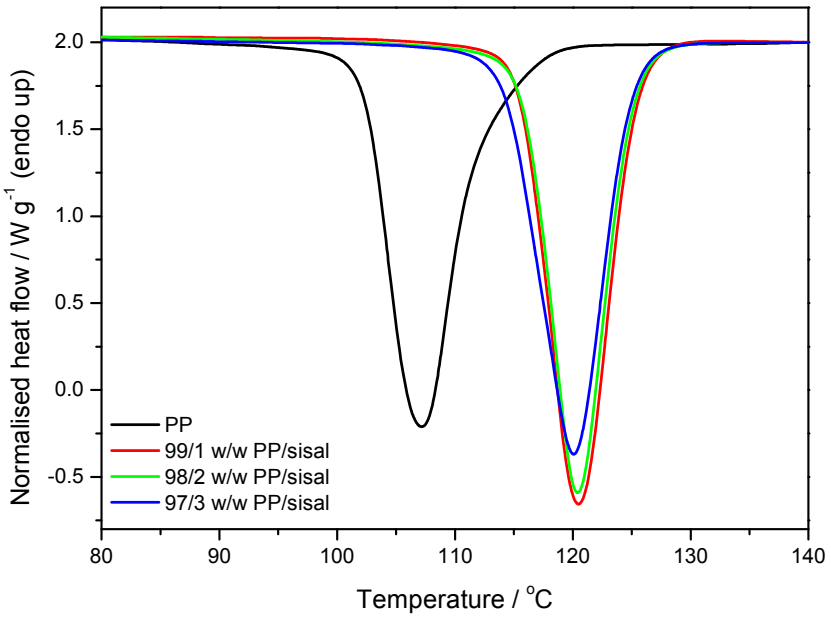

Figure 4.17 DSC cooling curves of PP and PP/sisal composites prepared at 190 ºC

4.5 Dynamic mechanical analysis (DMA)

Figures 4.18 to 4.29 show how the addition of different contents of sisal fibre influenced the storage modulus (E'), loss modulus (E'') and damping factor (tan δ) of PLA, PP and their respective composites. The storage modulus (E') below the glass transition of PLA changed with the fibre content for both the PLA systems (as prepared and annealed samples). The as prepared PLA composites exhibit larger E' values than the neat PLA. This is due to an increase in the stiffness as a result of fibre reinforcement [8,25]. The E' for the annealed PLA is even higher than those of the as prepared samples (neat PLA and composites) due to the annealing process which increased the crystallinity of the PLA. In this case the presence of fibre did not further increase the modulus in this temperature range. Mathew *et al.* [25] studied the crystallisation of PLA in the presence of different cellulose-based reinforcements. They reported that the heat treatment was not expected to result in 100% crystallinity, but that the crystalline regions might restrict the chain mobility. Therefore the introduction of fibre decreased the stiffness.

The sharp decrease in the storage modulus (around 59-63 ºC for most of the samples) for both the as prepared and annealed samples, corresponds to the α-relaxation of the amorphous regions in PLA [25]. The glass transition temperature (T_g) for as prepared samples shows no correlation with the sisal fibre content, so no specific trend was observed. The T_g for the annealed samples seems to increase with increasing sisal fibre content. This shows that the presence of fibre restricts the segmental motion of the polymer chains. The storage modulus started to increase again at temperatures around 100 ºC for both systems, which is the result of the cold crystallization which is typical for PLA [26], and which was also observed in the DSC curves. The decrease in modulus at temperatures around 140 °C indicates the softening of the sample before the onset of melting, which was observed from 140 °C in the DSC curves.

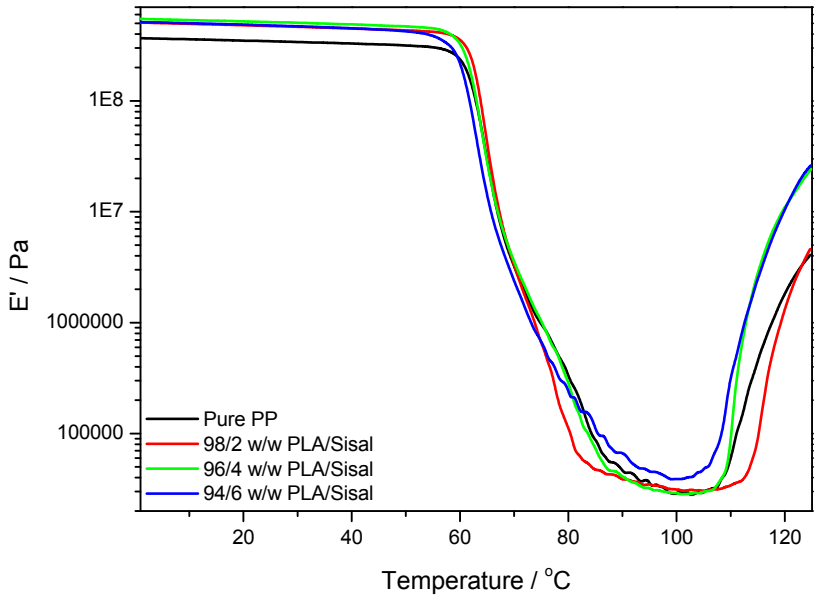

Figure 4.18 DMA storage modulus (E') as function of temperature of as prepared PLA and PLA/sisal fibre composites prepared at 205 ºC

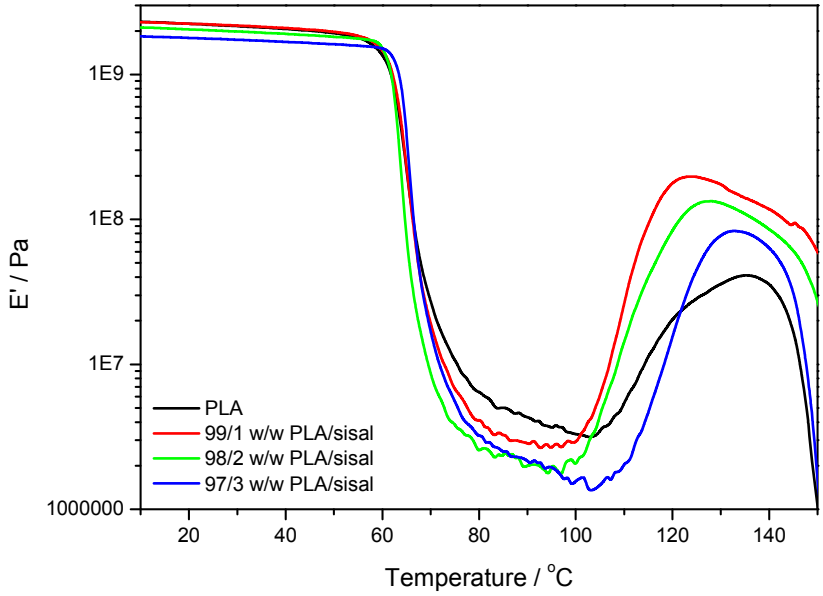

Figure 4.19 DMA storage modulus (E') as function of temperature of PLA (annealed at 120 °C) and PLA/sisal fibre composites prepared at 190 ºC

Figures 4.20 and 4.21 show the temperature dependence on the E' for neat PP and its composites for samples prepared at 205 ºC and at 190 ºC. In both the systems the E' increased when sisal fibre was introduced in the respective system. The increase in the E' indicates an increase in the stiffness of the polymer, which may be the result of a restriction in the segmental motion. The E' of the samples prepared at 190 ºC are much higher than those for the ones prepared at 205 ºC. There is no apparent reason for this, except that different polypropylenes may have been used in the preparation of the respective composites. Possible reasons for this have been discussed in the DSC section 4.4. The E' of all the PP and composite samples show more significant decreases starting around -5 to 0 ºC. This is related to the glass transition of PP [27].

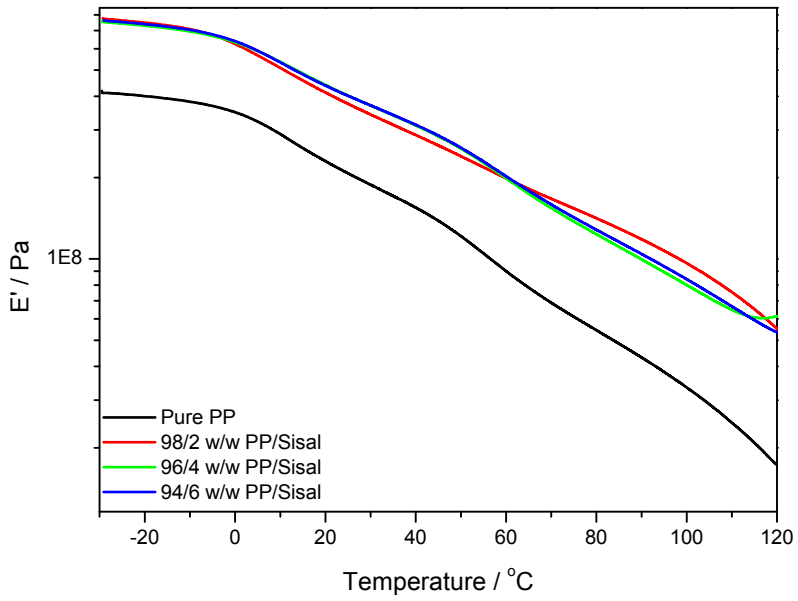

Figure 4.20 DMA storage modulus (E') as function of temperature of PP and PP/sisal fibre composites prepared at 205 ºC

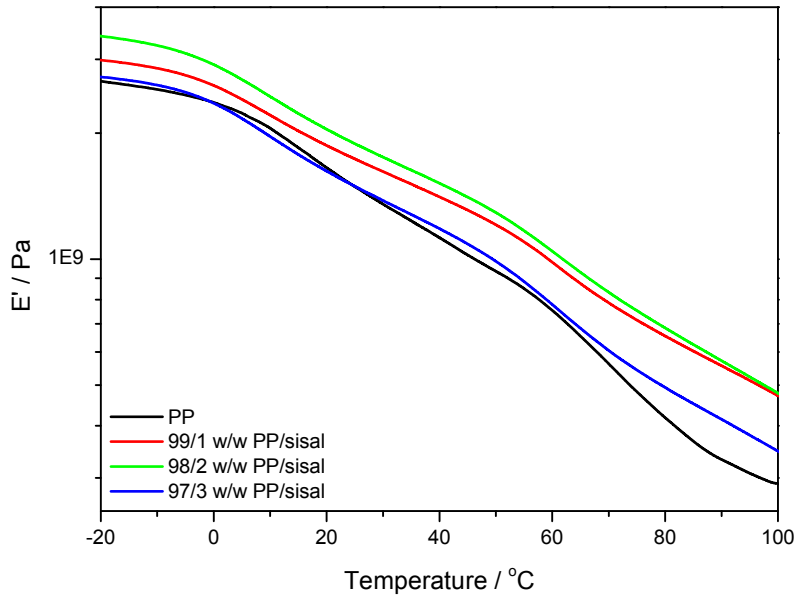

Figure 4.21 DMA storage modulus (E') as function of temperature of PP and PP/sisal fibre composites prepared at 190 ºC

The loss modulus curves of the as prepared PLA and its composites show a general decrease in glass transition temperature (T_g) with increasing sisal fibre content (Figure 4.22). This shows that the segmental motion increased in the presence of fibre. The reason for this is not immediately apparent, but it is possible that the fibre in some way plasticized the PLA matrix, as have already been discussed in DSC and tensile results sections 4.4 and 4.6 respectively. The T_g of the annealed PLA (Figure 4.23) samples slightly increased with the increasing fibre content, which shows that the segmental motion of the PLA was restricted in the presence of the fibre [8,26]. This is a more common and expected observation, but the change is too small to conclude that the fibres had a significant influence on the polymer chain mobility.

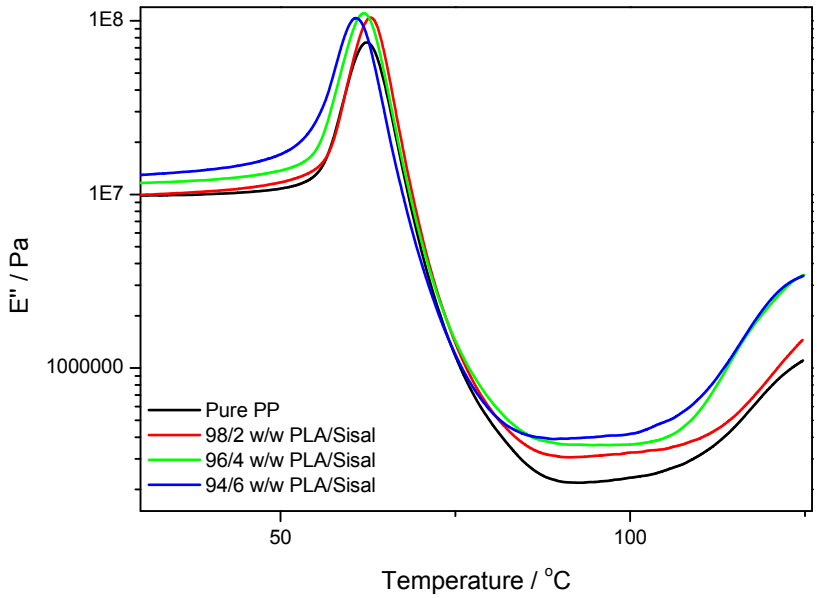

Figure 4.22 DMA loss modulus (E") as function of temperature of as prepared PLA and PLA/sisal fibre composites prepared at 205 ºC

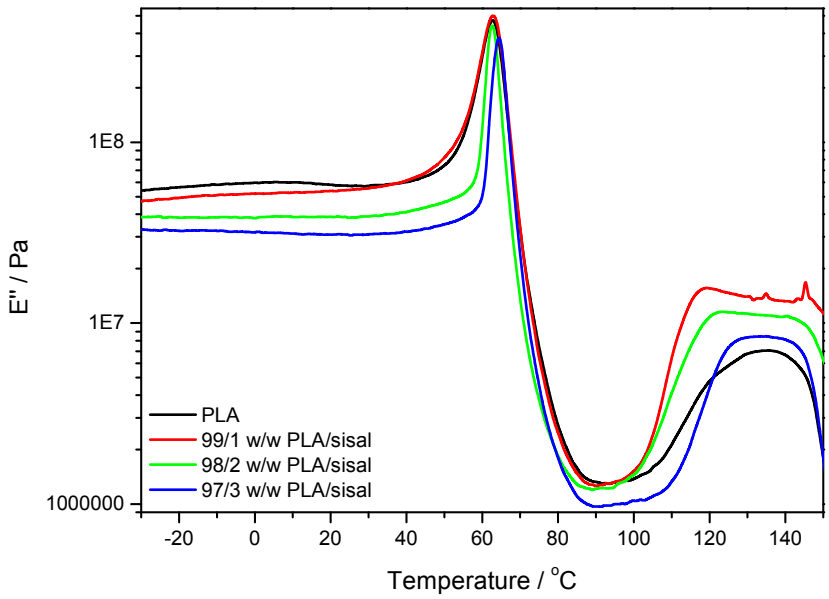

Figure 4.23 DMA loss modulus (E") as function of temperature of PLA (annealed at 120 °C) and PLA/sisal fibre composites prepared at 190 ºC

The loss modulus curves (Figure 4.24) for the PP samples prepared at 205 ºC show a T_g around 9 ºC for the neat PP, and this temperature decreases for the fibre containing samples. This may indicate that the partially degraded sisal fibres act as a plasticizer, increasing the mobility of the PP chains. In the case of the samples prepared at 190 ºC (Figure 4.25) the T_g of the fibre containing samples are observably higher than that of the pure PP. This may be characteristic of a better interaction between the PP and the fibre, which is probably the result of a different PP used in the preparation of these composites. As already mentioned above and in other sections, we could not conclusively establish whether the same PP from the same batch was used for the preparation of the composites at 205 °C and at 190 °C.

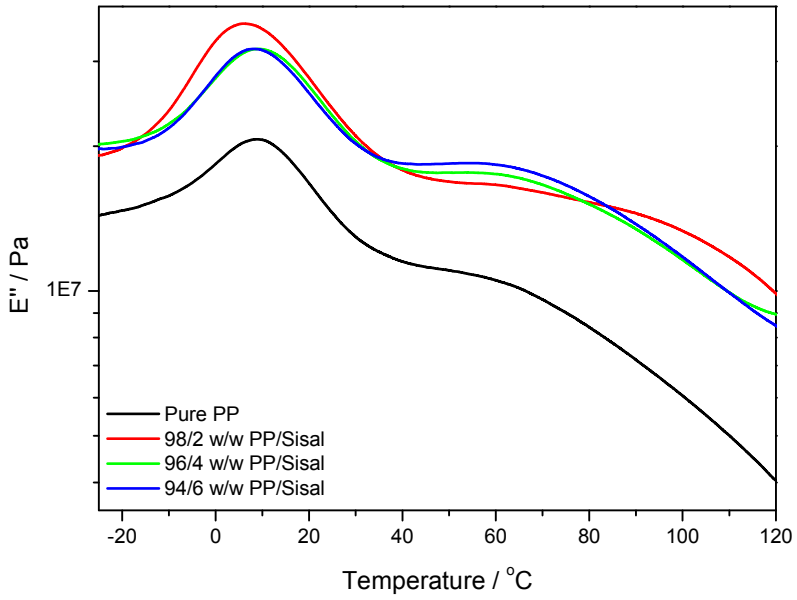

Figure 4.24 DMA loss modulus (E") as function of temperature of PP and PP/sisal fibre composites prepared at 205 ºC

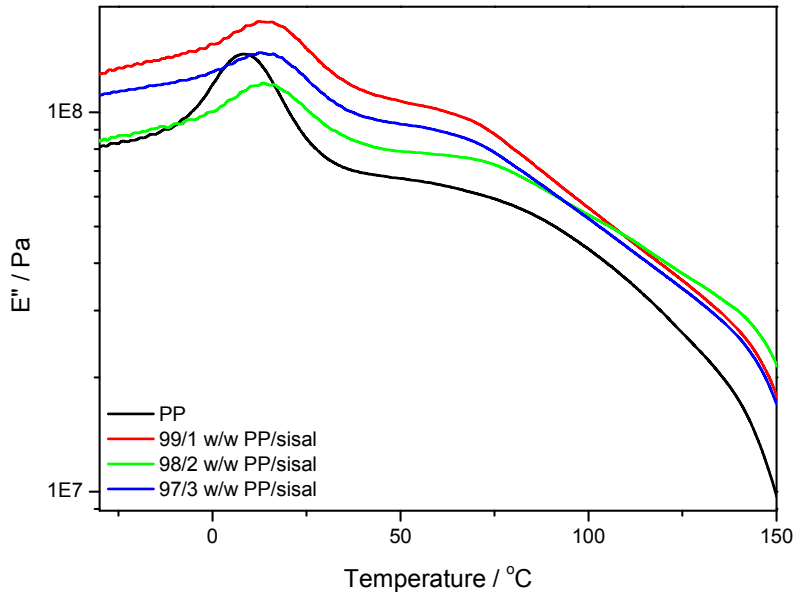

Figure 4.25 DMA loss modulus (E") as function of temperature of PP and PP/sisal fibre composites prepared at 190 ºC

A larger area under the α-relaxation peak in the tan δ curves of a polymer indicates that the molecular chains exhibit a higher degree of mobility, thus better damping properties [23]. The area under this peak (at about 67 °C) for both the as prepared and annealed PLA composites (Figures 4.26 and 4.27) seems to be slightly larger for the fibre composites, and shows no specific trend with increase in the fibre content. There is very little difference between the peak temperatures of this peak for the PLA and the composite samples, and there is no increasing or decreasing trend with increasing fibre content, which indicates that at these levels the fibre had very little influence on the chain mobility in the amorphous phase of PLA. The broad transition (between 75 and 120 ºC for as prepared samples and between 90 and 130 ºC for the annealed samples) for all the samples relates to the cold crystallisation of PLA in this temperature region. The high intensity transition in the as prepared samples (Figure 4.26) clearly indicates that there is a large amorphous content in the polymer. Annealing considerably reduced the amount of amorphous material, and the extent of cold crystallization is much smaller for these samples (Figure 4.27).

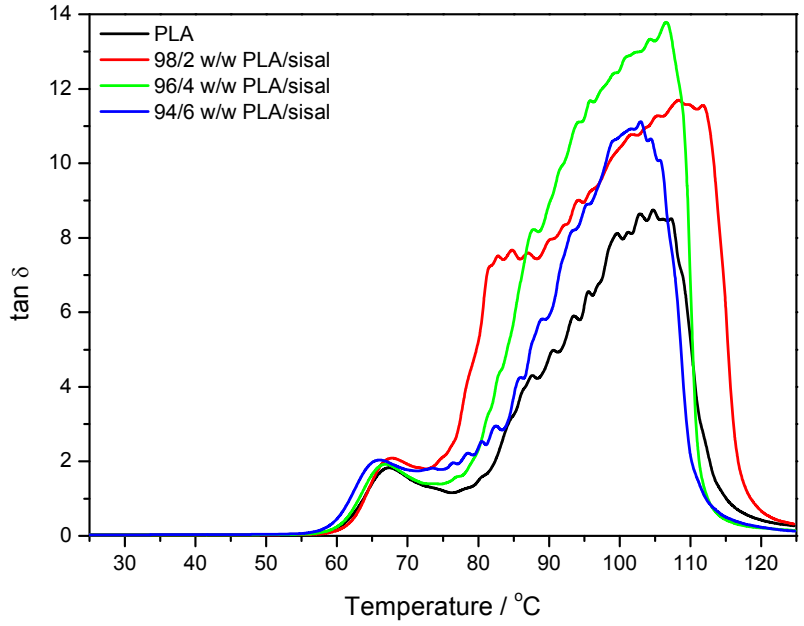

Figure 4.26 Damping factor (tan δ) as function of temperature of as prepared PLA and PLA/sisal fibre composites prepared at 205 ºC

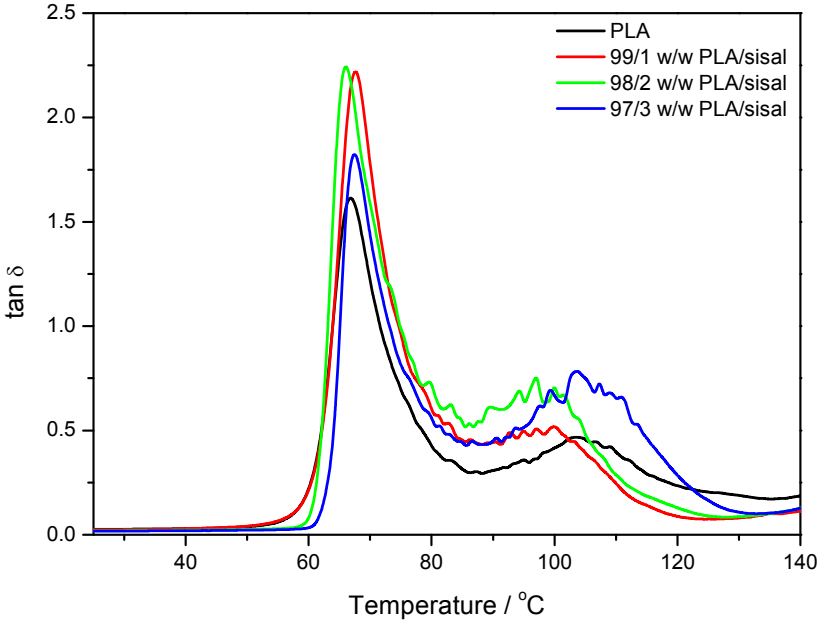

Figure 4.27 Damping factor (tan δ) as function of temperature of PLA (annealed at 120 °C) and PLA/sisal fibre composites prepared at 190 ºC

All the PP and PP/sisal composite curves show two relaxation peaks at about 15 ºC and 70 ºC. The low-temperature peak is related to the β-transition of the amorphous fractions of PP, and is taken as the glass transition. The higher temperature peak corresponds to the α-transition related to the PP crystalline fractions [28]. There is very little difference between the peak temperatures and intensities of the β-transition for the samples prepared at 205 ºC (Figure 4.28). The α-transition seems to disappear for the fibre containing composites, indicating that some fibre may have been located in the interlamellar amorphous regions, giving rise to immobilization of these polymer chain sections. For the annealed samples the composite β-transitions are observed at a slightly higher temperature than that of the pure PP (Figure 4.29), which indicates an immobilization effect of the fibre on the PP chains. The α-relaxation peak is observed for pure PP and all the composite samples, indicating that the fibre was more concentrated in the pure amorphous phase of the polymer, because it had very little influence on the interlamellar chain mobility.

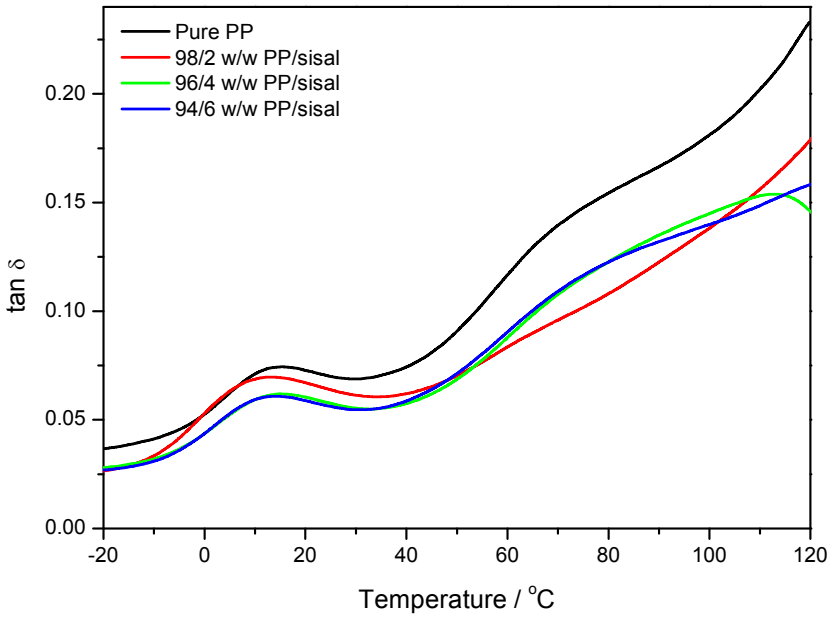

Figure 4.28 Damping factor (tan δ) as function of temperature of PP and PP/sisal fibre composites prepared at 205 ºC

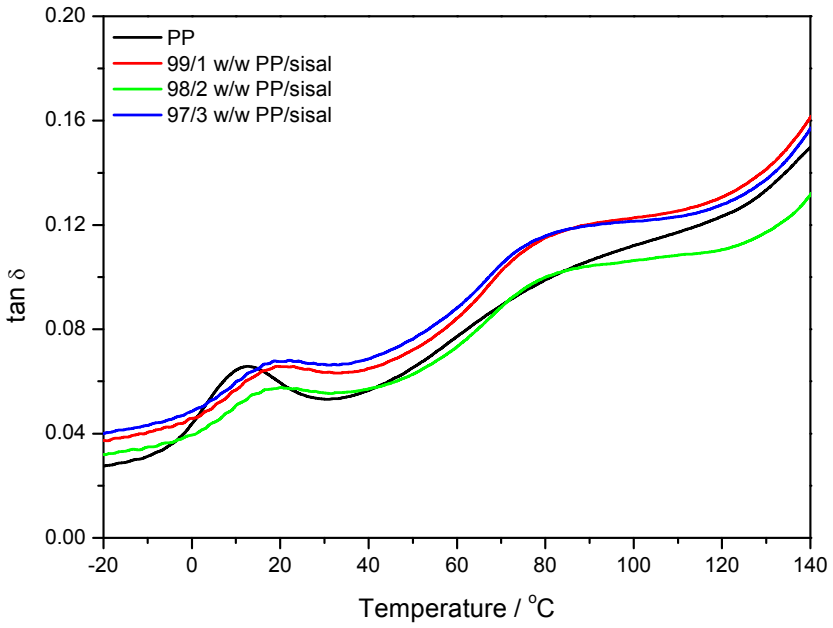

Figure 4.29 Damping factor (tan δ) as function of temperature of PP and PP/sisal fibre composites prepared at 190 ºC

4.6 Mechanical properties

In Figure 4.30 the effect of sisal fibre content on the tensile modulus of PLA is shown. The tensile modulus of PLA remained fairly constant within experimental error (Table 4.4). Since the tensile analyses were performed at room temperature, which is below the Tg of PLA, the polymer already had a high modulus and the addition of sisal fibre (especially at these small contents) is not expected to significantly change the tensile modulus of the polymer [18-19].

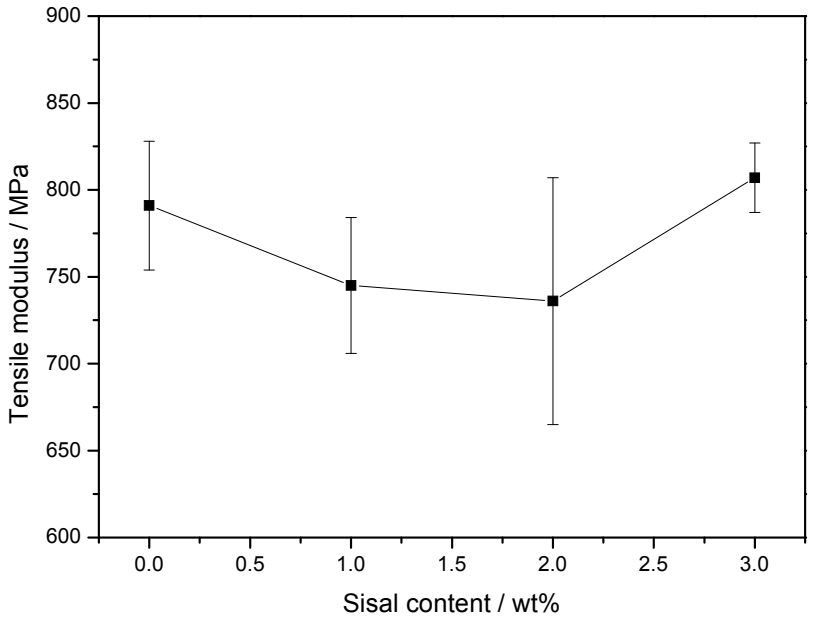

Figure 4.30 Tensile modulus as function of sisal fibre content for PLA and its composites

The tensile strength of PLA decreased (Figures 4.31 and 4.32) when sisal fibre was introduced. This means that the small fibre loadings could not impart reinforcement, and that the fibres acted as defect centres because of poor stress transfer across the interface. The reason for this is insufficient interfacial bonding between the reinforcing fibre and the polymer matrix, although the SEM and FTIR results indicated interaction and intimate contact between the fibres and the PLA matrix. Krishnaprasad *et al.* [29] investigated the influence of micro-fibrils from raw bamboo on polyhydroxybutyrate (PHB) biocomposites. They reported that the tensile strength was found to decrease at lower fibre loadings, and that the microfibrils were insufficient to reinforce the PHB matrix, but rather acted as flaws or stress concentration points. Joseph *et al.* [18] also reported that at low fibre content the fibres may act as flaws in the matrix, reducing the tensile strength of the composite.

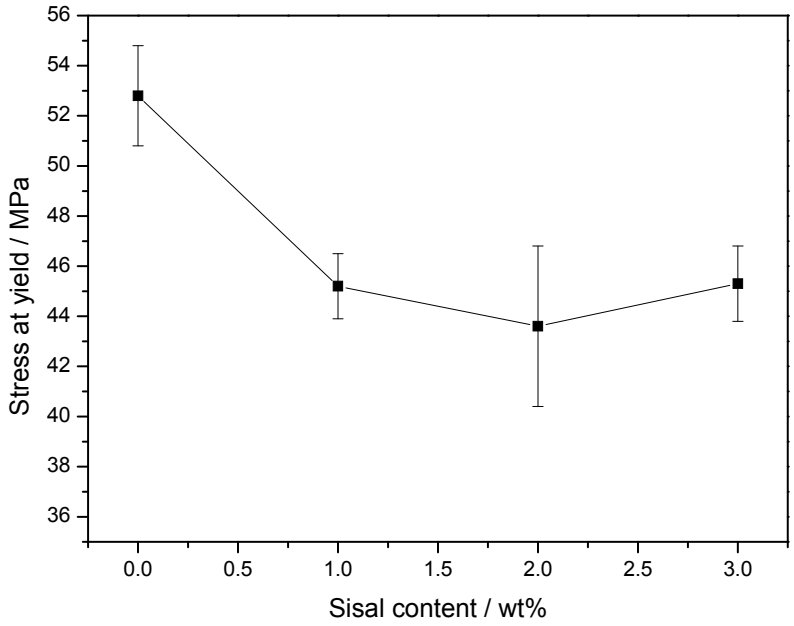

Figure 4.31 Stress at yield as function of sisal fibre content for PLA and its composites

Table 4.4 Tensile results of all the investigated samples

Sample	σ_y / MPa	ε_y / %	σ / MPa	ε / %	**E** / MPa
PLA	52.8 ± 2.0	8.2 ± 0.4	45.3 ± 1.9	12.7 ± 1.7	791 ± 37
99/1 w/w PLA/sisal	45.2 ± 1.3	7.5 ± 0.3	44.3 ± 1.6	8.0 ± 0.3	745 ± 39
98/2 w/w PLA/sisal	43.6 ± 3.2	7.4 ± 0.2	42.7 ± 3.3	8.0 ± 0.1	736 ± 71
97/3 w/w PLA/sisal	45.3 ± 1.5	7.4 ± 0.3	44.3 ± 1.6	8.1 ± 0.7	807 ± 20
PP	29.4 ± 1.9	11.9 ± 0.6	30.3 ± 2.7	938 ± 72	361 ± 22
99/1 w/w PP/sisal	29.4 ± 0.5	11.3 ± 0.3	25.8 ± 0.4	17.4 ± 1.3	605 ± 15
98/2 w/w PP/sisal	28.4 ± 0.6	10.7 ± 0.8	25.1 ± 2.0	15.7 ± 3.4	615 ± 35
97/3 w/w PP/sisal	28.0 ± 0.9	10.5 ± 0.4	24.5 ± 1.2	16.2 ± 1.2	614 ± 29

Modulus (E), stress at yield (σ_y), elongation at yield (ε_y), stress at break (σ), elongation at break (ε)

The elongation at yield and at break (Figure 4.33 and 4.34) decreased with an increase in fibre content. This is a normal observation for short fibre filled composites, because the fibres restrict the matrix from elongating by forming stress concentration points. Mathew *et al.* [26], in their studies of PLA reinforced with microcrystalline cellulose (MCC), reported a reduction in elongation with the addition of fibres into a thermoplastic polymer matrix as a common trend observed in these types composites. This is due to the change of the material from tough to being stiffer after the incorporation of the cellulose fibre.

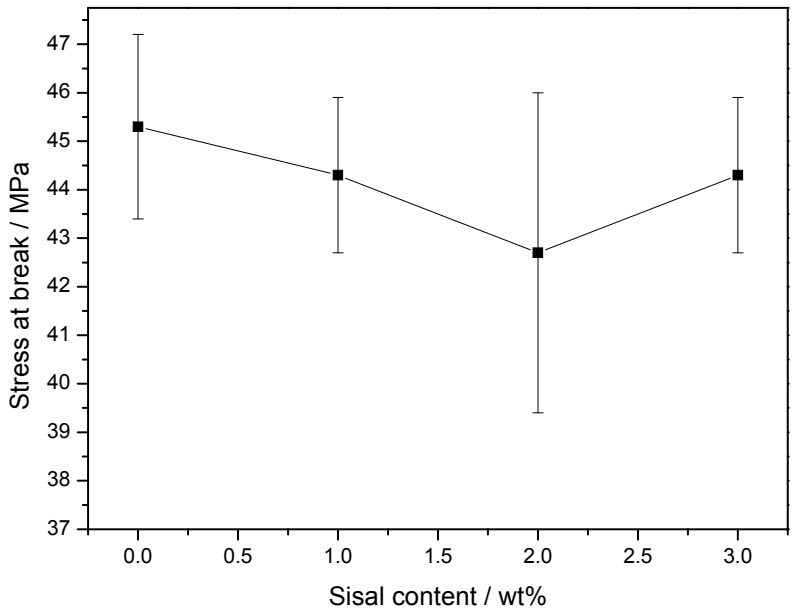

Figure 4.32 Stress at break as function of sisal fibre content for PLA and its composites

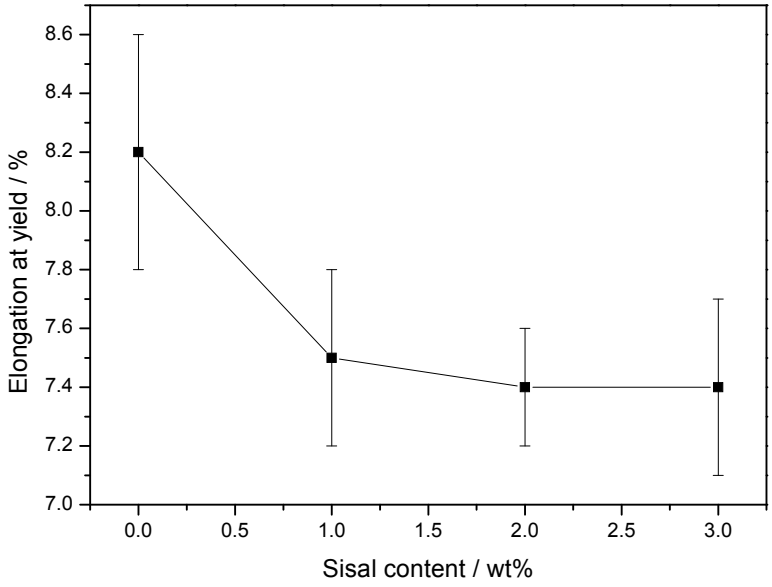

Figure 4.33 Elongation at yield as function of sisal fibre content for PLA and its composites

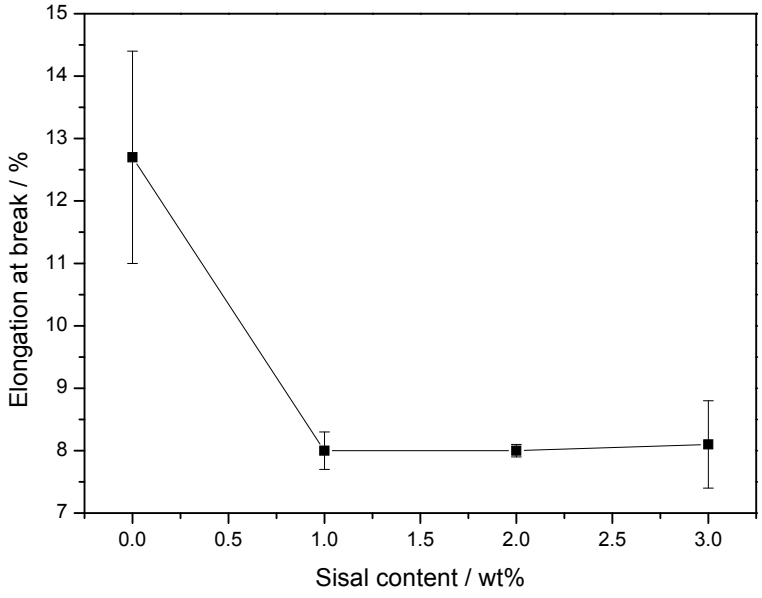

Figure 4.34 Elongation at break as function of sisal fibre content for PLA and its composites

It is well known that a strong effect cannot be obtained if the interfacial interaction between the non-polar polypropylene (PP) matrix and the polar sisal fibre is not strong enough. On the other hand, rigid fillers such as fibres are usually added into polymers to reinforce the matrix by bearing the load [30]. The tensile properties of the PP samples filled with different contents of sisal fibres are summarised in Table 4.4. The effect of sisal fibre loading on the tensile modulus of the PP composites is shown in Figure 4.35. The effect of adding sisal fibre to PP produced a significant increase in the tensile modulus, even at the lowest fibre content of 1%. The tensile modulus of PP almost doubled from 360 to 615 MPa. This is a common phenomenon in composites reinforced with cellulose fibres [16,19]. Since the sisal fibre is stiffer; it increases the stiffness in the polymer matrix resulting in an increase in the composite modulus [31].

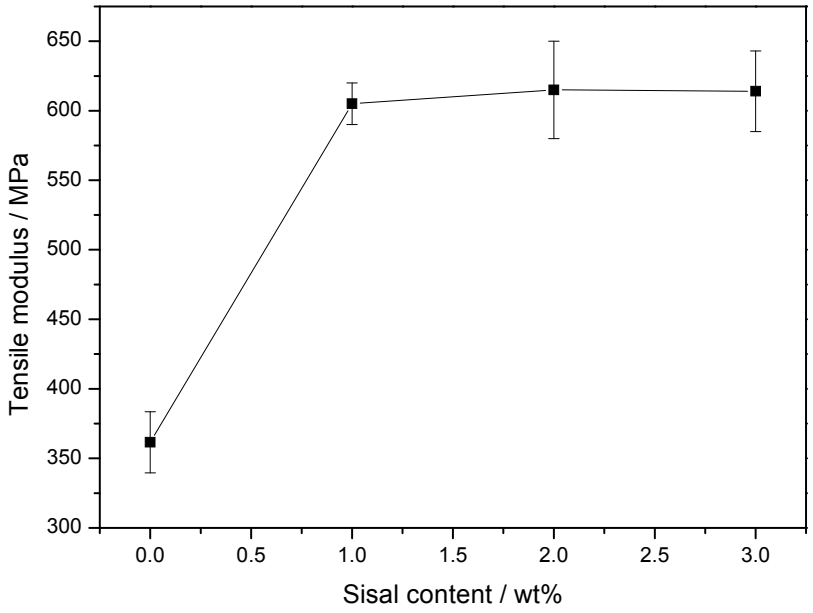

Figure 4.35 Tensile modulus as function of sisal fibre content for PP and its composites

It is evident that incorporation of fibres in the matrix had little effect on the tensile strength at yield of PP (Figure 4.36). An observable decrease in tensile strength at break is observed with increasing fibre content (Figure 4.37), which can be explained on the basis of poor adhesion between the polar sisal fibres and the non-polar PP [32]. The lack of interfacial bonds causes

inefficient load transfer from the matrix to the fibres. In fact, the fibres disturb the continuity of the matrix and act as defect centres, instead of reinforcing it.

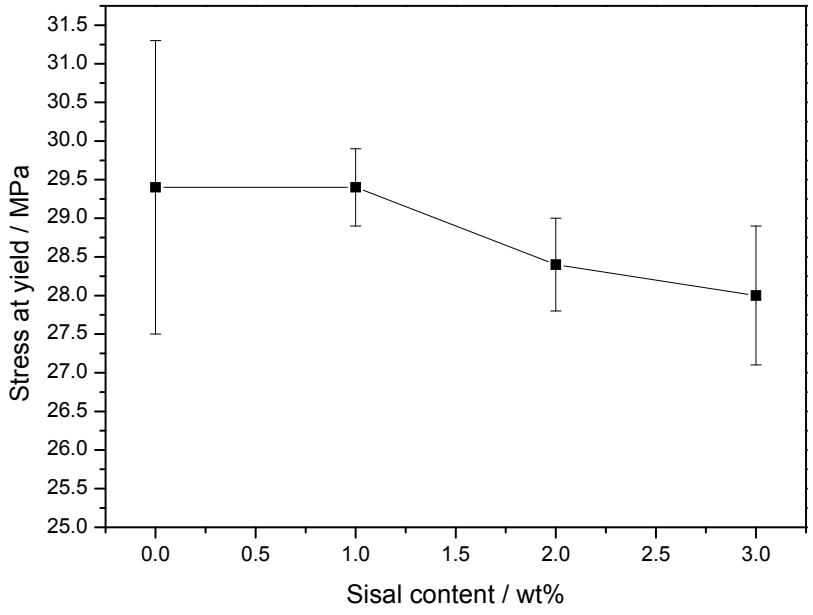

Figure 4.36 Yield stress as function of sisal fibre content for PP and its composites

Figure 4.39 shows the effect of fibre content on the elongation at break of the composites. Even at 1% sisal fibre content there is a significant decrease in elongation at break. This can be explained by the fact that the sisal fibres act as defect centres for crack initiation and suppress the ability of the PP matrix to undergo a plastic deformation process. It appears that the behaviour of the PP matrix shifted from ductile to brittle in the presence of sisal fibre

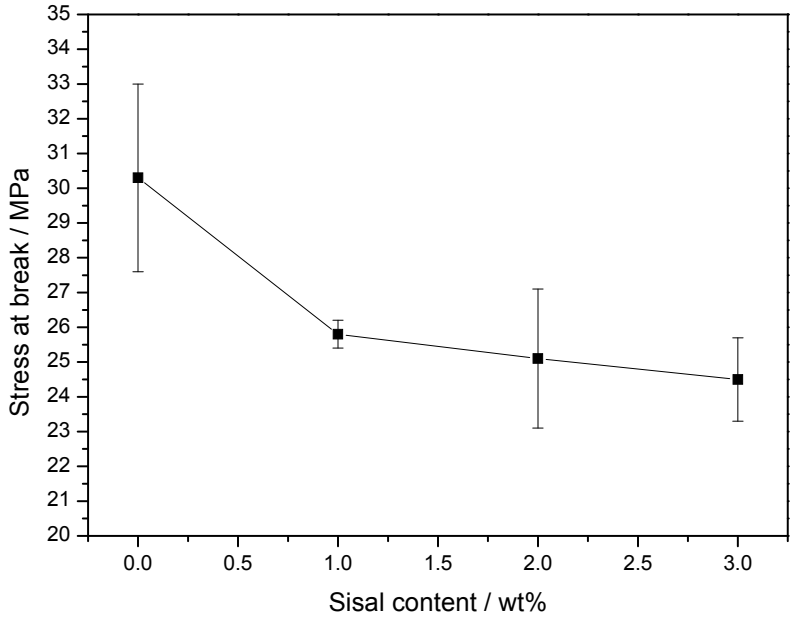

Figure 4.37 Stress at break as function of sisal fibre content for PP and its composites

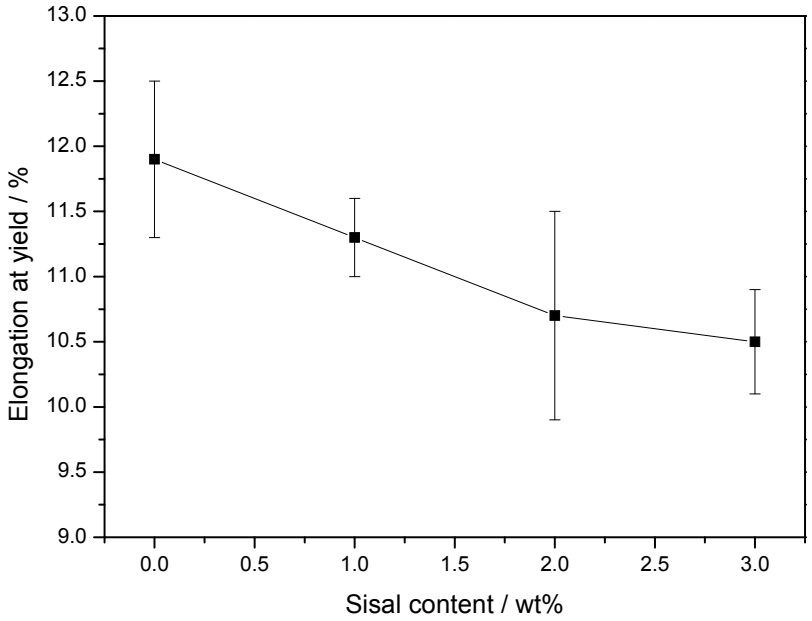

Figure 4.38 Elongation at yield as function of sisal fibre content for PP and its composites

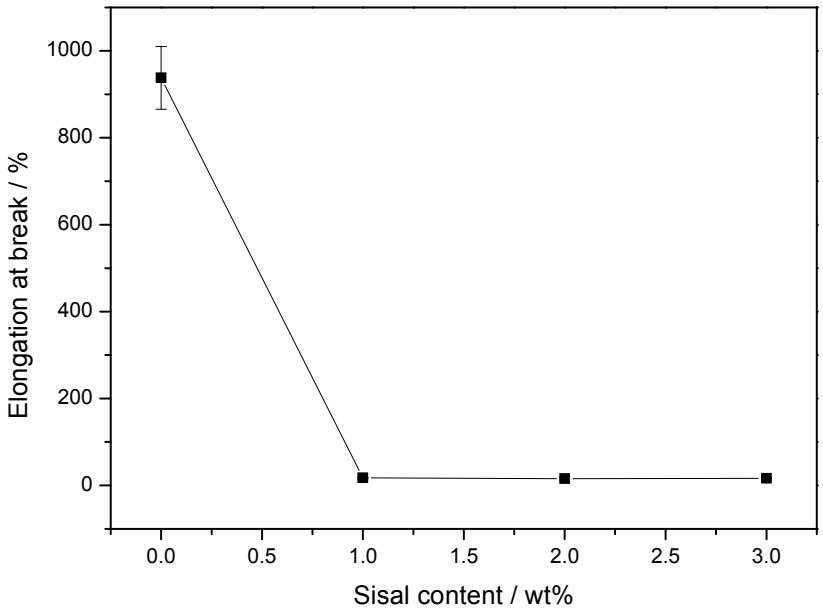

Figure 4.39 Elongation at break as function of sisal fibre content for PP and its composites

4.7 Biodegradability through hydrolysis

The mass loss results of PLA and PP samples after being immersed in distilled water at 80 ºC for ten days are shown in Figures 4.40 and 4.41, and the percentage mass loss is summarized in Table 4.6. The mass loss of neat PLA and its composites initially increased fast (Figure 4.40), but the rate of increase decreased as time progressed. A total mass loss of 46% was observed for neat PLA after ten days. At this point the neat PLA sample was very soft and it was difficult to decant water and rinse the sample without losing some material, therefore the experiment was discontinued after ten days. This mass loss was due to the removal of PLA from the surface upon biodegradation. In PLA biodegradation, moisture susceptibility is the primary driving force and involves the following four steps: water absorption, ester cleavage forming oligomers, solubilization of oligomer fractions, and diffusion of bacteria into soluble oligomers [26,33-34]. The mass loss of the composites followed the same trend and show mass loss values within the

same order of magnitude as those of neat PLA. The observed mass loss is due to the removal of the PLA matrix on the surface as a result of biodegradation [4], together with the removal of some substances from the sisal fibre during the immersion. Chow *et al.* [35] studied the effect of water absorption (at 90 ºC) on the mechanical properties of sisal fibre/polypropylene (SF/PP) composites. They reported that the mass loss of the composites was due to the removal of certain fractions from the sisal fibre during the water immersion. They analysed the samples' morphology before and after immersion by using SEM. The results of the tensile broken samples before immersion showed that the fibre was intact in the PP matrix. For the samples immersed in the hot water for 72 h, serious de-bonding between the fibre and the matrix was observed, but the sisal fibre did not show any signs of degradation. After 216 h immersion, the interface between the SF and PP was totally removed, a significant portion of the lignin and hemicellulose had been leached out, and the sisal fibre showed micro-fabrillation. Lee and co-worker [16] studied the biodegradation of PLA/bamboo fibre (BF) and they reported that the degradation of PLA was slow but enhanced in the presence of BF. The SEM results indicated that most of the matrix was degraded even though the degradation time was short. Shibata *et al.* [36] studied the biodegradation of PLA/abaca fibre, and reported higher mass loss of the untreated fibre composites compared to the neat polymer. They could not conclude whether the biodegradation of the matrix polymer was promoted by the presence of abaca fibre. However, they did not exclude the possibility that the presence of the highly hydrophilic fibre promoted the biodegradation of the matrix, probably by an action of hydrolytic depolymerisation.

No degradation was anticipated for PP during the immersion in water at 80 ºC. The neat polypropylene (PP) showed no mass loss up to ten days of immersion (Figure 4.41). All the PP/sisal fibre composites showed less than 1% mass loss after ten days, which is probably due to limited degradation of the fibre on the sample surface. The fibre in the bulk would have been protected by the surrounding PP. This mass loss of the PP composites was significantly lower than those of the PLA and its composites. Unfortunately there was not enough material to analyse several samples of the same composition in order to obtain statistically reliable results.

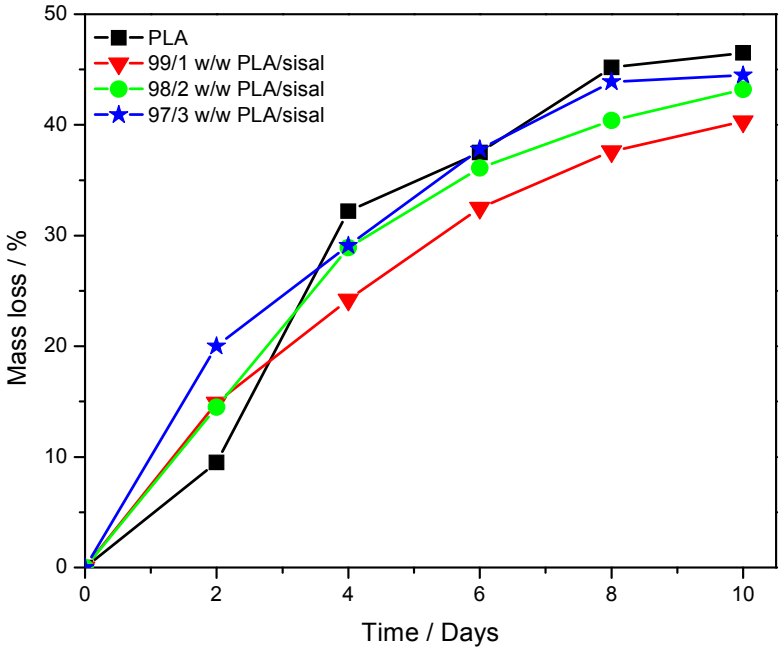

Figure 4.40 Loss in weight of PLA and PLA composites in water at 80 ºC for ten days

Table 4.5 Percentage mass loss of the PLA, PP and their composites after exposure in water at 80 ºC

Sample	2 days	4 days	6 days	8 days	10 days
PLA	9.5	32.2	37.5	45.2	46.5
99/1 w/w PLA/sisal	14.9	24.2	32.5	37.6	40.3
98/2 w/w PLA/sisal	14.5	28.9	36.1	40.4	43.2
97/3 w/w PLA/sisal	20.0	29.1	37.8	43.9	44.5
PP	0.0	0.0	0.0	0.0	0.0
99/1 w/w PP/sisal	0.0	0.0	0.2	0.6	0.4
98/2 w/w PP/sisal	0.00	0.1	0.1	0.1	0.2
97/3 w/w PP/sisal	0.0	0.1	0.1	0.2	0.2

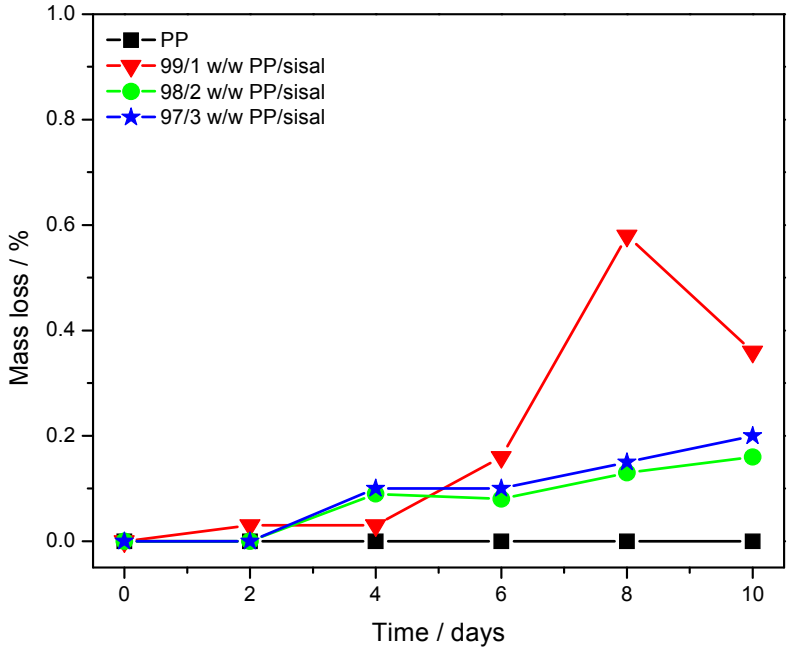

Figure 4.41 Loss in weight of PP and PP composites in water at 80 ºC for ten days

The SEM micrographs of the surface of the biodegraded samples immersed in water at 80 ºC for 2, 8 and 10 days are displayed in Figures 4.42, 4.43 and 4.44 respectively. The neat PLA at 2 days show only some small cracks, but the cracks become larger when the sisal fibre content increases. This shows that fibre enhance the biodegradability of PLA. Figure 4.42 (d) show the exposed fibre after the PLA matrix has been eroded. The exposed fibre also show some disintegrated parts in which the fibrils are formed. Figure 4.43 shows the samples that were immersed for 8 days, and the cracks for the neat PLA are propagating with the increase in immersion time. The composites at fibre content 2 and 3 wt% (Figure 4.43 (c) and (d)) show the collapsed surface of the samples. This indicates that the fibre itself degrade in the process of immersion in water at 80 ºC, therefore, resulting in further biodegradation of the PLA matrix. Figure 4.44 (a) shows visible lines and pores that were formed on the surface of neat PLA during the increase in immersion time (10 days). In this figure the composites surface is almost completely collapsed. More damaged fibres are exposed, showing that the fibres undergone severe degradation.

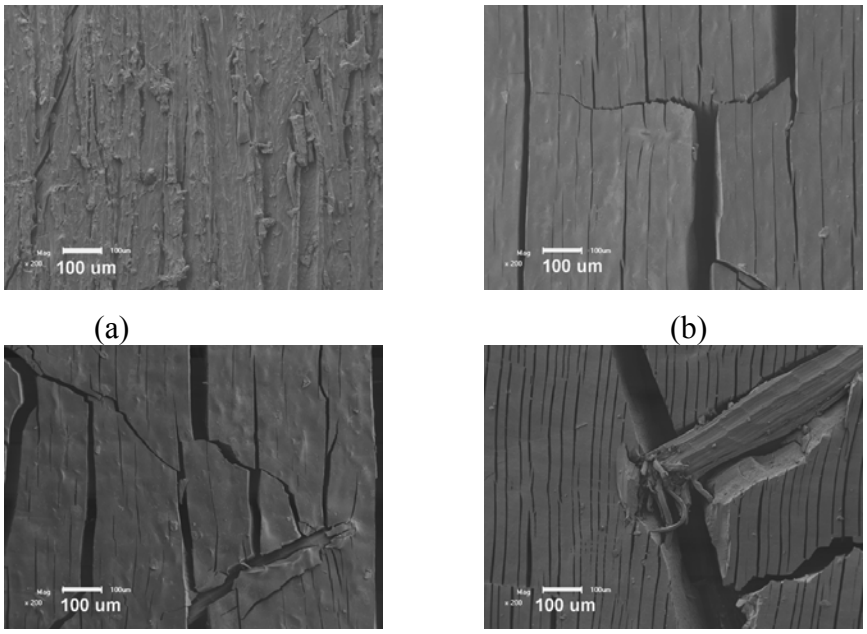

(a) (b)

(c) (d)

Figure 4.42 SEM micrographs of the biodegraded surfaces of PLA ((a) 99/1 w/w PLA/sisal (b) 98/2 w/w PLA/sisal (c) and the 97/3 w/w PLA/sisal (d) 200x after 2 days of immersion.

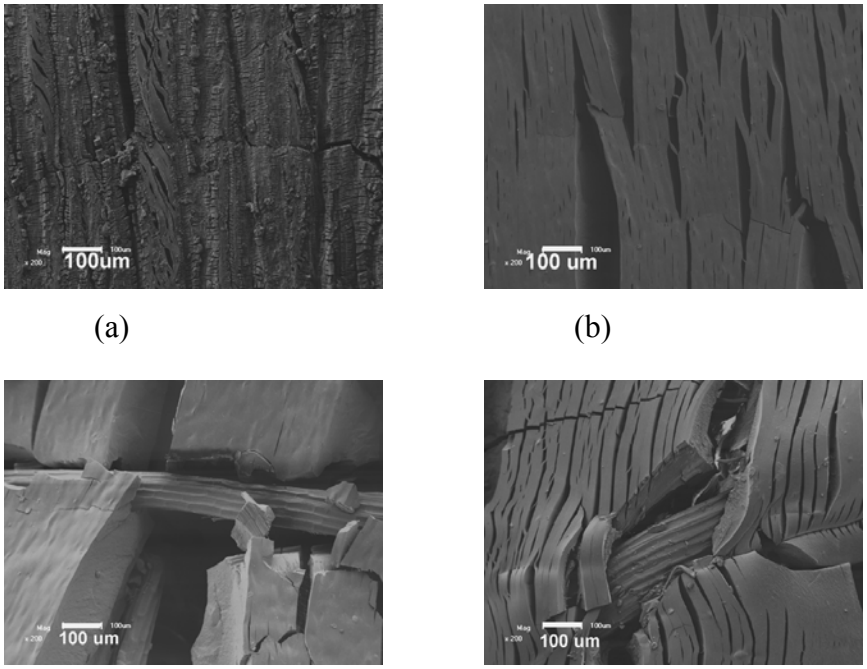

(a) (b)

(c) (d)

Figure 4.43 SEM micrographs of the biodegraded surfaces of PLA ((a) 99/1 w/w PLA/sisal (b) 98/2 w/w PLA/sisal (c) and the 97/3 w/w PLA/sisal (d) 200x after 8 days of immersion.

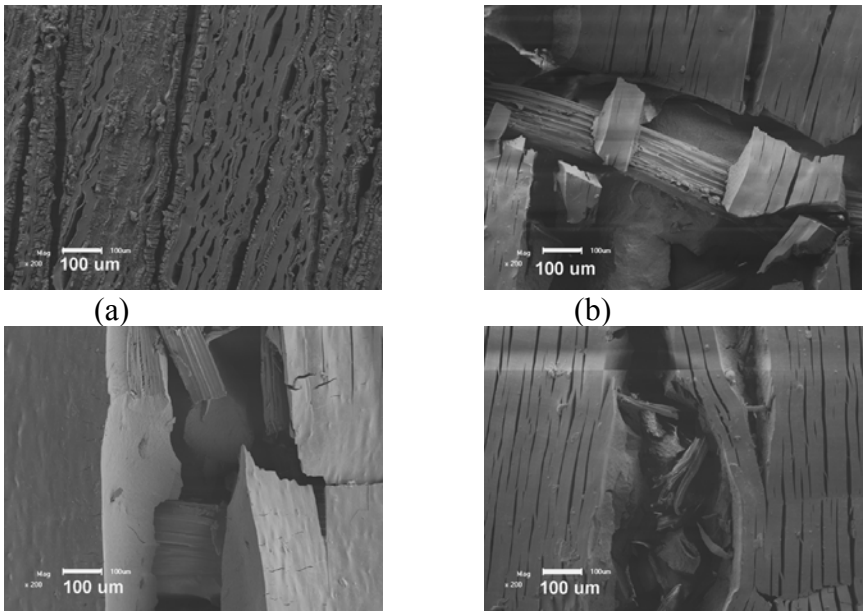

(a) (b)

(c) (d)

Figure 4.44 SEM micrographs of the biodegraded surfaces of PLA ((a) 99/1 w/w PLA/sisal (b) 98/2 w/w PLA/sisal (c) and the 97/3 w/w PLA/sisal (d) 200x after 10 days of immersion.

4.8 References

1. M.S. Huda, L.T. Drzal, A.K. Mohanty, M. Misra. Wood fibre reinforced poly(lactic acid) composites. 5th Annual SPE Automotive Composites Conference, Troy, Michigan, 12-14 September 2005.
2. S. Wong, R. Shanks, A. Hodzic. Interfacial improvements in poly(3-hydroxybutyrate)-flax fibre composites with hydrogen bonding additives. Composites Science and Technology 2004; 64:1321-1330.
   DOI: 10.1016/j.compscitech.2003.10.012
3. PV. Joseph, K. Joseph, S. Thomas, C.K.S. Pillai, V.S. Prasad, G. Groeninckx, M. Sarkissova. The thermal and crystallisation studies of short sisal fibre reinforced polypropylene composites. Composites: Part A 2003; 34:253-266.
   PII: S1359-835X(02)00185-9
4. R. Kumar, M.K. Yakubu, R.D. Anandjiwala. Biodegradation of flax fibre reinforced poly(lactic acid). eXPRESS Polymer Letters 2010; 14:423-430.

DOI: 10.3144/expresspolymett.2010.53

4 J.I. Morán, V.A. Alvarez, V.P. Cyras, A. Vázquez. Extraction of cellulose and preparation of nanocellulose from sisal fibres. Cellulose 2008; 15:149-159.
DOI: 10.1007/s10570-007-9145-9

5 C. Chuai, K. Almdal, L. Poulsen, D. Plackett. Conifer fibres as reinforcing materials for polypropylene based composites. Journal of Applied Polymer Science 2001; 80:2833-2841.

7. L. Petersson, I. Kvien, K. Oksman. Structure and thermal properties of poly(lactic acid)/cellulose whiskers nanocomposites materials. Composites Science and Technology 2007; 67:2535-2544.
DOI:10.1016/j.compscitech.2006.12.012.

8. M.S. Huda, L.T. Drzal, M. Misra, A.K. Mohanty, K. Williams, D.F. Mielewski. A study on biocomposites from recycled newspaper fiber and poly(lactic acid). Industrial & Engineering Chemistry Research 2005; 44:5593-5601.
DOI: 10.1021/ie0488849.

9. J.K de Verney, M.F.S. Lima, D.M. Lenz. Properties of SBS and sisal fiber composites: ecological material for shoe manufacturing. Materials Research 2009; 11:447-451.

10. C. Albano, J. González, M. Ichazo, D. Kaiser. Thermal stability of blends of polyolefins and sisal fiber. Polymer Degradation and Stability 1999; 66:179-190.
DOI:10.1016/S0141-3910(99)00064-6

11. F. Mengeloglu, K. Karakus. Thermal degradation, mechanical properties and morphology of wheat straw flour filled recycled thermoplastic composites. Sensors 2008; 8:500-519.

12. K.L. Fung, X.S. Xing, R.K.Y. Li, S.C. Tjong, Y.-W. Mai. An investigation on the processing of sisal fibre reinforced polypropylene composites. Composites Science and Technology 2003; 63:1255-1258.
DOI:10.1016/S0266-3538(03)00095-2.

13. L-T. Lim, R. Auras, M. Rubino. Processing techniques for poly(lactic acid). Progress in Polymer Science 2008; 33:820:852.
DOI: 10.1016/j.progpolymsci.2008.05.004.

14. M.S. Huda, L.T. Drzal, M. Misra, A.K. Mohanty. Wood-fiber-reinforced poly(lactic acid) composites: Evaluation of the physicomechanical and morphological properties. Journal of Applied Polymer Science 2006; 102:4856-4869.
DOI: 10.1002/app.24829

15. M. Avella, G. Bogoeva-Gaceva, A. Bežarovska, M.E. Errico, G. Gentile, A. Grozdanov. Poly(lactic acid)-based biocomposites reinforced with kenaf fibers. Journal of Applied Polymer Science 2008; 108:3542-3551.
DOI: 10.1002/app.28004

16. S-H. Lee, S. Wang. Biodegradable polymers/bamboo fiber biocomposite with bio-based coupling agent. Composites: Part A 2006; 37:80-91.
DOI: 10.1016/j.compositesa.2005.04.015

17. M.G. Salemane, A.S. Luyt. Thermal and mechanical properties of polypropylene-wood powder composites. Journal of Applied Polymer Science 2006; 100:4173-4180.
DOI: 10.1002/app.23521.

18. P. V. Joseph, G. Mathew, K. Joseph, S. Thomas, P. Pradeep. Mechanical properties of short sisal fiber-reinforced polypropylene composites: comparison of experimental data with theoretical predictions. Journal of Applied Polymer Science 2003; 88:602–611.
DOI: 10.1002/app.11498.

19. H.D. Rozman, K.W. Tan, R.N. Kumar, A. Abubakar, Z.A.M. Ishak, H. Ismail. The effect of lignin as a compatibilizer on the physical properties of coconut fibre polypropylene composites. European Polymer Journal 2000; 36:1483-1494.
PII: S0014-3057(99)00200-1

20. J.D. Menczel, R.B. Prime, P.K. Gallagher. Differential scanning calorimetry. In: J.D. Menczel, R.B. Prime. Thermal Analysis of Polymers – Fundamentals and Applications. John Wily & Sons: New Jersey (2009).

21. E. Lezak, Z. Kulinski, R. Masirek, E. Piorkowska, M. Pracella, K. Gadzinowska. Mechanical and thermal properties of green polylactide composites with natural fillers. Macromolecular Bioscience 2008; 8:1190–1200.
DOI: 10.1002/mabi.200800040.

22. R. Masirek, Z. Kulinski, D. Chionna, E. Piorkowska, M. Pracella. Composites of poly(L-lactide) with hemp fibers: Morphology and thermal and mechanical properties. Journal of Applied Polymer Science 2007; 105:255–268
DOI 10.1002/app.26090.

23. S. Pilla, A. Kramschuster, L. Yang, J. Lee, S. Gong, L-S. Turng. Microcellular injection-molding of polylactide with chain-extender. Materials Science and Engineering C 2009; 29:1258-1265.
DOI: 10.1016/j.msec.2008.10.027.

24. K.S. Anderson, M.A. Hillmyer. Melt preparation and nucleation efficiency of polylactide stereocomplex crystallites. Polymer 2006; 47:2030–2035.
DOI:10.1016/j.polymer.2006.01.062

25. A.P. Mathew, K. Oksman, M. Sain. The effect of morphology and chemical characteristics of cellulose reinforcements on the crystallinity of polylactic acid. Journal of Applied Polymer Science 2006; 101:300-310.
DOI: 10.1002/app.23346

26. A.P. Mathew, K. Oksman, M. Sain. Mechanical properties of biodegradable composites from poly lactic acid (PLA) and microcrystalline cellulose (MCC). Journal of Applied Polymer Science 2005; 97:2014-2025.
DOI: 10.1002/app.21779

27. K.L. Fung, R.K.Y. Li, S.C. Tjong. Interface modification on the properties of sisal fibre-reinforced polypropylene composites. Journal of Applied Polymer Science 2002; 85:169-

28. A. Amash, P. Zugenmaier. Morphology and properties of isotropic and oriented samples of cellulose fibre–polypropylene composites. Polymer 2000; 41:1589-1596.
PII: S0032-3861(99)00273-6.

29. R. Krishnaprasad, N.R. Veena, H.J. Maria, R. Rajan, M. Skrifvars, K. Joseph. Mechanical and thermal properties of bamboo microfibril reinforced polyhydroxybutyrate biocomposites. Journal of Polymers and the Environment 2009; 17:109-114.
DOI: 10.1007/s10924-009-0127
DOI: 10.1002/app.21779.

30. S.E. Selke, I. Wichman. Wood fibre/polyolefin composites. Composites: Part A 2004; 35:321-326.

DOI:10.1016/j.compositesa.2003.09.010.

31. P.R. Hornsby, E. Hinrichsen, K. Tarverdi. Preparation and properties of polypropylene composites reinforced with wheat and flax straw fibres – Part II. Analysis of composite microstructure and mechanical properties. Journal of Materials Science 1997; 32:1009-1015.

32. L.M. Arzondo, C.J. Pérez, J.M. Cerella. Injection molding of long sisal fibre-reinforced polypropylene: Effects of compatibilizer concentration and viscosity on fibre adhesion and thermal degradation. Polymer Engineering and Science 2005; 45:613-621.
DOI: 10.1002/pen.20299.

33. H-S. Yang, J-S. Yoon, M-N. Kim. Dependence of diodegradability of plastics in compost on the shape of specimens. Polymer Degradation and Stability 2005; 87:131-135.
DOI: 10.1016/j.polymdegradstab.2004.07.016.

34. N. Lucas, C. Bienaime, C. Belloy, M. Queneudec, F. Silvestre, J-E. Nava-Saucedo. Polymer biodegradation: Mechanisms and estimation techniques. Chemosphere 2008. 73:429-442.
DOI: 10.1016/j.chemosphere.2008.06.064.

35. C.P.L. Chow, X.S. Xing, R.K.L. Li. Moisture absorption studies of sisal fibre reinforced polypropylene composites. Composites Science and Technology 2007; 67:306-313.
DOI: 10.1016/j.compscitech.2006.08.005.

36. M. Shibata, K. Ozawa, N. Teramoto, R. Yosomiya, H. Takeishi. Biocomposites made from short abaca fiber and biodegradable polyesters. Macromolecular Materials and Engineering 2003; 288:35-43.

Chapter 5

Conclusions

The aim of this project was to compare the properties of a biodegradable polymer (PLA) and a non-biodegradable polymer (PP) as matrices, in the presence of sisal fibre as the reinforcement. The effect of the presence and amount of fibre on the morphology, thermal, and mechanical properties as well as biodegradability, was studied in order to find if synthetic, non-biodegradable polymer (PP) composites can be substituted by biodegradable (PLA) composites. The most important factor is to find a perfect replacement with the same or very similar properties.

The morphology of the PLA/sisal fibre composites was studied, and it was found that there was a good interaction between the fibre and the polymer matrix. Fewer fibre pull-outs or debonding were observed, and there was also hydrogen bonding as determined by FTIR. Because of this interaction in the PLA/sisal composites there was an increase in crystallinity with increasing fibre content in the composites. The melting temperature of both the annealed and un-annealed samples increased with an increase in fibre content, and it was more evident in the annealed samples. The glass transition temperature of as prepared PLA samples decreased with an increase in the fibre content. The glass transition temperature of annealed samples was higher than that of the as prepared samples, and it did not change for the fibre-containing samples. The Young's modulus and tensile strength of PLA did not chance much in the presence of sisal fibre. The fibre played a role in decreasing the toughness of the matrix as the elongation at break decreased in the presence of fibre. The storage modulus of the annealed PLA did not change much in the presence of the fibre, as the modulus was already high due to the annealing process. In the case of as prepared PLA the storage modulus increased with an increase in fibre content. The biodegradation of PLA was almost 50% in just ten days, and the presence of the fibre seemed to have enhanced this biodegradation process.

Unexpected good adhesion was observed in the PP/sisal fibre composites, because only a few fibre pull-outs were observed in the SEM pictures, but this interaction could not be confirmed by FTIR. The presence of fibre increased the melting temperature, cystallisation temperature as well

as the enthalpy of melting of the PP samples prepared at 190 ºC. This showed that the crystallinity of the PP increased in the presence of sisal fibre. The opposite was observed for the PP samples prepared at 205 ºC, as the presence of fibre decreased the melting temperature, and the enthalpy of melting. The thermal stability of both PPs increased in the presence of sisal fibre, and it was more significant for the samples prepared at 190 ºC. The storage and Young's modulus of the PP samples increased as a result of presence of the stiffer sisal fibres, with the Young's modulus almost double. The PP composites showed little (> 1%) or no biodegradation after 10 days of immersion in water at 80 ºC.

Both the PLA and PP composites showed similar morphologies as indicated by the SEM results. Better polymer-fibre interaction was observed for the PLA composites, and this was confirmed by the FTIR results. The differences in thermal properties of the PP samples prepared at different temperatures (190 and 205 ºC) could be due to the partial degradation of fibre at higher temperatures, although it was more probably the result of two different batches of PP used in the preparation of the composites. If the properties of the comparable PLA and PP composites are compared, it is clear that the PLA and PP composites melt at very similar temperatures, although the PLA has a higher glass transition temperature than PP. If processing is at temperatures close to or above the melting temperature of the polymer, then PLA can substitute PP in the preparation of these composites. Although the PP composites seem to be thermally more stable than the PLA composites, both of them are thermally stable at least up to 330 °C, which is sufficient for most applications. Except for the elongation at yield and break, which is lower for the PLA than for the PP composites, the PLA composites generally show better tensile properties than the PP composites. On a balance of properties it is possible that PLA composites containing small amounts of sisal fibre can replace equivalent PP composites in a number of applications. The biodegradation of PLA is its biggest attribute, and therefore PP can be replaced by PLA as a matrix in a number of applications (packaging, household, and disposable products), especially where environmental concerns are important as almost all the properties are the same, with an additional property of environmental friendliness of PLA.

Acknowledgements

First of all I will like to thank **God** who gave me strength, courage, and perseverance to achieve most of my dreams, and most of all the gifts of life.

I also would like to express my profound gratitude and deep appreciation to my honourable supervisor **Professor Adriaan Stephanus Luyt** for his guidance, support, enthusiastic encouragement throughout the entire period of this research that enabled me to complete this important milestone in my life, and for his efforts to explain things clearly and cleanly. I would like to thank him for his sound advice, good teaching, and lots of good ideas. His overly enthusiasm and integral view on research and his mission for providing only the best and high-quality work, has made a deep impression on me. I am very grateful that I had him as my supervisor and mentor and I learned a lot from his strong character and good conduct as well as the same treatment of all his students.

I acknowledge the Budapest University of Technology and Economics for allowing me to use their facilities for the preparation of the samples

I acknowledge the University of the Free State at large for proving me with an opportunity to study. I would also like to acknowledge the National Research Foundation (NRF) for providing me with financial support and the opportunity to fulfill my dream of achieving a masters degree.

I would like to thank the Old Apostolic Church (OAC) congregation for providing me with emotional support and strength through difficult times, mainly Mr. and Mrs Nkanyane, Mr. and Mrs Gosenyegang, Mr. and Mrs Motho for their great support always as my leaders.

Countless thanks to my mother Mme Mmakeletso Mofokeng, and my brothers Lefu and Lebohang Mofokeng for their love and support, I am proud to be part of this family. I would also like to thank my grandmother Mmamokgae Tibisa Mokoena and the entire Mokoena family who gave birth to this strong woman “my mother” and accepted me and my brothers as part of their

family. Not forgetting Hadebe's family from Phuthaditjhaba for their motivations and encouragement.

Many thanks to my fellow polymer science research group members (Mr. S. Jeremia Sefadi, Mr. Thabang Mokhothu, Mr. Sibusiso Ndlovu, Mr. Mokgaotsa Mochane, Mr Teboho Mokhena, Miss Motshabi Sibeko, Mr. Teboho Motsoeneng, Mr Tankiso Mokoena, Dr. He Wei, Mr. Bongane Msibi, Mr Lucky Dlamini, Ms Nomadlosi Nhlapo, Mr Tladi Mofokeng, Mrs. Moipone Mokoena, Mr. Tshwafo Motaung, Mr. Lulu Mohomane, Mr Tsietsi Tsotetsi, Mrs. Doreen Mosiangaoko, Mrs. Nomampondomise Molefe and Rantwa Papzen Moji), for all their help, support, interest and valuable hints. Especially I am grateful to Mr. Essa Esmail Mohammad Ahmad and Mr. Mfiso Mngomezulu.

I will also like to thank Dr Spirit Molefi, Dr Vladimir Djokovic, Mr Kamohelo George Tshabalala, Mrs Nomampondomise Molefe, Dr. Buiswa Hlangothi, Mr S. Percey Hlangothi, Dr. S. Ochigbo, Mrs Seadimo Mojaki, Miss Rethabile Marumo, Miss Dimakatso Mokalanyane, Mr Phakiso Malinga, Mrs Zanele Pasha, Mrs Makgadiete Mofokeng, Mrs Itumeleng Buthelezi, Mrs. Pholositswe Mpharu, Miss Makhosazana Mthembu, Miss Andisiwe Maandi Sangqu, Mrs Dilahlwane Mohono, Miss Zanele Clarke, Miss Meiki Lebeko, Mr Lehlohonolo Koao for their moral support and good friendship.

I would like to thank Mrs Marlize Jackson, and Mrs Mpho Patience Leripa for their kindheartedness, perseverance and administrative support.

Many thanks to Mrs Luyt who have let her husband work and help all his students, even when she needed him most, I really appreciate it.

I am thankful to the maintenance staff, Mrs Mmadibuseng Lemeko, Mrs Mmaanie Motaung, Mrs Mmalehlohonolo Moremi, Mrs Mmalehlohonolo Bereng and Mr Songame who are always making our working environment clean, and for their parental advice. Finally I would like to thank everyone who has supported me academically and emotionally throughout the entire study. May God bless you all.

Appendix

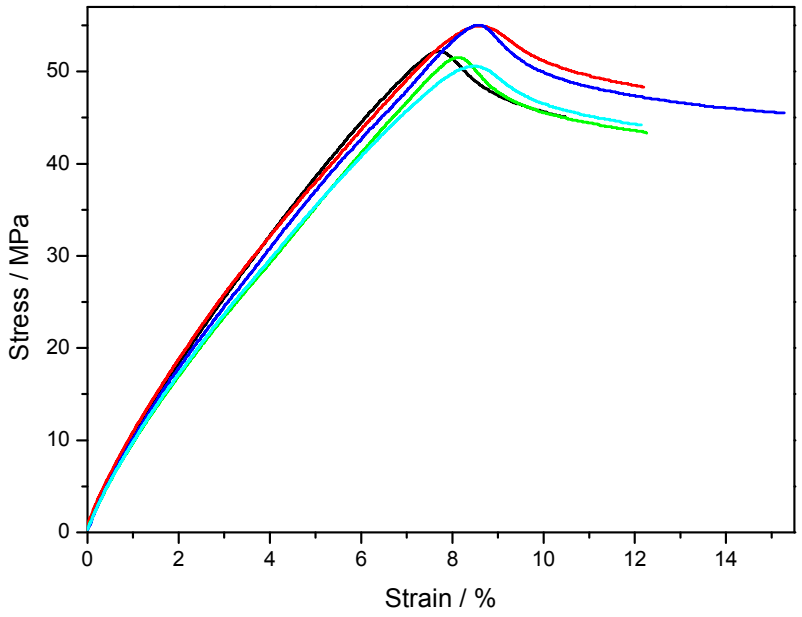

Figure A.1 Stress-strain curves of neat PLA

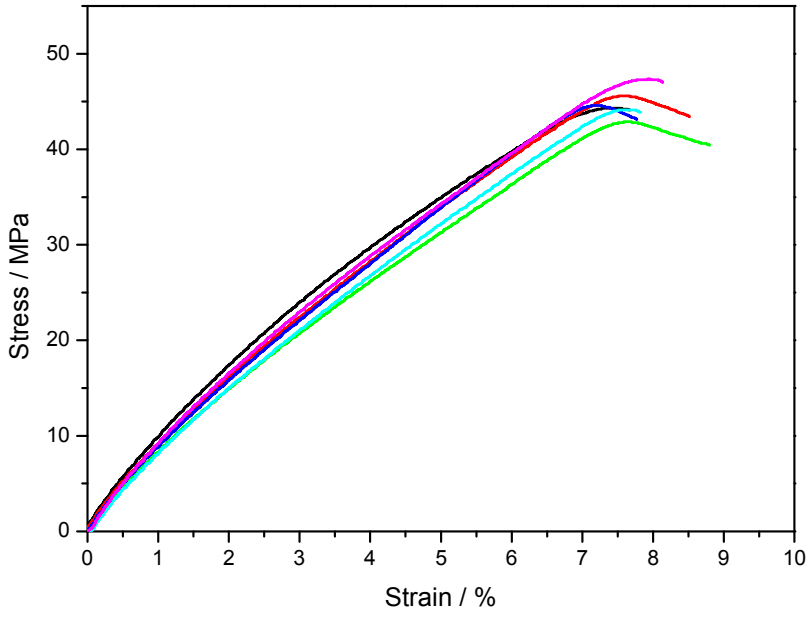

Figure A.2 Stress-strain curves of 99/1 w/w PLA/sisal

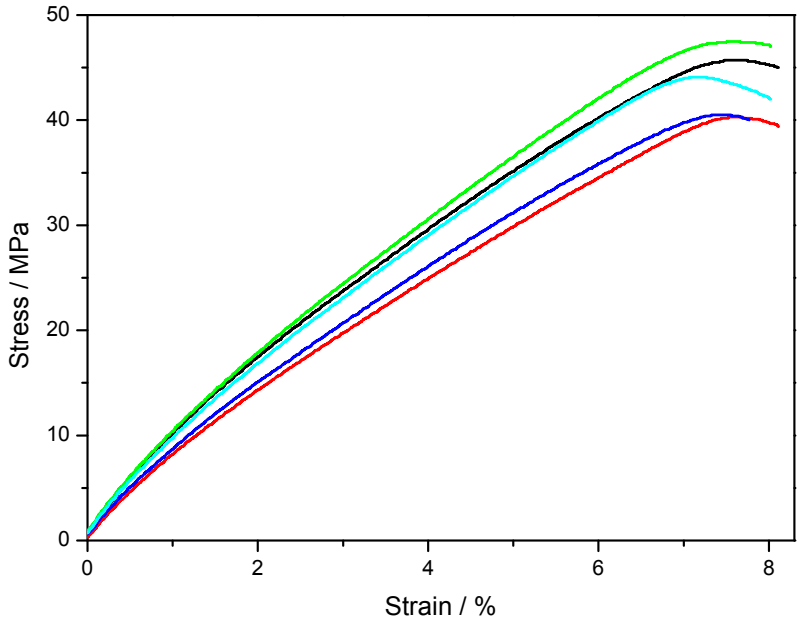

Figure A.3 Stress-strain curves of 98/2 w/w PLA/sisal

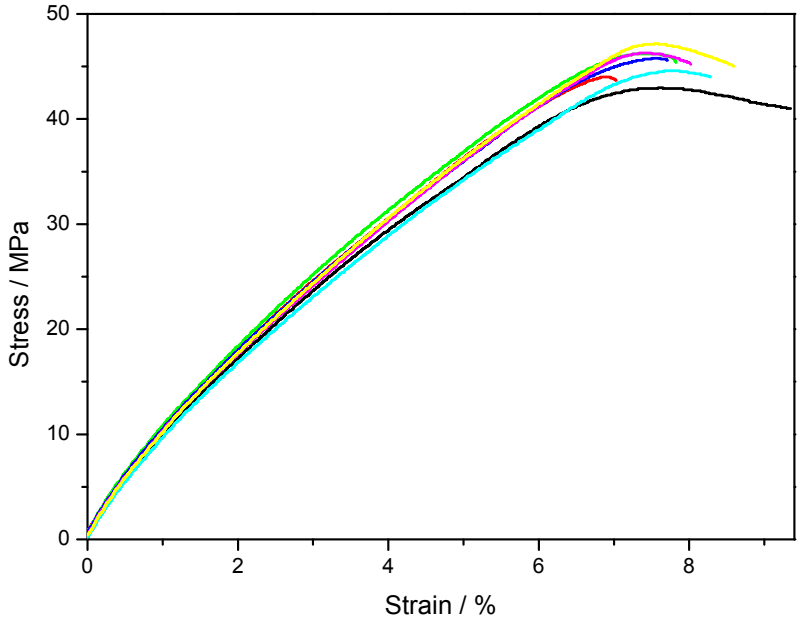

Figure A.4 Stress-strain curves of 97/3 w/w PLA/sisal

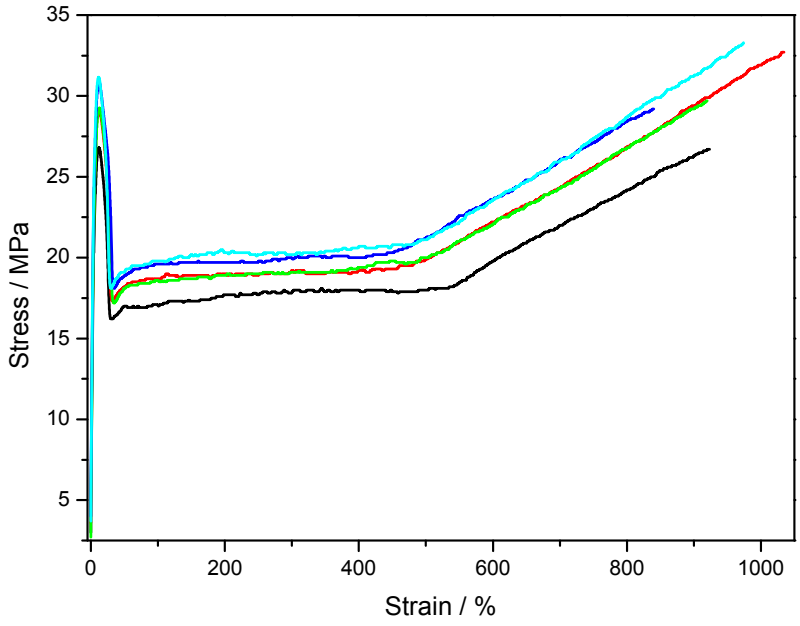

Figure A.5 Stress-strain curves of neat PP

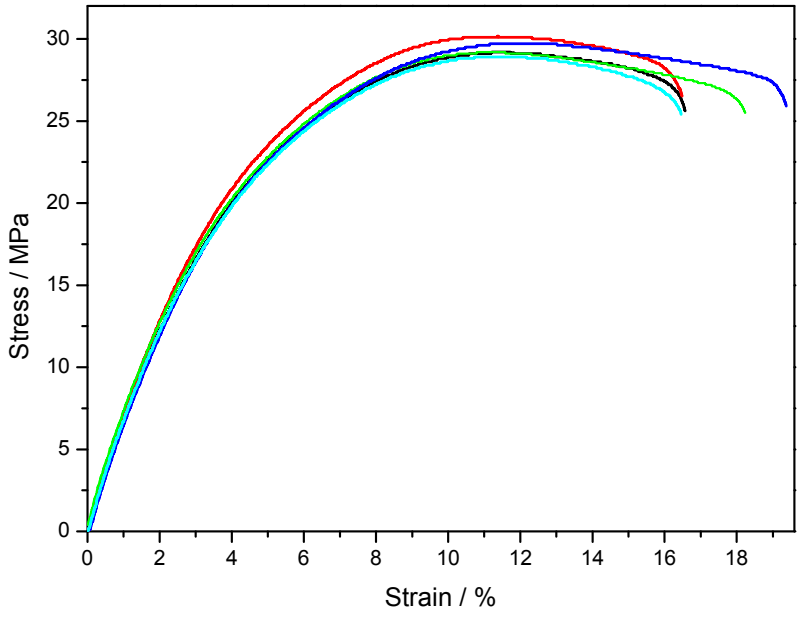

Figure A.6 Stress-strain curves of 99/1 w/w PP/sisal

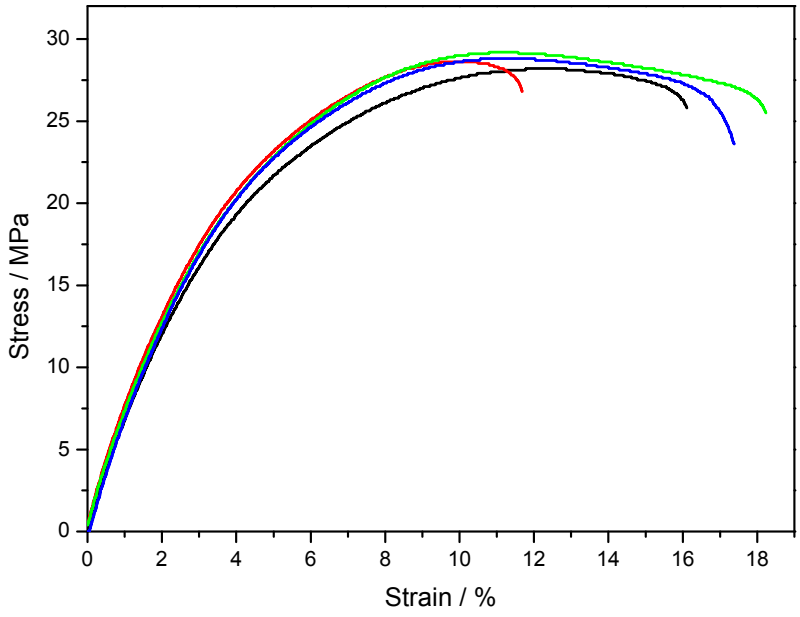

Figure A.7 Stress-strain curves of 98/2 w/w PP/sisal

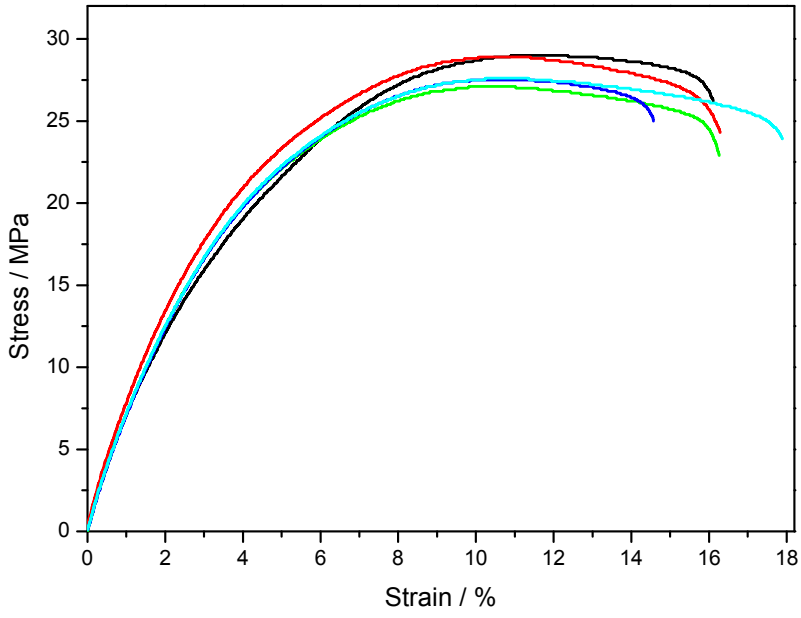

Figure A.8 Stress-strain curves of 97/3 w/w PP/sisal